Errata for the
Proceedings of the Nineteenth
Annual Precise Time and
Time Interval (PTTI) Applications
and Planning Meeting

A meeting held at the
Sheraton Hotel
Redondo Beach, California
December 1-3, 1987

ERRATA FOR THE 1987 PTTI PROCEEDINGS

Richard L. Sydnor

June 10, 1988

Enclosed are two articles and one sheet which are to be substituted for the corresponding parts of the Proceedings.

The single sheet, page 268 is a direct replacement for the original page 268. It corrects several typographic errors.

The article "PORTABLE HYDROGEN MASER CLOCK TIME TRANS-FER AT THE SUBNANOSECOND LEVEL" replaces the original on pages 345—364. Several figures were omitted in the original.

The article "A STUDY OF LONG–TERM STABILITY OF ATOMIC CLOCKS" replaces the original on pages 375—379. A number of pages and figures were omitted in the original.
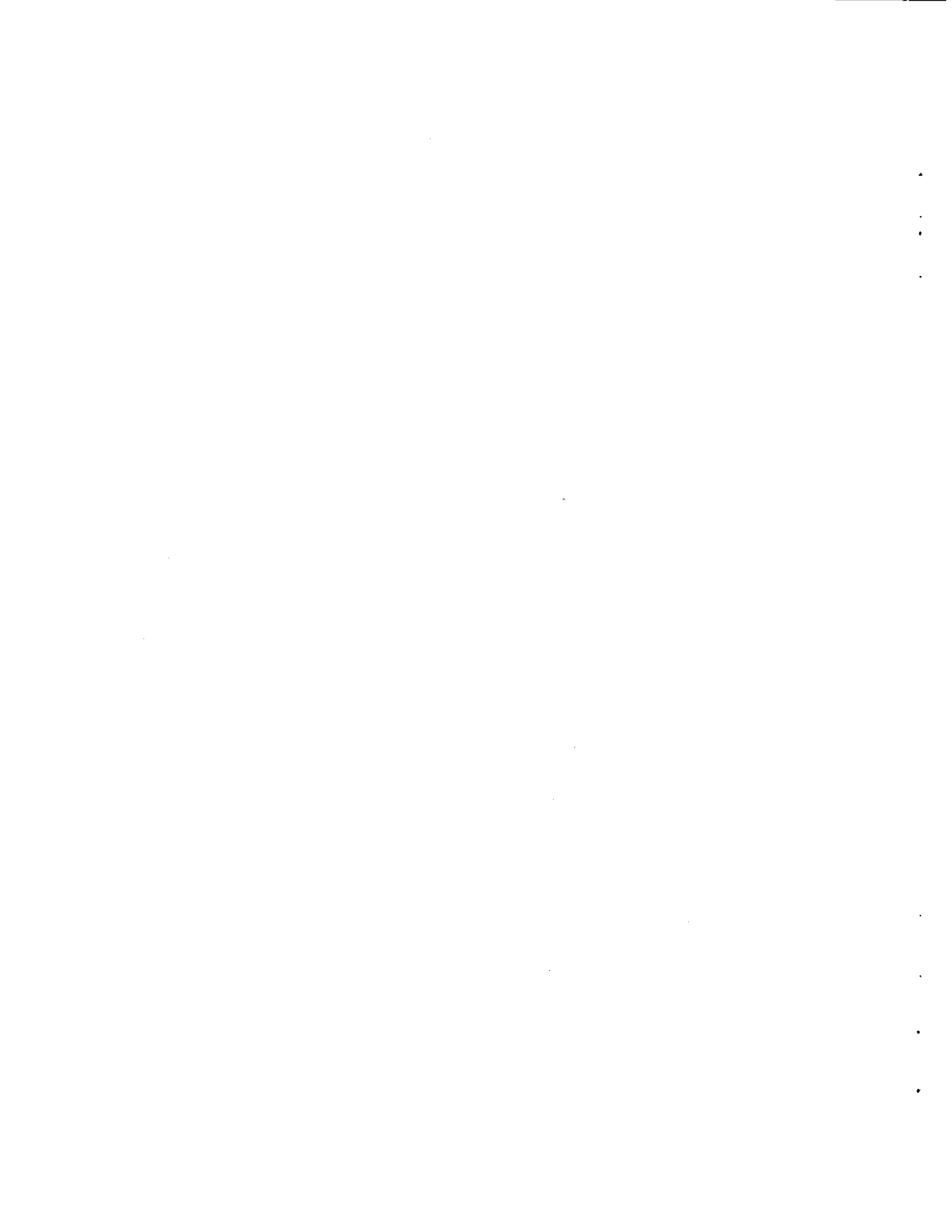
STABILITY TEST RESULTS FOR
GPS RUBIDIUM CLOCKS

F. Danzy
Naval Research Laboratory
Washington, DC

W. Riley
EG&G, Inc.
Salem, MA

ABSTRACT

This paper presents the results of further long-term stability tests on two prototype GPS rubidium frequency standards. These tests, currently underway at the U.S. Naval Research Laboratory, have resulted in the highest stabilities yet reported for such devices. Both units have smooth, highly modelable drift under 2×10^{-14}/day and a stability of about 1×10^{-14} at 10^5 to 10^6 seconds.

INTRODUCTION

EG&G, Inc., began the development of a high-performance rubidium frequency standard (RFS) for the Global Positioning System (GPS) satellites in early 1980. The design of that unit was described at this conference in 1981[1] and the results of stability, performance, and environmental tests on two prototypes were presented at this conference in 1983[2] and 1985[3]. This paper presents the results of further stability tests currently underway at the Naval Research Laboratory (NRL).

The active work at EG&G on these GPS Rb clocks ended in July 1985, when the units were transferred to NRL. Since that time they have been running nearly continuously. Both of these units have now accumulated a failure-free operating time comparable to their 7.5-year design life, mostly under thermovac conditions.

TEST SETUP

The Rb frequency standards under test were installed together in a thermovac chamber[4] in the NRL Space Applications atomic clock laboratory. For the long-term stability tests, these clocks were operated at a constant $+28°$ C baseplate temperature free of any deliberate environmental disturbances.

Phase and frequency measurements were made with an averaging time of 1 hour using a computer-controlled dual-mixer time difference measuring system[5]. The frequency reference for these measurements was an active hydrogen maser (N1)[6].

A photograph of the test setup is shown in Figure 1.

STABILITY TEST RESULTS

Figures 2-7 show the phase and frequency records for the two Rb clocks (EG&G1 and EG&G2) versus the NRL active H-maser reference (N1). The phase records (Figures 2 and 5) have the parabolic shape characteristic of a source having linear frequency drift, which is also visible in the frequency records (Figures 4 and 7). The drifts are very smooth and uniform and have least-squares fit values of -1.8 and -0.8 x 10^{-14}/day. Most of the largest frequency excursions (short spikes of about 2 x 10^{-13} peak) occur simultaneously on both records, and are therefore likely to be from the test setup. The largest drift-corrected phase excursions (about 20 nsec) are associated with small steps (under 1 x 10^{-13}) in the

frequency record. Since there is no deterministic cause for such disturbances, these are the largest nonmodelable clock errors.

The stability of these GPS Rb clocks is also shown in the Allan variance plots of Figures 8-11. The nondrift-corrected plots (Figures 8 and 10) show a $\tau^{-1/2}$ white frequency noise characteristic (at a level of about $3 \times 10^{-12}\tau^{-1/2}$) and a τ^{+1} frequency drift characteristic, with a $\sigma_y(\tau = 10^5)$ seconds) of 1-2 x 10^{-14}, well below the GPS specification shown as the solid line. With the drift removed, this value of stability extends to 10^6 seconds, which, we believe, is the highest level of stability yet reported for a Rb clock. Both units have demonstrated this performance after many years of operation, and one (EG&G2) after two exposures to qualification levels of shock, vibration, and temperature cycling.

A summary of the stability test results is shown in Table I.

TEMPERATURE TEST RESULTS

The two Rb frequency standards were also subjected to a temperature stability test over their operating temperature range of +20 to +45°C. Both units showed excellent temperature insensitivity ($<1 \times 10^{-13}$/°C) over the low-temperature portion of this range, but both had anomalies at the high-temperature end. For EG&G1, this anomaly is due to a secondary loop crystal oscillator that loses oven control above +35°C. For EG&G2, the high-temperature problems seem to be caused by internal temperature rise due to poor thermal transfer between the internal RFS chassis and the thermovac baseplate. Previous tests on this unit showed a temperature sensitivity of -1 x 10^{-13}/°C over its entire operating temperature range.

DESIGN FACTORS

The very high performance of the EG&G GPS RFS is an expected result of its design, which is carefully implemented using classical RFS principles. The low level of white frequency noise is directly related to the high signal-to-noise ratio of the discriminator signal. The low environmental sensitivity is a result of careful error budget analysis relating to the physics package and electronic sensitivities (such as C-field stability and Rb cell temperature coefficients). The low drift is primarily a result of careful control of such physics package parameters as light and rf power shifts. For example, the lamp exciter is both voltage and current regulated; the lamp is well heat-sunk and temperature-controlled; and the discrete filter cell is adjusted to achieve a very close-to-zero light shift coefficient.

Lamp life tests are continuing at both EG&G and Aerospace Corporation using differential scanning calorimetry to measure their Rb consumption.[7] Over a 6-year test period these lamps have consistently shown a low Rb consumption rate (0.2 μgram/$\sqrt{\text{hour}}$) without random failures, thus allowing a relatively low fill (100 μgram) for low noise while assuring a long life ($\geq$ 20 years).

The RFS is specifically designed and adjusted for best performance under vacuum, where the light and signal parameters are optimized, the ovens have their highest stabilization factors, and the unit is freest of such perturbations as thermal gradients and barometric sensitivity. These, and other, design considerations have also resulted in a unit that is remarkably free of the frequency jumps and wandering that usually limit the medium-term stability and modelability of Rb frequency standards. There is, therefore, good reason to believe that the performance of these two prototypes can be duplicated or exceeded as further experience is gained as more units are built.

PORTABLE HYDROGEN MASER CLOCK TIME TRANSFER
AT THE SUBNANOSECOND LEVEL

L. J. Rueger, M. C. Chiu, S. D. Deines
Johns Hopkins University/Applied Physics Laboratory
Laurel, MD 20707

R. A. Nelson, J. T. Broomfield, C. O. Alley
Department of Physics and Astronomy, University of Maryland
College Park, MD 20742

ABSTRACT

A subnanosecond time transfer between the Johns Hopkins University Applied Physics Laboratory (JHU/APL) and the United States Naval Observatory (USNO) was carried out using a portable hydrogen maser. The maser was contained within a temperature controlled enclosure which was supported on pneumatic shock isolators inside an air-conditioned van. The comparisons of the portable maser time with the APL base station maser time used the National Bureau of Standards technique of dual balanced mixers with picosecond resolution.

I. INTRODUCTION

Time transfers between major time and frequency laboratories have been accomplished via portable cesium clocks for the past 15 to 20 years. In more recent times, GPS common view time transfers have been utilized at a great savings in time and operational expense. The GPS transfers, however, are based on differential measurements over periods of several days. Portable clocks are still used to provide an absolute time difference measurement. It is customary to use cesium frequency standards for this function.

The high precision of hydrogen masers, in the range of a few parts in 10^{15}, has been recognized for several years[1-4]. However, there has been no attempt to use these standards to transfer time as a portable clock. Few laboratories could benefit from comparisons of time at the subnanosecond level. APL, NBS and the USNO are among the few. Four portable clock experiments using a hydrogen maser were performed over a three day period in July 1987. This paper describes these experiments and discusses the results.

II. BACKGROUND

Over the past 28 years, the Johns Hopkins University Applied Physics Laboratory (JHU/APL) has maintained an atomic based frequency and time standard facility in support of research and development activities in precision time and frequency measurements for a number of government agencies. To satisfy DOD and non-DOD traceability requirements, these in-house standards have been linked over the years by various means to the United States Naval Observatory (USNO) and National Bureau of Standard (NBS) reference clocks and frequencies. For the last nine years, JHU/APL frequency and time standards have been linked via the United States Naval Observatory to the Bureau International de L'Heure (BIH) and contribute to the international definition of Coordinated Universal Time (UTC).

The APL facility currently has an ensemble of five hydrogen masers and one commercial Hewlett-Packard option 4 cesium standard. Since January 1986, the day to day link of these standards to other laboratories has been through common view monitoring of GPS satellites with an NBS designed GPS receiver. The APL GPS receiver is driven directly from the APL master clock hydrogen maser, NR6. The GPS antenna has a clear 360° view

above 10° from the horizon on a position known to an uncertainty of a few centimeters relative to a prime Defense Mapping Agency (DMA) survey point in the east coast geodetic survey. Prior to the GPS link, a portable Cs standard was used on a weekly trip between APL and the United States Naval Observatory, approximately 72 km (45 miles) round trip, with clock transfer closures typically in the 5 to 10 nanosecond range. The clock transfer closure refers to a laboratory time measurement of the portable Cs clock operating in a curbside vehicle before and after a round trip between APL and USNO, using a straight line interpolation.

Since the Cs standard clock transfers had been so successful in the past, it was proposed to use a hydrogen maser clock known to have stabilities far superior to the Cs clocks as a portable clock. The size of the hydrogen maser with portable standby power is considerably larger than the Cs clock, so a larger vehicle is required. APL salvaged a surplus radio truck equipped with an auxiliary motor generator and air-conditioning unit and refitted the side access door to accommodate the large entry needed for the APL masers. A first experiment was tried in November 1985 in which a maser built by Sigma Tau for APL was mounted on shipping pads and an auxiliary precision measurement instrumentation rack was mounted inside the truck. The results of this first experiment were very encouraging; a curb to curb closure of less than 0.5 nanoseconds was measured.

This trip yielded much information on various techniques needed to perform such a precise time transfer. First, it was noted that the cables used to reach from the APL T& F Lab to the curbside portable clock, located on the outside of the building, were subject to delay changes depending on the cable temperatures (e.g., exposed to sunlight or in the shade of clouds). These delay changes could be as much as 1.2 nanoseconds on the 2-way, 200-ft cables. To alleviate this effect, the cable has been rerouted inside the building to a box on the wall outside nearest to the curb. Now there is only a 20-ft building to curb span exposed to the weather. A second major factor affecting our measurements occurred at the USNO. The USNO was using a microstepper to correct for the drift of their hydrogen maser (the USNO masers do not have automated tuning mechanisms which are incorporated into both the NR and Sigma Tau masers). It was found that in measuring the APL maser against USNO's maser with the microstepper in the circuit, there were peak to peak modulations of 200 picoseconds. This modulation disappeared when the two masers were measured directly. Since this time, USNO has improved its method of compensating for the drift rate of its masers by adjusting the maser internal synthesizer.

There were also other factors affecting the operation of the maser during the trip which were identified. These include temperature, vibration, and acceleration effects. Better control of these factors was considered essential in order to achieve the desired goal of transferring time between APL and USNO with 100 picosecond uncertainty.

III. DESCRIPTION OF EQUIPMENT

A. APL Truck

The air-conditioned truck used to transport the hydrogen maser carries a 15 kW single phase, 220 volt motor generator set for primary power during portable operations. The power supplied to the maser, the enclosure heater and box temperature control system is via an Uninterruptable Power System (UPS) capable of delivering 920 watts for up to 20 minutes. The UPS takes input power from the vehicle motor/generator and charges up a 70 volt battery; the battery feeds a crystal controlled 60 hertz oscillator and power amplifier. This arrangement removes all vehicle motor generator transients, spikes, and frequency variations from the electrical loads. There is a rack of precision time and frequency measurement instrumentation that can be carried in the van; this is identified as the 5 MHz system, and is described later. The APL Truck is shown in Figure 1.

346

B. Hydrogen Maser

The portable hydrogen maser clock used for the APL time transfers was designed and fabricated by Sigma Tau, Inc. for APL. This maser, designated ST1, is fairly small in size and mass compared to most types of masers. The Sigma Tau maser, however, is unique in its tuning capability. By modulation of the maser cavity frequency, the ST1 maser can tune without reference to another maser[5]. This feature is a key factor in the performance of the portable hydrogen maser clock. Many disturbances to which the maser was subjected while being transported were essentially corrected internally through this self-tuning process. A picture of the ST1 maser is shown on the left in Figure 2, an NR maser is shown on the right.

C. Environmental Monitors and Controls

(i) Clock Enclosure

The portable clock must have a stable temperature. For a few parts in 10^{15} frequency stability, a temperature stability of about 0.1°C is needed. The APL van can be either air-conditioned or heated. Temperature is regulated with a thermostat which provides stability of a few degrees. To obtain greater temperature stability for the clock a special enclosure was constructed. The dimensions are 1.72 m high x 1.24 m wide x 0.93 m deep. This volume can accommodate either the Sigma Tau maser used in these experiments or the APL NR-series of masers. Air is drawn into the enclosure through a duct by two fans whose speeds can be regulated. An airflow of 0.15 m³/s (315 CFM) was found to be satisfactory that allowed for both cooling of the air and removal of the 150 W maser heat dissipation. The interior temperature is controlled slightly above ambient room temperature by a commercial system manufactured by Watlow. Heat is added by a 49-cm long stainless steel heating element with blades mounted perpendicular to the axis. The maximum power is 1450 W at 120 V. The current to the heating element is provided by a silicon rectifier power supply that is regulated by a Watlow series "910" digital controller. The sensor is a platinum Resistor Temperature Device (RTD) placed on the surface of the maser. The controller has a microprocessor that has proportional-integral-derivative (PID) action. The PID parameters can be programmed on the face of the instrument.

Considerable effort was made to test this system in the laboratory to obtain the optimum combination of parameters. It was found that an internal temperature stability of 0.1°C could be maintained in the laboratory when the external temperature fluctuated by a few degrees. However, the road trips were undertaken on hot summer days when the air temperature exceeded 32°C. The van air conditioner was not able to provide sufficient cooling while the van was in motion on the longer trips described in this report. Consequently, the temperature within the clock enclosure actually varied by a degree or more during the trips and the full temperature control capability was not realized in these specific tests.

Several measurements were made on the temperature stability of the Sigma Tau maser while maintained at a constant temperature of 24.0±0.1°C within the clock enclosure in the laboratory. The change in slope of the chart record for the 200 MHz system (described below) was measured for consecutive 1, 2, and 3-hour intervals over a time span of 72 hours to determine the stability and prediction of time keeping. Histograms of the data are presented in Figure 3. The standard deviation in the time change relative to a laboratory standard is about 25 ps over 1 hour.

The clock enclosure was also used to measure the temperature coefficient of the Sigma Tau maser. The temperature controller setpoint was raised from 24°C to 28°C and a new equilibrium was later observed. From the change in slope of the chart record for three trials it was found that the temperature coefficient was $1.8 \pm 0.6 \times 10^{-14}/°C$. This result is consistent with earlier tests conducted in a small room whose temperature could

347

be regulated. It was also found that between 1 and 1 1/2 hours elapsed between the time when the temperature setpoint was changed and the clock responded by changing its frequency. This delay is due to a combination of the maser thermal time constants and the self-tuning feature of the maser.

The clock must also be protected from strong vibration. Shock isolation was obtained by mounting the enclosure on four pneumatic supports, each with a load rating of 150 to 600 lb, manufactured by Barry Controls. This required a special loading procedure. The clock enclosure was supported on wheels and a set of rails was constructed that can be erected to extend out the side of the van. The enclosure with the portable clock secured inside is lifted onto the rails by a forklift and the enclosure is rolled into the van onto a frame bolted to the floor. One rail has an inverted "vee" shape to index on grooved wheels on one side of the enclosure. A picture of this clock enclosure being loaded into the APL Truck is shown in Figure 4. When the clock is inside the van, the shock isolators are pressurized with a nitrogen cylinder, thereby raising the enclosure off the rails slightly, and the rails are removed. The shock system provided good high frequency vibration isolation during road trips. The pneumatic supports provided adequate lateral stability while limiting the vertical vibration to a few hertz with a maximum amplitude of about 2 cm.

Provision was also made to attach a pair of wheel assemblies to the outside of the clock enclosure to facilitate moving it in and out of the laboratory with the maser inside. The wheels are removed when the enclosure is supported by the forklift prior to being loaded onto the rails. The time required to move the system out of the laboratory and load it into the van is between 30 and 45 minutes.

(ii) Van Velocity

Provision was made to have a complete record of the van velocity over the duration of the trip, in order to apply small relativity corrections where applicable in the reduction of the data. A small permanent magnet dc motor was mounted on a bracket that could pivot about a support clamp. A large rubber wheel was attached to the motor axle. The device was bolted to the underside of the van so that the rubber wheel rested on the top of the van driveshaft. The electrical leads to the motor were extended through the truck floor where they could be connected to a strip chart recorder. When the van was in motion the motor, acting as a generator, produced a voltage directly proportional to the velocity. Periods when the van was moving in reverse or was at rest could also be identified. The resolution of the strip chart is about 2 mph. Figure 5 shows the truck velocity for one of the portable clock experiment trips.

D.   Measurement Systems

Three time and frequency stability measurement systems were used during the time transfer experiments. Having more than one measurement system was considered necessary both for redundancy and in accounting for any ambiguities in the more precise systems. These three systems included a 1 PPS signal system, a 5 MHz signal based system and a 200 MHz signal based system. Block diagrams of the systems are shown in Figures 6-8.

(i) 1 PPS System

The 1 PPS (Pulse Per Second) system (Figure 6) uses the 1 PPS signals from the portable clock (PC) maser and NR6 maser as the start and stop functions on an HP 5345 counter in the time interval mode. At least ten consecutive measurements are made and averaged for a precision of ±0.3 nanoseconds.

(ii) 5 MHz Signal System

The 5 MHz signal system (see Figure 7) compares the 5 MHz output signals from ST1 and NR6 using a heterodyne method. The individual 5 MHz signals are mixed with the signal from a 5 MHz VCO (voltage controlled oscillator) with a 10 Hz offset. The resulting 10 Hz beats are then input to a counter which measures the time interval between the zero crossings. The resolution of this counter is 100 picoseconds, and with the multiplication factor the resolution is less than 0.1 picosecond. The ambiguity of this system is 200 nanoseconds. This system was placed in a portable rack to transport in the APL Truck with the hydrogen maser.

(iii) 200 MHz Signal System

The 200 MHz system compares the 5 MHz signals from PC (ST1) and NR6 after a multiplication to 200 MHz using a heterodyne method (see Figure 8). The 5 MHz signal from PC is input to one of our reference APL masers, offset in frequency by 5×10^{-8}. The 5 MHz signals from PC and the 5 MHz (1 to 5×10^{-8}) signal from the reference maser are mixed producing a 10 Hz beat. A similar procedure is performed with the 5 MHz signal from NR6. The two resulting 10 Hz beats are then measured by HP 5300 counters with a resolution of 1 microsecond. The overall precision of this system (accounting for the multiplication factor) is 0.05 picoseconds, and the ambiguity is 5 nanoseconds. However, during these experiments only a strip chart was used to record the data. The reading resolution for the strip chart was only 10 picoseconds.

As one can see, the three systems are both redundant and complementary. The 1 PPS system can measure time differences without ambiguity (at least to the second) but is rather coarse in resolution. The 5 MHz and 200 MHz systems have much finer resolution but have ambiguities which can be resolved with the 1 PPS system. In addition to measuring the time differences between NR6 and ST1 in the time transfer experiments, measurements were also made between NR6 and two other, undisturbed NR masers in APL's Time and Frequency Laboratory. This was to verify that NR6 did not experience any disturbances during the time transfers that might contaminate the data.

IV.   ANALYSIS OF TRIPS

Four trips were made with the portable hydrogen maser in which closure times were measured. The general procedure for these trips is as follows. The PC (ST1 maser) in the clock enclosure was wheeled from the APL Time and Frequency Laboratory (located on the third floor) down to the first floor and outside onto the sidewalk. A forklift was then used to lift the maser up to the rails extending from the APL truck side door (as described in a previous section). It was then rolled into the APL Truck and secured. When the portable 5 MHz measurement system was used, it was loaded at this time. The APL Truck was then driven to the curb outside located nearest to the Time and Frequency Laboratory to measure the PC relative to NR6. The APL truck was parked in this location for a period of time to monitor the performance of PC, and to allow the PC maser to recover from any disturbances caused by the move. After transporting the PC it was again parked in this location for a period of time to measure its performance. Afterwards it was returned to the APL Time and Frequency Laboratory.

Four trips were made between July 29 and July 31. The routes for the four trips are illustrated in Figure 9. A more detailed description of the individual trips is given below.

A.   Trip 1

The first trip was made from APL curbside, on Johns Hopkins Road, across Route 29, along local roads to MD-216 and I-95. The route proceded south to the MD-212 cloverleaf

at Calverton and returned over the same path to APL. The trip took about 35 minutes, covering 34.4 km (21.6 miles), and provided a clock closure of +140±10 picoseconds as measured by the 200 MHz system. A strip chart display of Trip 1 and Trip 2 using the 200 MHz measurement system is shown in Figure 10 as the left interrupted trace. The right trace in Figure 10 is another maser also compared to the NR6 house standard to verify that NR6 provided a stable reference during the various trips. The 1 PPS system measurement was consistent within its known resolution limits. A measurement on the 5 MHz system was not taken in the beginning of the trip. Figure 5 shows the truck velocity data for this trip.

B. TRIP 2

The same route as for trip 1 was followed and the trip time between departure and return was 36 minutes, providing a clock closure of +110±10 picoseconds as measured by the 200 MHz system (see Figure 10) and +150 picoseconds by the 5 MHz system. The 1 PPS system measured 0±300 picoseconds, which is still consistent with the above measurements.

C. Trip 3

A measure of the clock stability during a road trip lasting 1.75 hours was provided by a trip from APL, proceeding south on Interstate Rt. 95, counter clockwise around the Washington Capital Beltway, and back. The total distance was 139.4 km (86.6 mi). The range of temperature within the clock enclosure was 1.5°C. As shown in Figure 11, a closure of 300±10 picoseconds (using the 200 MHz system) was obtained between the times of disconnect and reconnect at curbside.

It is interesting to estimate what the effects of relativity would be for this trip. At an average speed of 80 km/h (50 mph) the time dilation effect would represent a loss of 17 ps of the portable clock compared to the stationary laboratory clock. Rt. 95 and the Beltway have average differences in elevation with respect to APL of -46 m and -76 m, respectively. The total gravitational redshift correction corresponds to a loss of 41 ps. In addition there is a Sagnac effect loss of 1 ps. The approximate total loss in time of the portable clock compared to the laboratory is thus 59 ps. If one is permitted to extrapolate the trend in the chart record after reconnect back to the point of disconnect, there is a shift to the right corresponding to a loss of about 60 ps. This agreement may be fortuitous, but it is significant that the technology of precise timekeeping has advanced so far that subtle relativity effects may be within the range of measurement for travel at the level of ordinary experience.

D. Trip 4

This trip was to the USNO and included a time transfer from the USNO curbside service. The trip took 3 hours and provided a time closure at APL of -200±10 ps using the 200 MHz system. The 1 PPS system yielded -600±300 picoseconds. The 5 MHz system was not used for the closure. A strip chart of this trip (using the 200 MHz system) is shown in Figure 12.

The trip started at curbside at APL as shown in Figure 13; proceeded to the curbside at USNO as shown in Figure 14.

Figure 15 shows the USNO time transfer in diagram form. The resultant time difference measured between USNO and NR6 (GPS) reference is 4247.8 ns via the time transfer using the portable hydrogen maser. As a comparison, the GPS time transfer between NR6 (GPS) and USNO for the same day was 4249±4 ns. (The 4 ns error bar on our data is rather small compared to other facilities' GPS receivers. APL appears to be in a radio-quiet area and, in addition, the GPS receiver is driven by the hydrogen maser, a much more stable source than the cesiums normally used.)

V. PERFORMANCE OF APL TIME STANDARDS

The time keeping data from three NR continually tuned hydrogen masers is shown in Figure 16, relative to UTC (APL) for 250 days. The portable clock (ST1) time keeping data against NR6 is shown in Figure 17 for 250 days; the step in time resulted from adding a 46-foot cable to the portable clock to allow it to be moved to another room capable of accommodating the temperature controlled enclosure. The portable clock is continuously tuning against a selfcontained frequency modulation of the resonant cavity.

The APL master clock, the NBS master clock and the USNO master clock time keeping performances are compared against UTC (BIH) in Figure 18 via the GPS common view receiver systems. These plots show the relative stability as long term clocks of the portable clocks and the APL ensemble of hydrogen masers over a period before and after the time transfer experiments were performed.

VI. DISCUSSION OF RESULTS

It has been established that APL has a master clock system capable of keeping time with subnanosecond uncertainty over periods of days. The use of a hydrogen maser based clock as a portable clock has been demonstrated to provide subnanosecond performance over periods of hours in an environment available in an air-conditioned vehicle as evidenced from clock time closures.

Data taken via GPS receiver common monitoring over periods of months has provided data relating the performance of the APL master clock relative to precision master clocks at USNO and NBS, Boulder.

The hydrogen maser clock performance seems to have been degraded by a factor of 3 in the vehicle environment from the performance in the laboratory environment. Greater care in the control of temperature and vehicle accelerations should reduce the moving clock degradation factor significantly. In addition, a recently installed external power cable at APL will permit longer periods of clock stabilization and monitoring before and after a trip without having to rely on the van generator.

Future activities, more demanding on the maser clock performance, are planned. An additional time comparison between APL and USNO is planned. A new road test will also be performed in which longer monitoring and improved temperature control is expected.

Better control of these factors is considered essential in order to reach the performance needed for the maser's role in a forthcoming relativistic light propagation experiment in preparation at the University of Maryland. The optical link to be used in this experiment was described in a previous PTTI paper[6].

ACKNOWLEDGEMENTS

REFERENCES

1. L. J. Rueger, "Characteristics of the NASA Research Hydrogen Maser," Journal of the Institution of Electronics and Telecommunication Engineers, Vol. 27, No. 11, 1981, pp. 493-500.

2. L. J. Rueger and M. C. Chiu, "Development of Precision Time and Frequency Systems and Devices at APL," Johns Hopkins APL Technical Digest, Vol. 6, No. 1, pp. 75-84.

3. L. J. Rueger and M. C. Chiu, "Long-Term Performance of The Johns Hopkins Built Hydrogen Maser," IEEE Trans. on Instrumentation and Measurement, Vol. IM-36, No. 2, June 1987, pp. 594-595.

4. A. G. Bates, M. T. Boies, M. C. Chiu, R. Kunski, and J. J. Suter, "Precision Time and Frequency Sources and Systems Research and Development at The Johns Hopkins University Applied Physics Laboratory," Proc. of the Eighteenth Annual Precise Time and Time Interval Applications and Planning Meeting, December 1986, pp. 55-70.

5. H. E. Peters and P. J. Washburn, "Atomic Hydrogen Maser Actions Oscillator Cavity and Bulb Design Optimization," Proc. of the Sixteenth Annual Precise Time and Time Interval Applications and Planning Meeting, December 1984, pp. 313-336.

6. C. O. Alley, J. D. Rayner, C. A. Steggerda, J. V. Mullendore, L. Small and S. Wagner, "Time Transfer Between the Goddard Optical Research Facility and the United States Naval Observatory Using 100 Picosecond Laser Pulses," Proc. of the Fourteenth Annual Precise Time and Time Interval Applications and Planning Meeting, December 1982, pp. 243-267.

LIST OF FIGURES

Figure 1. APL Truck used for Portable Clock Experiments
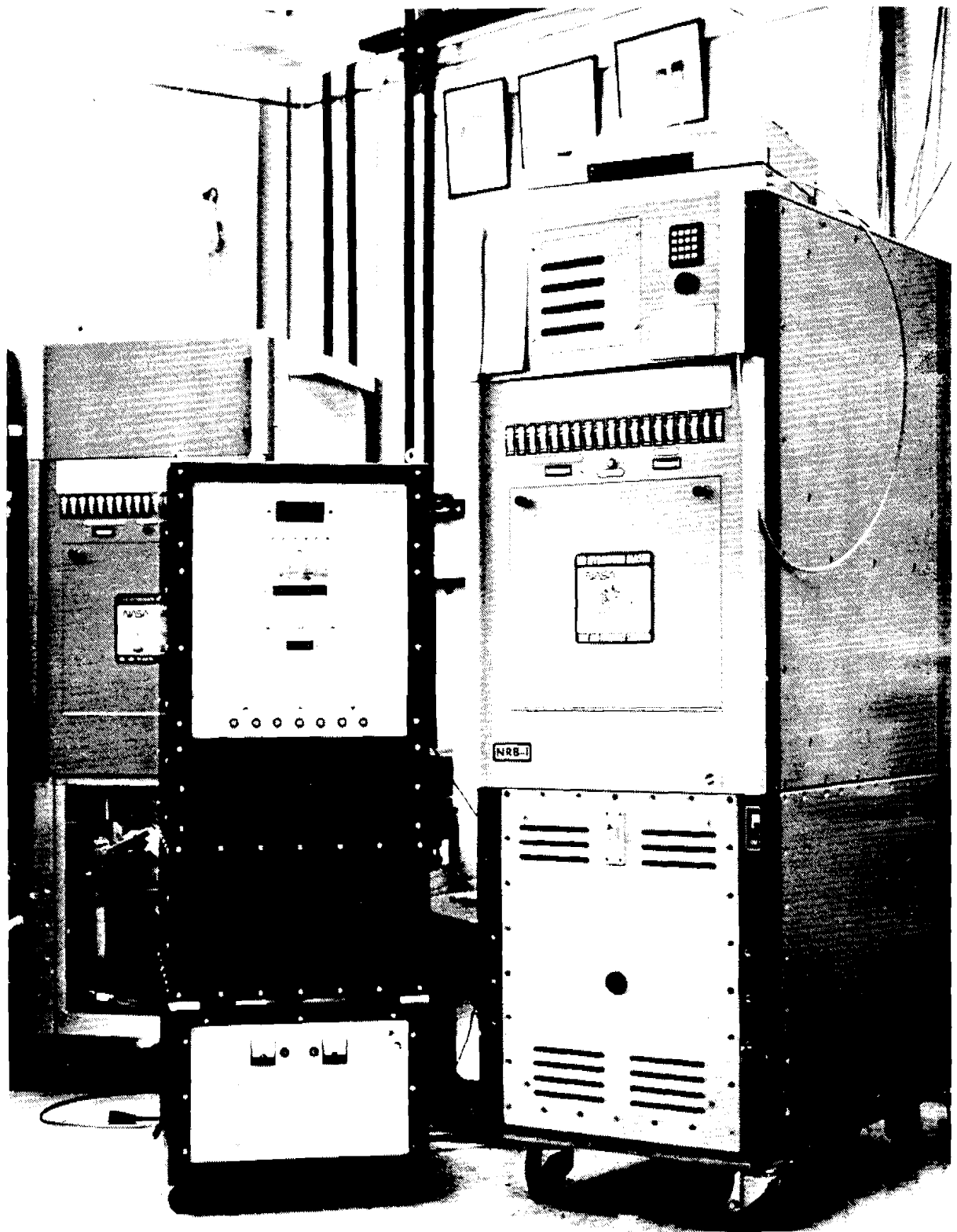
Figure 2. ST-1 Maser (left) and NR MASER

Figure 3. ST-1 Maser Short Range Stability for 1, 2 and 3 Hour Intervals

356
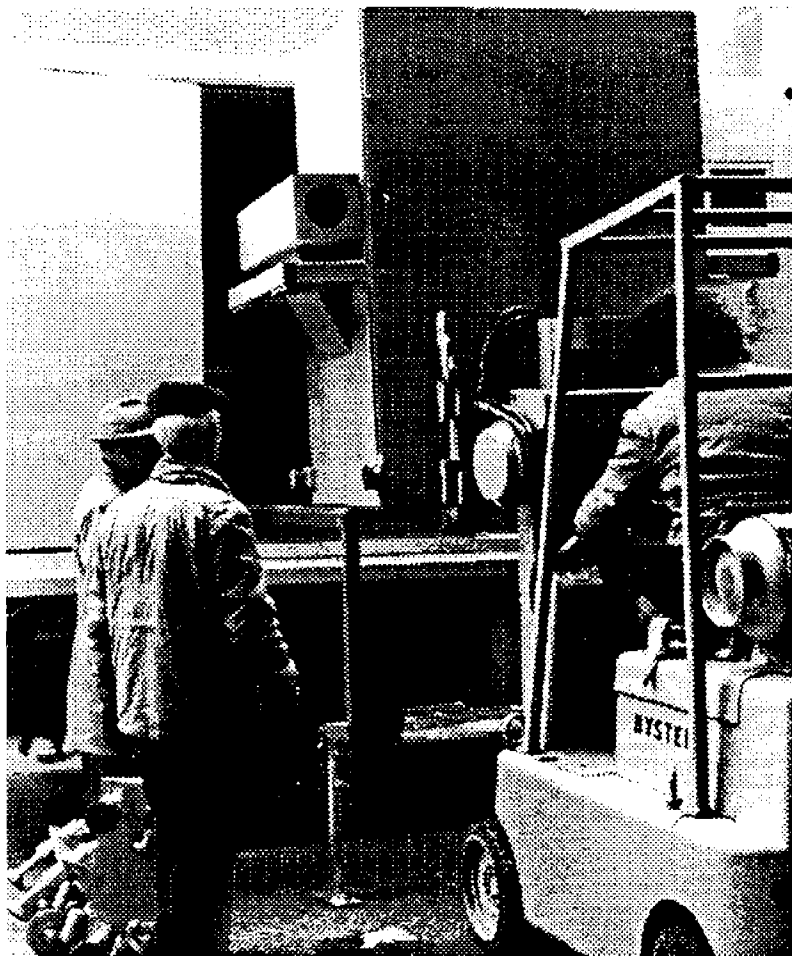
Figure 4. Clock Enclosure being loaded into APL Truck
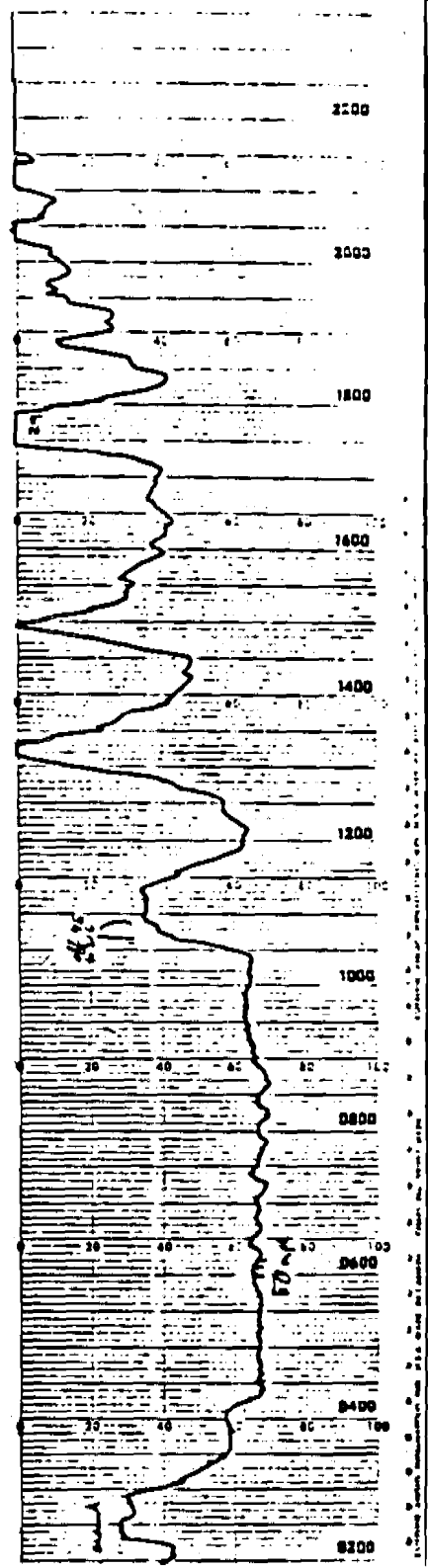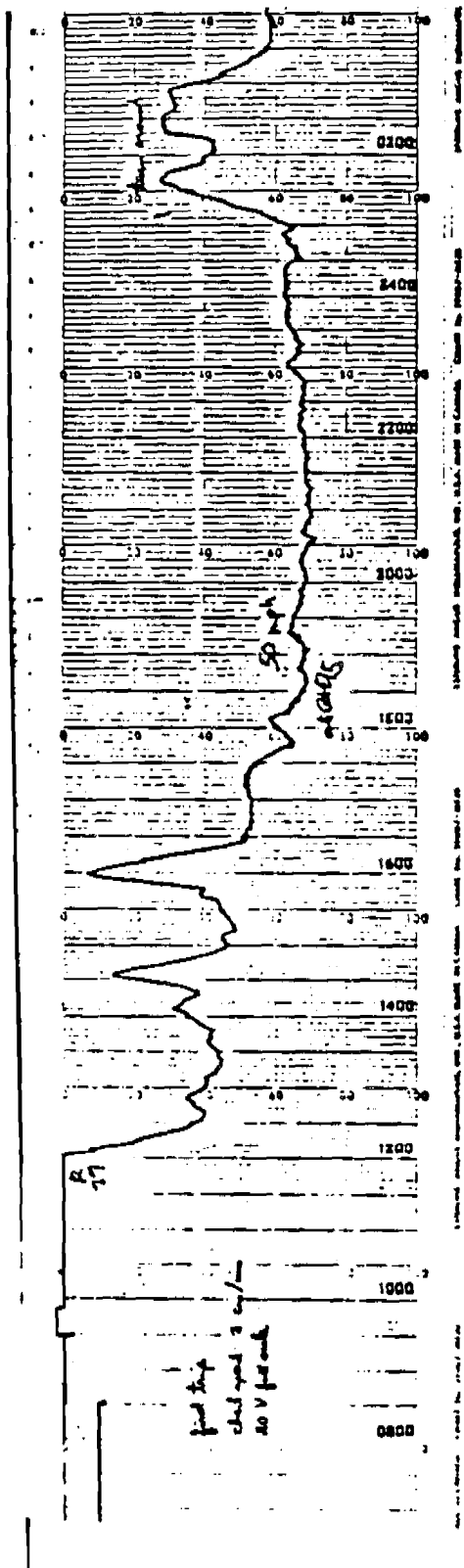
Figure 5. SAMPLE Record of Velocity for Portable Clock Experiment (Trip 1)

358
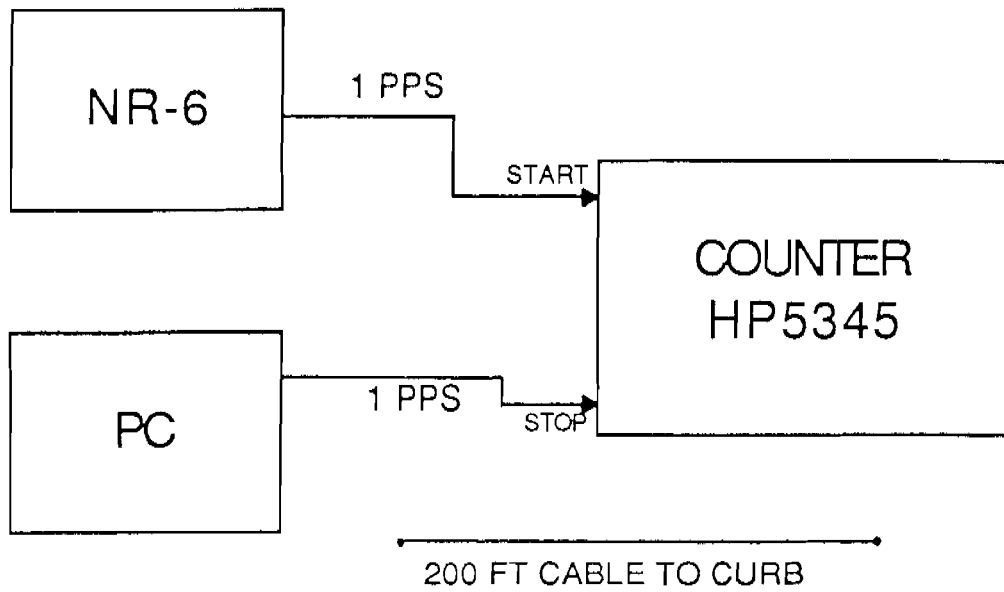
A) MEASUREMENT CONFIGURATION
AT APL
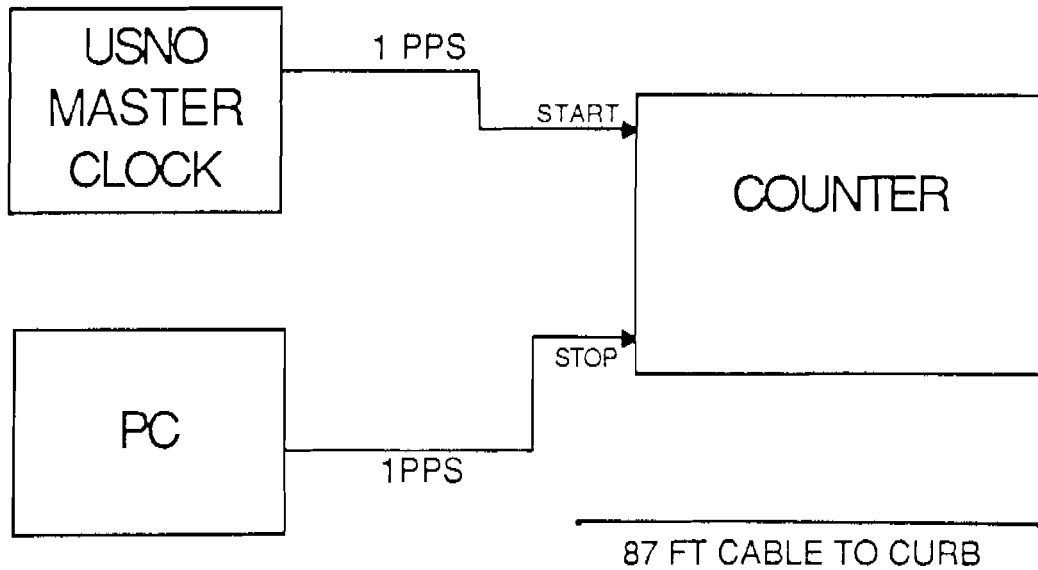
B) MEASUREMENT CONFIGURATION
AT USNO

Figure 6. 1 PPS Measurement System
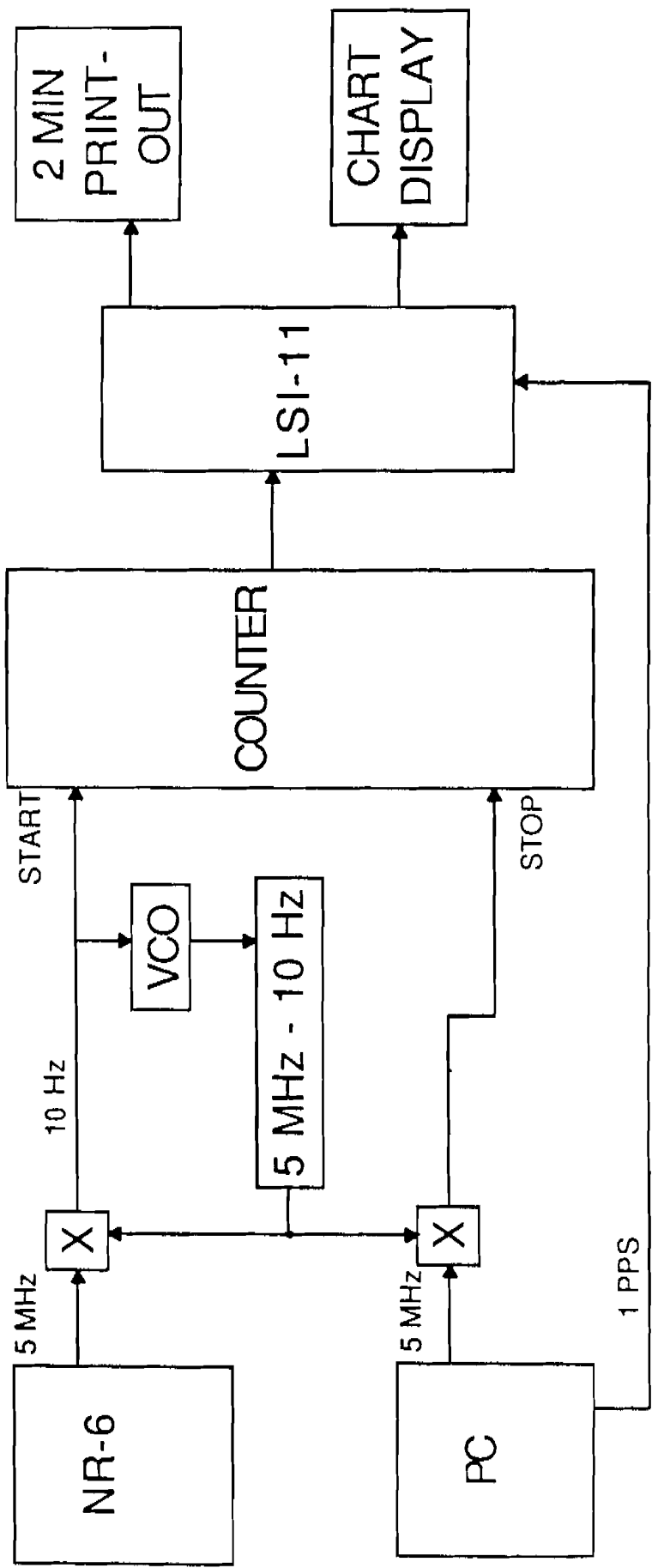
Figure 7. Measurement System Based on 5 MHz Signals

360
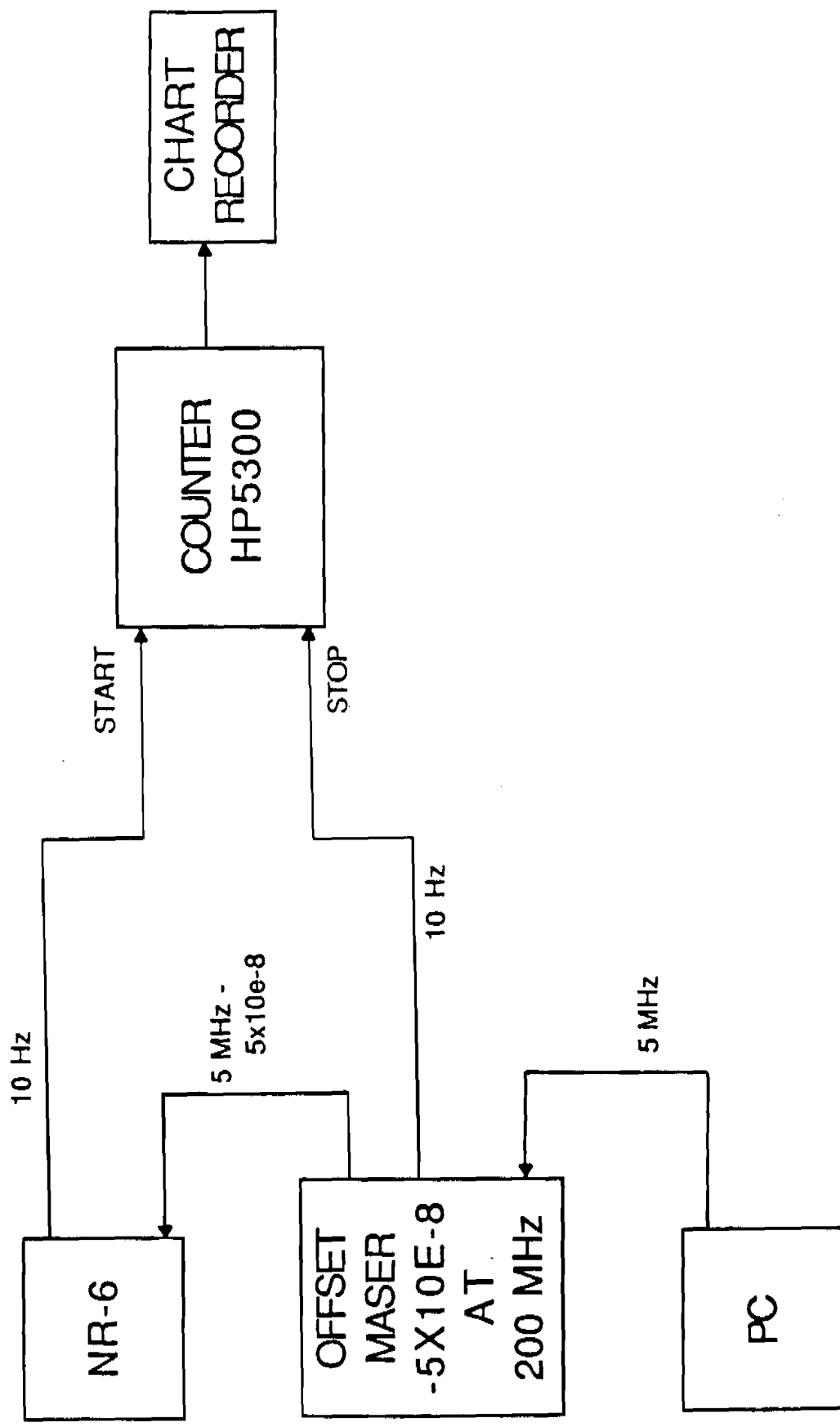
Figure 8. Measurement System Based on 200 MHz Signals
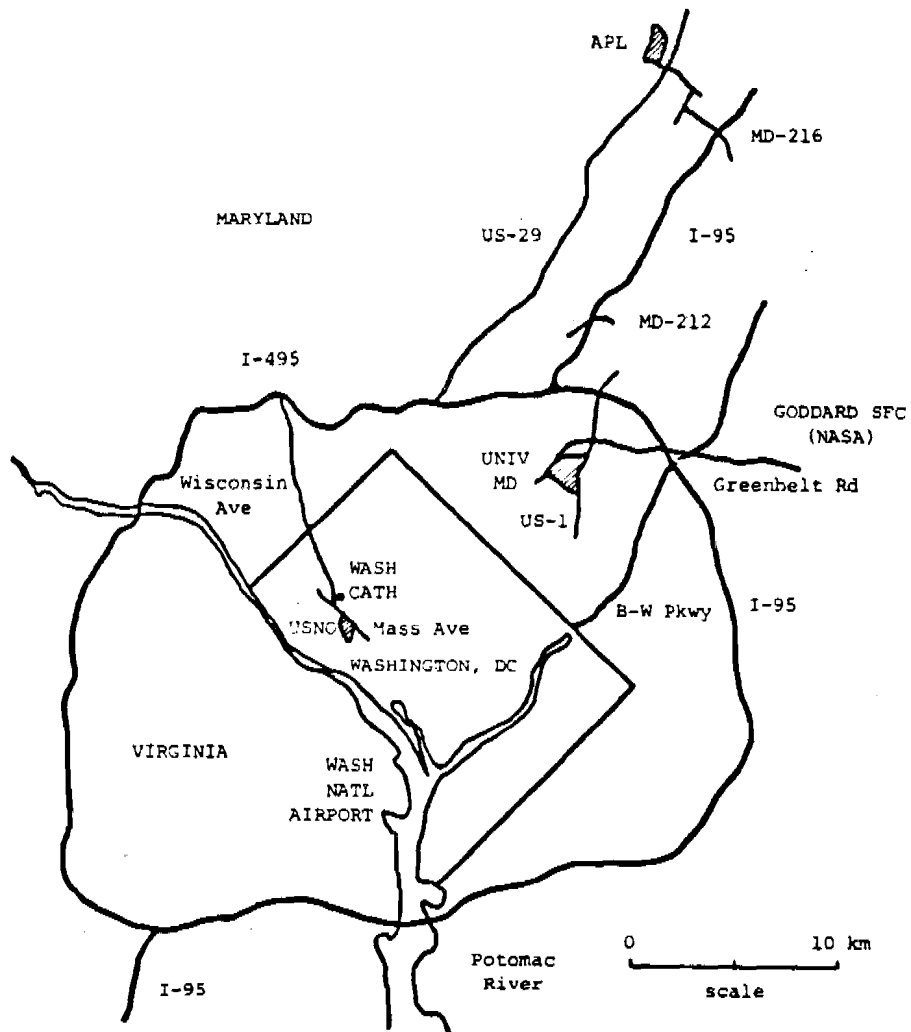
Figure 9. Routes for Portable Clock Experiments

reduced to it speed

1.55×10^{-14}

$\Delta S = 2.4 \times 10^{-14}$

-3.17×10^{-14}

Recount

deviant for trip
12:20 PM

at cwt

29 July 87

|← 1 ns →|
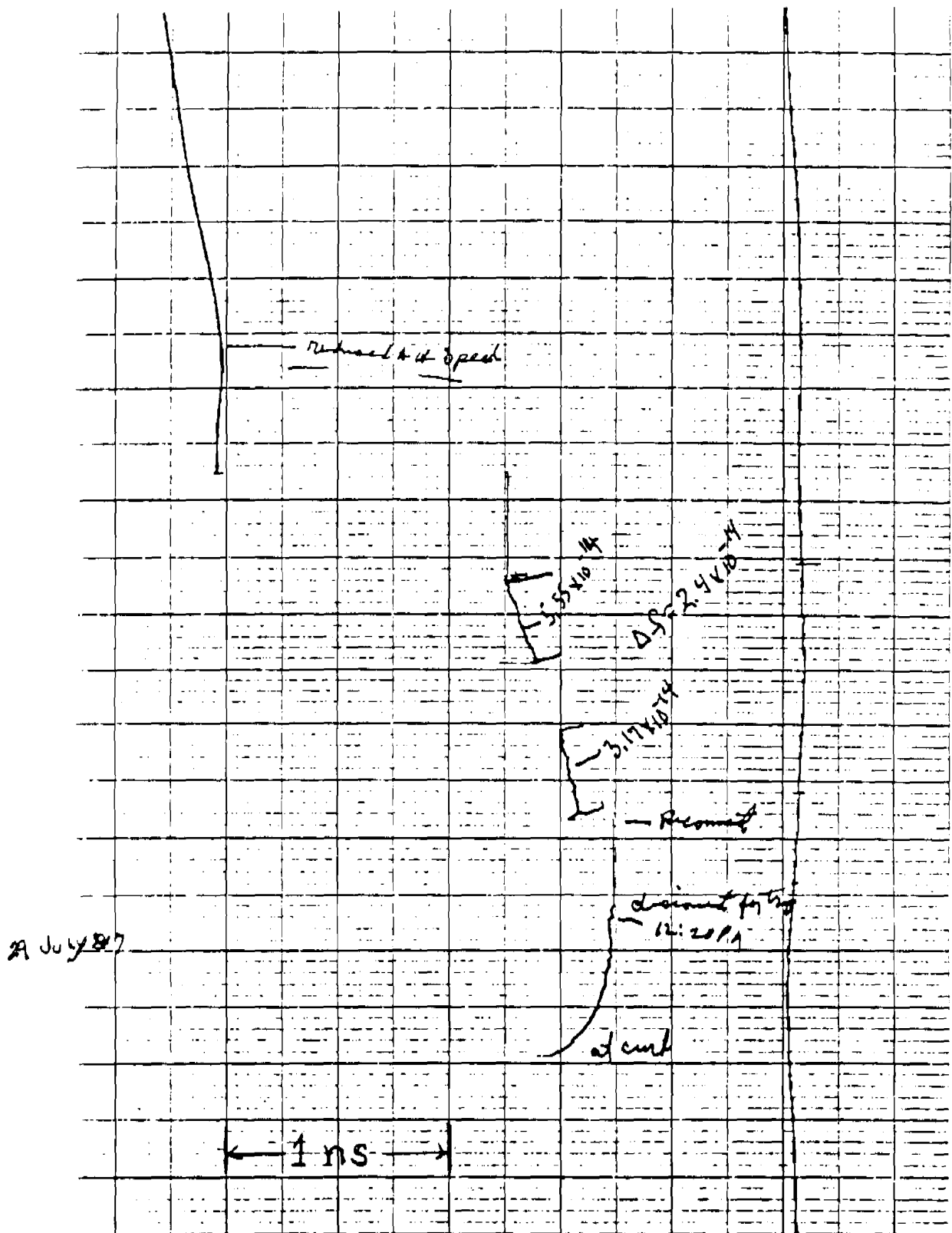
Figure 10. Strip Chart from 200 MHz Measurement System for Trips 1 and 2
(July 29, 1987)

363
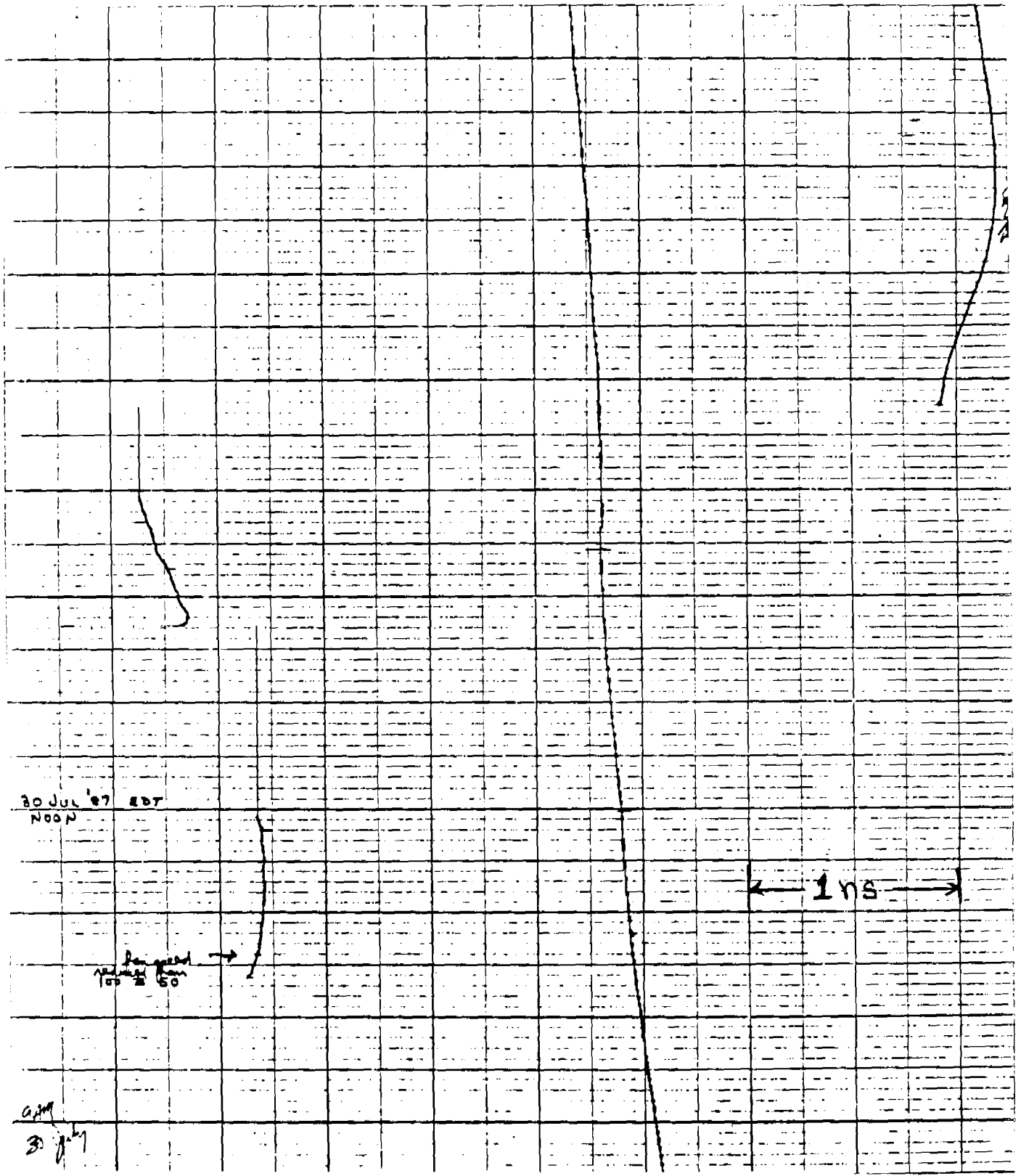
Figure 11. Strip Chart from 200 MHz Measurement System for Trip 3 (July 30, 1987)
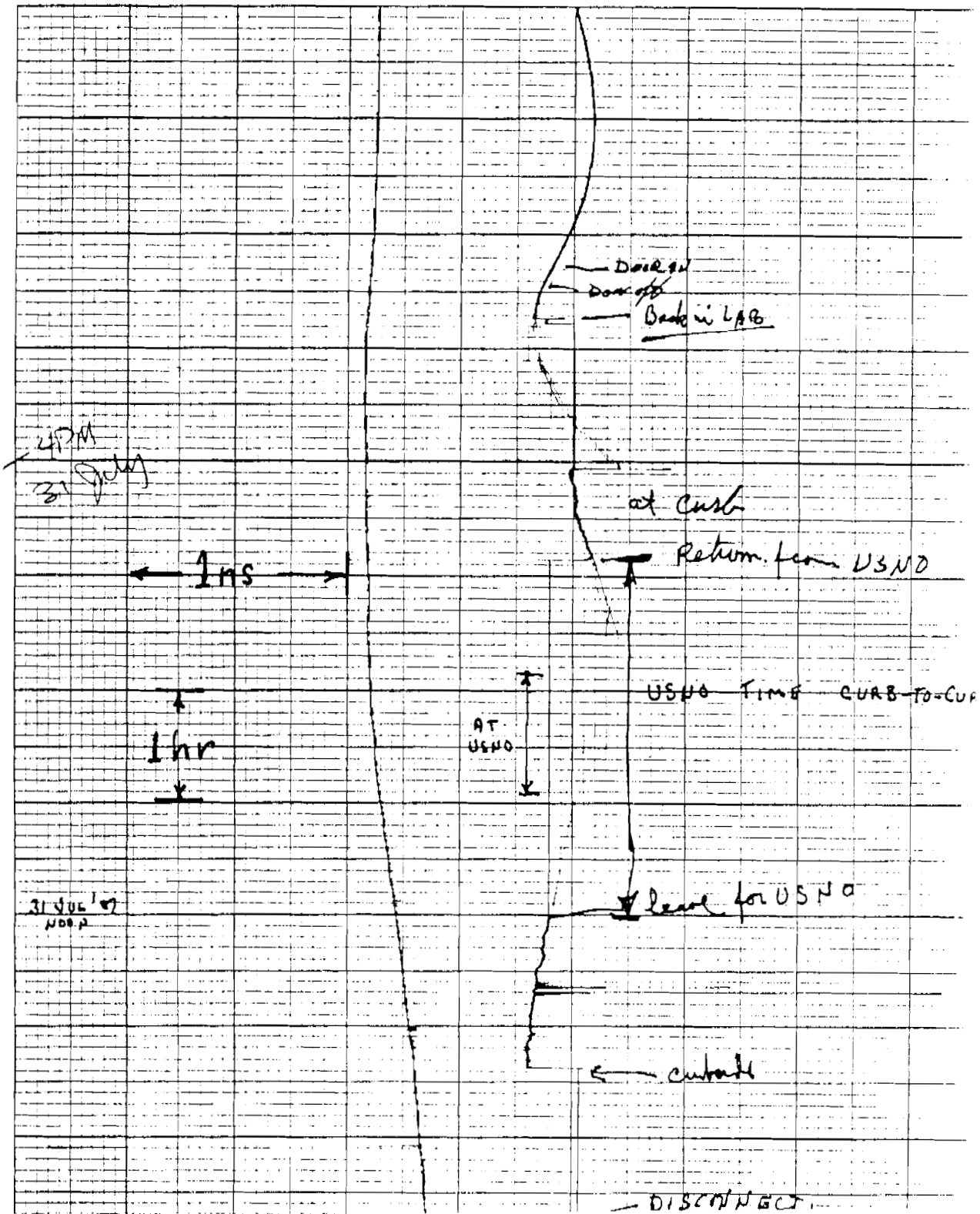
Figure 12. Strip Chart from 200 MHz Measurement System for Trip 4
(July 31, 1987)
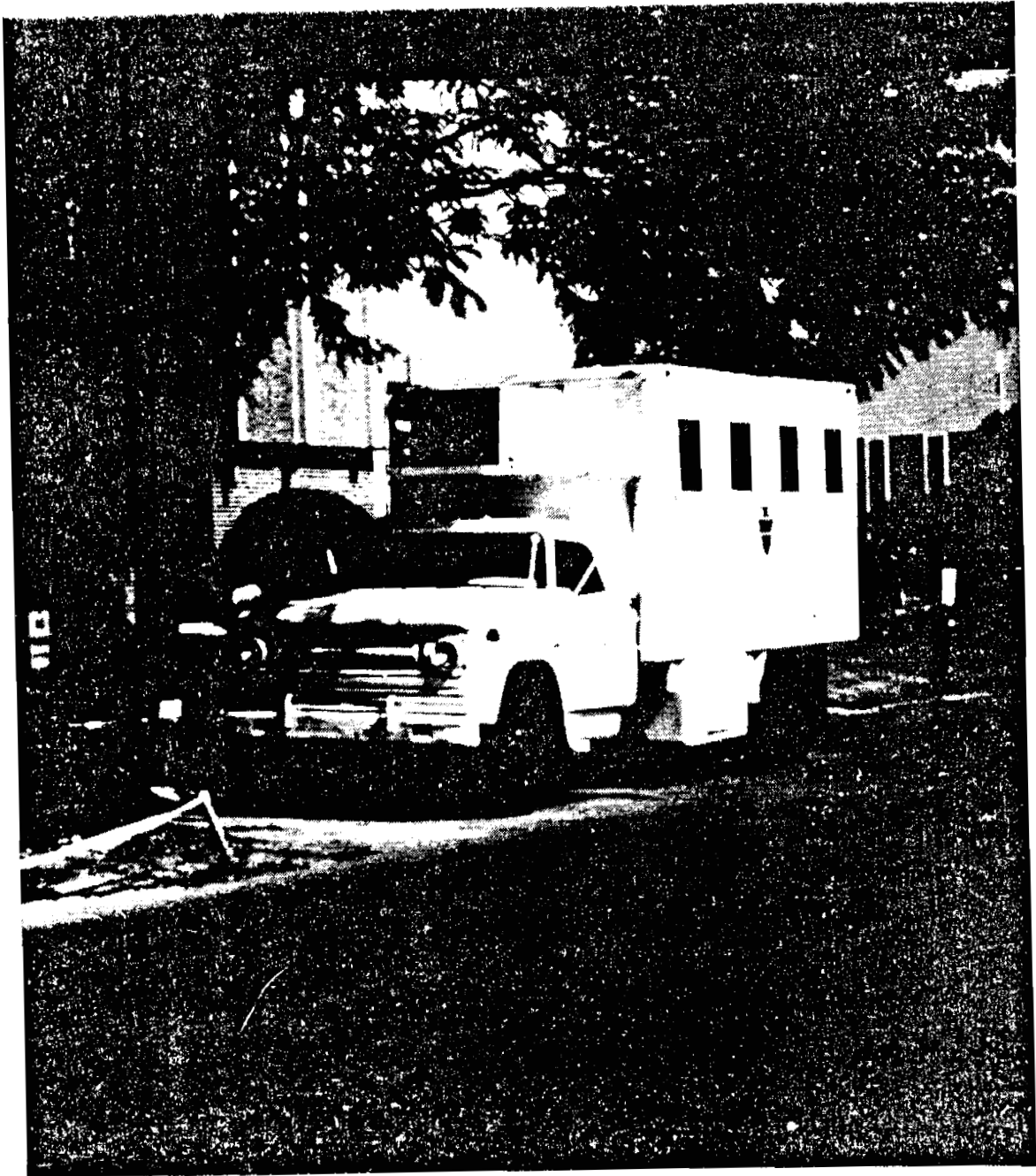
Figure 13. Curbside at APL
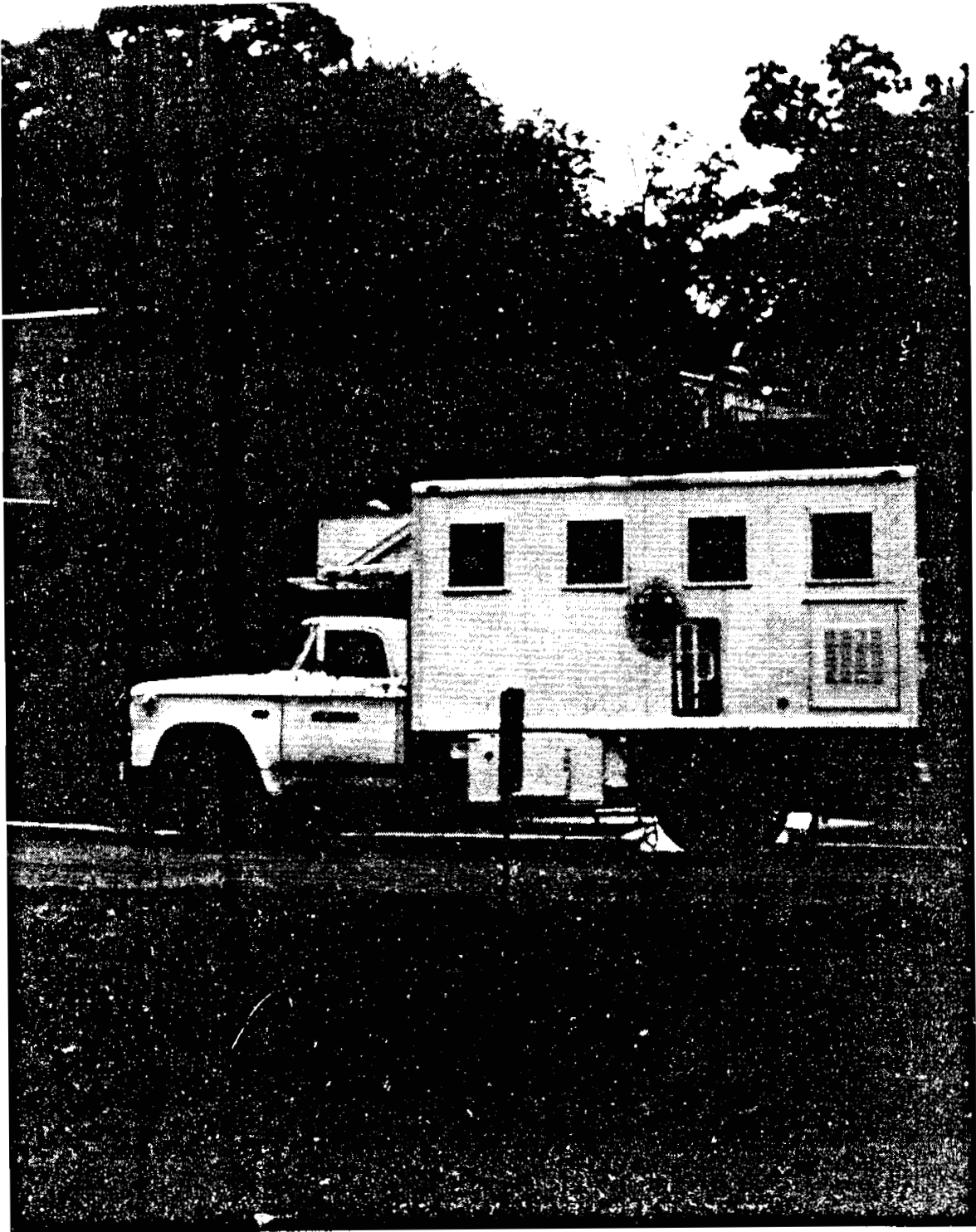
Figure 14. Curbside at USNO

CURBSIDE
MEASUREMENT
AT USNO

PC(curb)   PC   USNO

cable
├─130─┼──────── 4172.2 ────────┤
                USNO-PC

├───────────── 4302.2 ─────────────┤

CURBSIDE
MEASUREMENT
AT APL

MEAS.
SYS.
REF. PT

CABLE   PC   USNO

CURB CABLE
9 ├──── 298.8 ────┤───────── 4172.2 ─────────┤

├───── 239.7 ─────┼──────── 4240.3 ─────────┤
                  NR6   USNO-NR6

MEASUREMENTS
RELATIVE TO
APL GPS
RECEIVER

NR6
(GPS)

NR6
CABLE   USNO

7.5 ├─────────── 4240.3 ───────────┤

126 ├────────── 4247.8 ──────────┤
UTC(APL)   USNO-NR6(GPS)
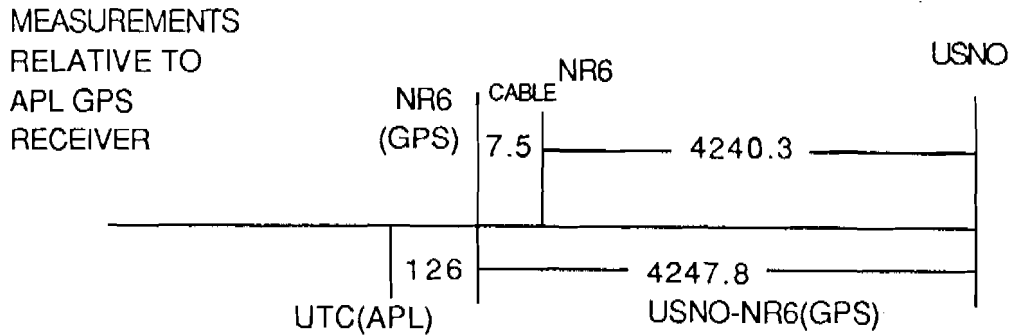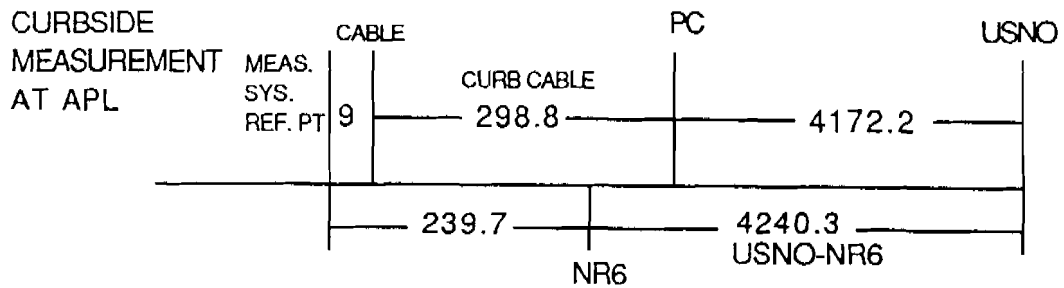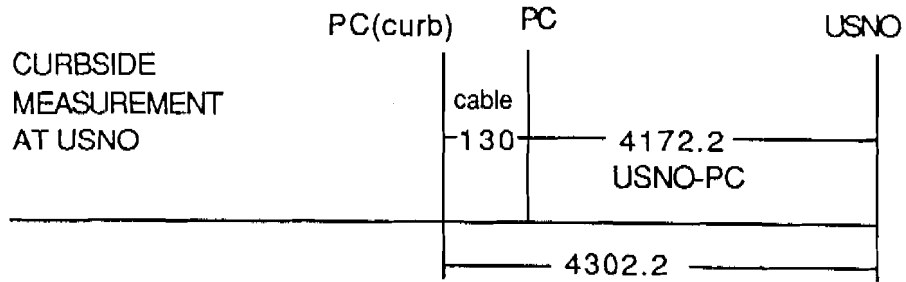
NOTE:
ALL MEASUREMENTS GIVEN IN NANOSECONDS
USNO-NR6 VIA GPS RECEIVERS = 4249 $\pm$ 4 NANOSECONDS

Figure 15. Measured Time Differences between Standards for
            31 July 1987 Time Transfer
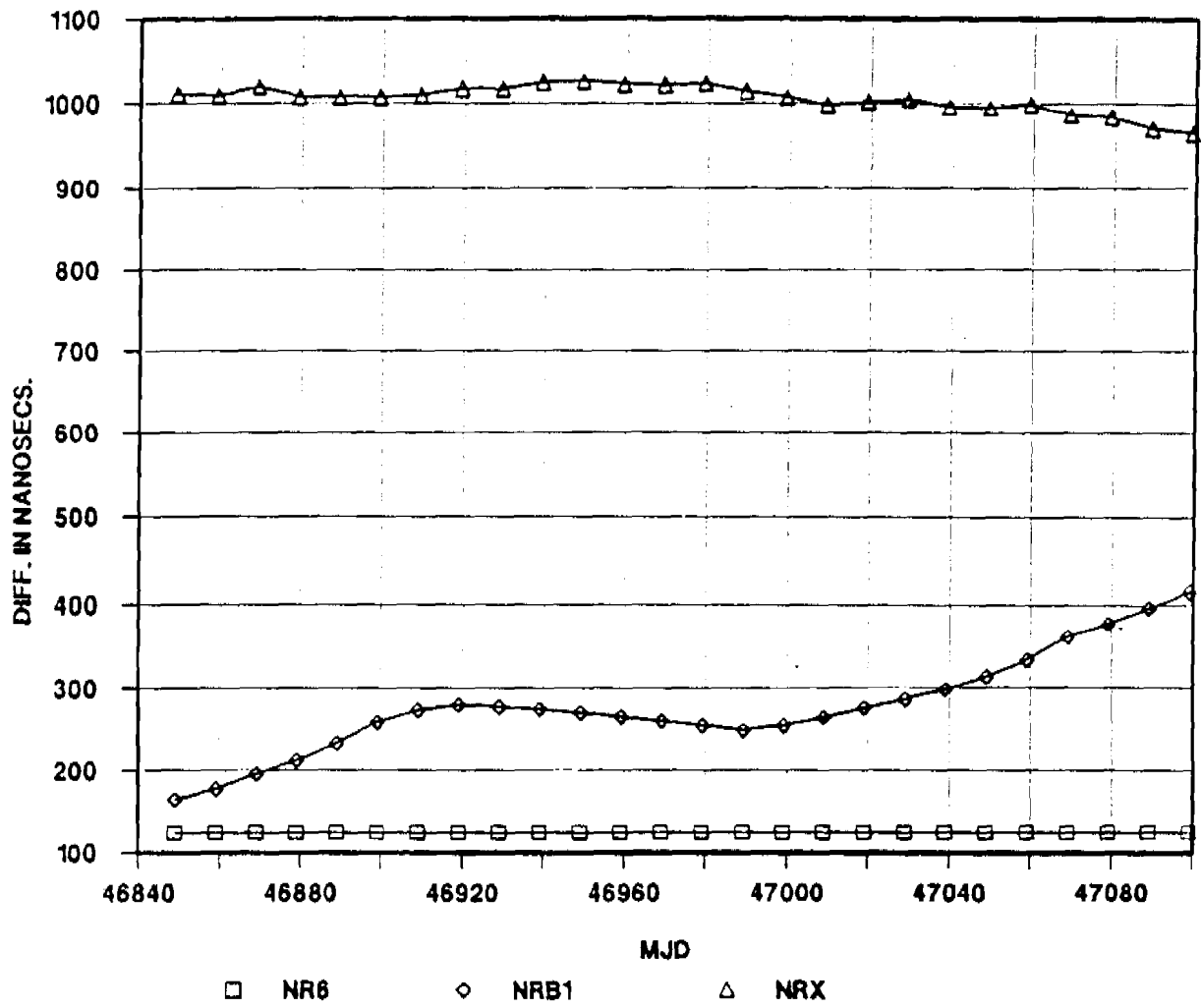
Figure 16. UTC (APL) - APL Masers
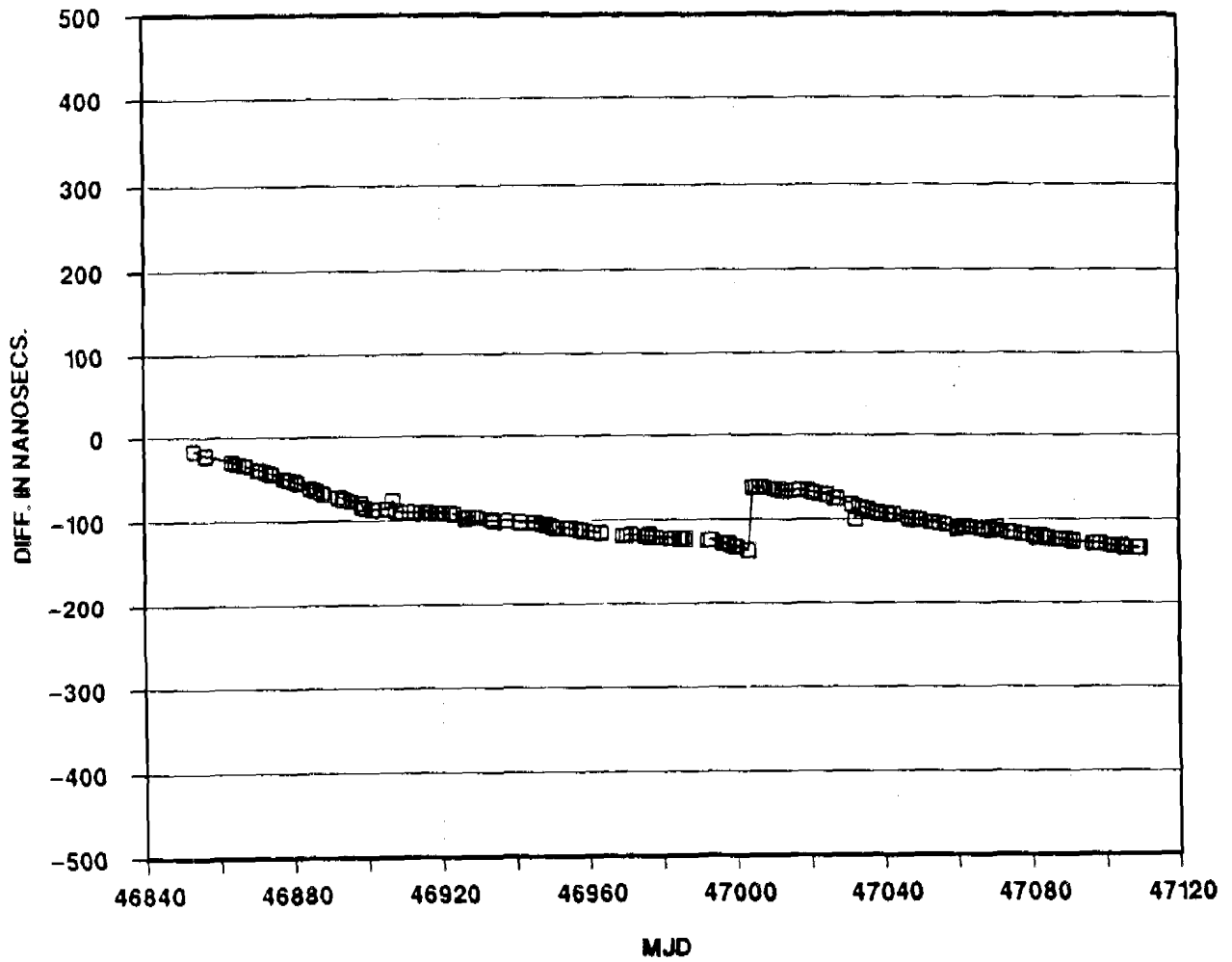
Figure 17. UTC (APL) - ST1
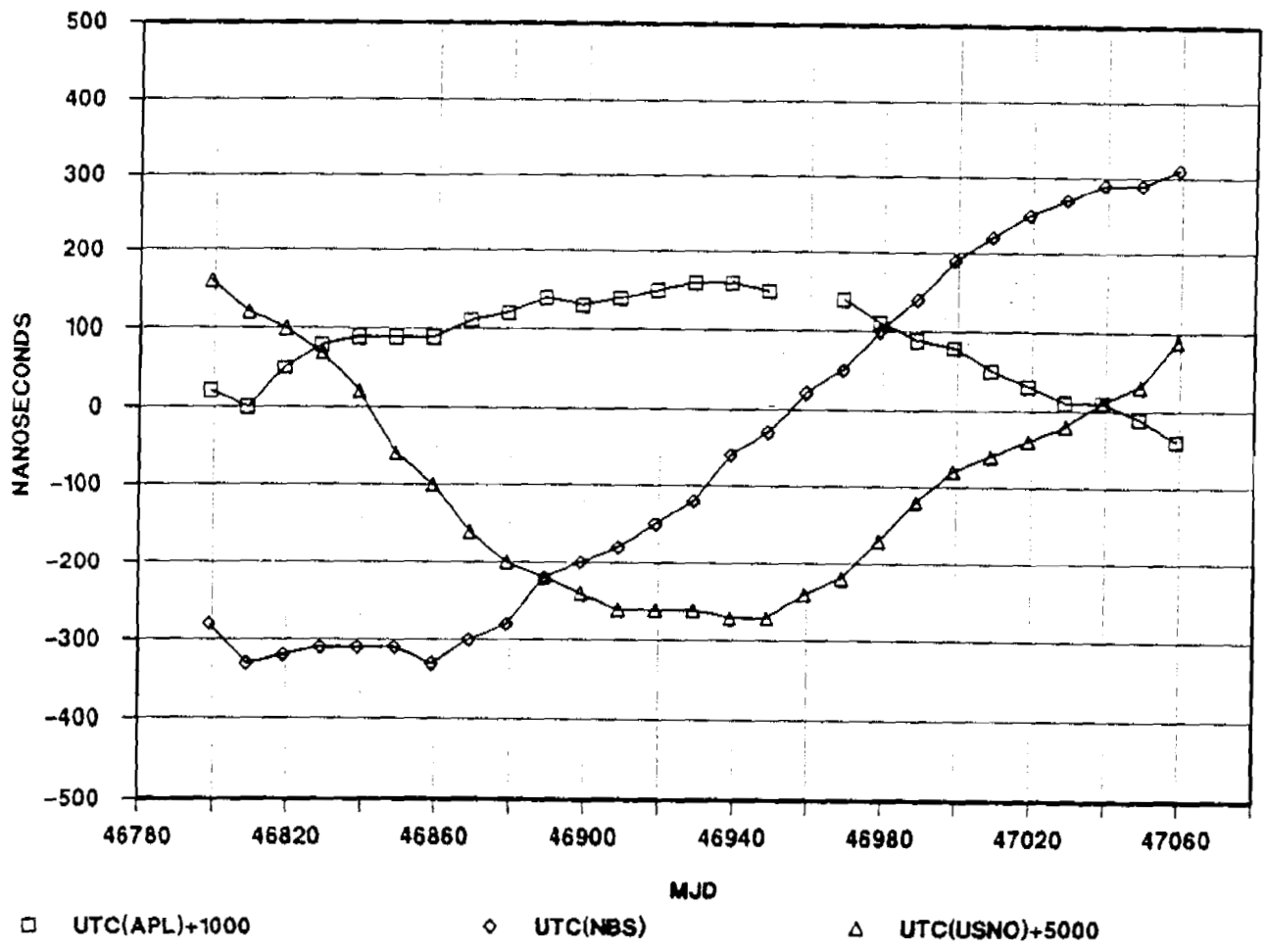
Figure 18. UTC (BIH) - UTC (i)

A STUDY OF LONG–TERM STABILITY OF ATOMIC CLOCKS

David W. Allan
National Bureau of Standards
Time and Frequency Division
325 Broadway
Boulder, Colorado 80303

ABSTRACT

The importance of long–term frequency stability has increased significantly in recent years because of the discovery of the millisecond pulsar, PSR 1937+21. In addition, long–term stability is extremely useful not only in evaluating primary frequency standards and the performance of national timing centers, but also in addressing questions regarding autonomy for the Global Positioning System (GPS) and syntonization for Jet Propulsion Laboratory's (JPL) Deep Space Tracking Network.

Over the last year, NBS has carried out several studies addressing questions regarding the long–term frequency stability of different kinds of atomic clocks as well as of principal timing centers. These analyses cover commercial and primary cesium–beam frequency standards, active hydrogen maser frequency standards and the new commercial mercury–ion frequency standards at United States Naval Observatory (USNO).

The support and cooperation of the timing centers involved have, along with the GPS common–view measurement technique, made these analyses possible. Fortunately, the measurement noise was significantly less than the clock noise for the long–term stability regions studied. Fractional frequency stabilities, $\sigma_y(\tau)$, of parts in 10^{14} down to parts in 10^{15} were observed for various of these standards. It is believed that frequency stabilities on the order of a part in 10^{15} will be necessary to measure the effects of gravity waves on frequency stability between millisecond pulsars and atomic clocks on or near the earth.

INTRODUCTION

The primary reasons for improved long–term stability in atomic clocks have been the study of millisecond pulsars[1,2], autonomy questions for GPS, maintaining syntonization for the JPL Deep Space Network and long term stability performance of new clocks at the primary timing centers throughout the world. As needs have arisen for improved stability in atomic time scales, several laboratories have responded with very strong efforts in producing new standards[3–8]. Some analysis techniques to ascertain current performance of the best operating clocks in the world have also been developed. Fortunately, the GPS common–view time–difference and frequency–difference measurement technique has allowed us to analyze long–term clock time deviations at state–of–the–art levels.

One analysis tool used was a statistical cross–correlation technique in the time domain in order to ascertain correlations at different integration times[1]. This tool was developed to study long term correlations in the presence of nonstationary processes in the clock deviations. The next tool was to employ the NBS algorithm for generating the time scale NBS(AT1) from the ensemble of clocks at NBS[9]. NBS(AT1) plus an equation generates UTC(NBS); the latter being the official time from the National Bureau of Standards. This same algorithm was used on the international set of clocks available through GPS common–view measurements. Each laboratory timing center's output was treated as an

independent clock and then combined with all the others in an optimum minimum squared error sense according to the NBS algorithm's design. The hope is to generate a "world's best" clock, which in turn could be used to analyze each of the constituent members and then better understand the long term stability performance of each. The next tool used was an N-cornered hat statistical approach under the assumption of independence of the member clocks[10]. In this way we can sort out the performance of each member of a set of N clocks in terms of its statistical characteristics. Last, a second-difference drift estimator was used to study long term frequency drift correlations among some of the clocks involved[10,11].

Figure 1 shows a plot of the fractional frequency stability between the millisecond pulsar (PSR 1937+21) and UTC(NBS), as well as the stability estimate of NBS(AT1) versus the "world's best" clock estimate. Figure 1 shows that with more integration time the millisecond pulsar might show better performance than the best clocks in the world. As indicated in the plot the possibility of measuring gravity waves at a few parts in 10^{15} at integration times of the order of a year is by itself a significant motivator.

GENERATION OF THE "WORLD'S BEST" CLOCK AND COMPARISON OF THE PERFORMANCE OF THE INTERNATIONAL TIMING CENTERS

The advantage of post-analysis is that we can more easily discern outliers and abnormal performance in the member clocks. Following this post analysis and removal of outliers and abnormal behavior, we can then employ optimal statistical processing techniques. These processing techniques can approach the ideal once the nonstochastic behavior has been filtered off. In contrast, the time from any timing center, including the generation of TAI has to be calculated or generated in near real time. In a real-time operation, subtle frequency steps and annual variations cannot readily be dealt with because of their low frequency character. Often they are best observed in post-analysis.

A period of time commensurate with the installation of the new measurement system for the millisecond pulsar (PSR1937+21) at Arecibo, Puerto Rico was picked. The time was a 1110 day period from MJD 45769 to MJD 46879. The data not available on the NBS computer file were accrued from the Princeton University computer file or were extracted from the BIH annual report. The UTC scales were used from the various timing centers as they were more readily available. Since some of the UTC scales are steered, we tried to remove the steering corrections so that the contributing scales would be independent. The post-analysis was performed removing known frequency steps in the time scales and outliers that would contaminate the stochastic analysis.

An N-cornered hat analysis between the times generated by the various timing centers was first performed in order to get a first order estimate of the 10 day stability and the longer term stability of each of the outputs from the timing centers. Preliminary parameters were then chosen for the optimization routine for the NBS algorithm to include each timing center's output as a clock member. One of the features of the NBS algorithm is that it is an adaptive filter so that as a clock improves or degrades with time the filtered estimate will adapt to the value commensurate with the clock's performance. The time constant of this filter for this experiment was set at three months. Once the parameters have been set and the clocks processed through the NBS algorithm, the "world's best" estimate could then be used to better ascertain the performance of each member clock, and the parameters could be appropriately fine tuned to reduce the minimum squared error of the estimate of the ensemble as well as of each individual member. Figures 2a and 2b through 14a and 14b list a modified $\sigma_y(\tau)$ fractional frequency stability plot and a time residual plot with a mean frequency and a mean time removed for each of the contributing timing centers. The abscissas and ordinates have been kept the same in the figures for convenience of comparison.

The contributing timing centers were: Applied Physics Laboratory at Johns Hopkins University, Laurel, MD; Commonwealth Scientific and Industrial Research Organization, Australia; Istituto Elettrotecnico Nazionale, Torino, Italy; National Bureau of Standards, Boulder, CO; National Physical Laboratory, Teddington, England; National Research Council in Ottawa, Canada; Paris Observatory, Paris, France; Physikalisch–Technische Bundesantalt, Braunschweig, Germany; Radio Research Laboratory Tokyo, Japan; and Tokyo Astronomical Observatory, Tokyo, Japan; Technische Universität Gras, Gras, Austria; US Naval Observatory, Washington, DC; and Van Swinden Laboratory, Delft, Netherlands.

Following are some highlights to note from the several figures. Though there was a limited set of data available on the hydrogen maser at APL, the stability at integration times of a few months is very impressive. The NBS algorithm generates from its own ensemble a scale called AT1, which is neither synchronized nor syntonized with any other scale. NBS(AT1) is optimized for frequency stability. Because NBS(AT1) had the largest weight among the set of clocks used in this "world's best" estimate, we removed it from the ensemble and looked at it independently against all the other optimally weighted clocks in order to see whether a similar stability performance was still obtained. This independent analysis confirmed the stability plots shown in Figures 5a and 5b.

Most of the timing centers have clock output stabilities at levels of a few parts in 10^{14} for integration times from 10 days out to the order of a year. Figures 9a and 9b for PTB show exceedingly good stability from year to year, though there may be inadequate confidence of the estimate to confirm this. This stability may be because UTC(PTB) is steered with their primary cesium clock. Also annual variations appear in the time deviations of the PTB output. The excellent performance of the TUG clock may be because this single commercial clock is temperature controlled, humidity controlled and voltage controlled. The apparent quadratic behavior observed in the residuals of the USNO clock is of concern because most of these clocks are high performance cesium beam clocks. We are led to ask whether there is a systematic frequency drift in a particular production line series. On the other hand, the month–to–month stability is very good.

A STUDY OF THE ANNUAL VARIATIONS

For the most stringent of timing users, B. Guinot at the International Bureau of Weights and Measures (BIPM) has generated a scale called Terrestrial Time BIPM TT(BIPM). Figure 15 shows the fractional frequency differences between TT(BIPM) and International Atomic Time (TAI) over the last several years. The noticeable frequency step is associated with the 1972 adjustment in the SI second used for TAI to conform with the NBS, NRC and PTB primary frequency standards. Annual variations are apparent between these two scales. Since PTB Cs 1 is believed to be one of the best primary clocks in the world, its weight in generating TT(BIPM) is quite high, and the annual term shown earlier in the PTB plot in Figures 9a and 9b corresponds with the annual variations shown in Figure 15. We are led to the questions: are these annual variations in all of the clocks in the world ensemble, moving up and down together on an annual basis, or are they in PTB Cs 1, or a combination of both? At the few parts in 10^{14} level it is very difficult to ascertain which conclusion is the most nearly correct.

In an effort to obtain an independent estimate regarding this problem, the data from the millisecond pulsar were analyzed. The pulsar data have much larger variations from week to week and month to month — primarily due to the 4 k parsec (13,000 light–years) path of the signal. The variations can be fairly well characterized as a white noise phase modulation (PM) process at about the 300 ns level. Because such noise integrates as $\tau^{-3/2}$ on a mod $\sigma_y(\tau)$ plot, the long term variations can be meaningful. PSR1937+21 is plotted against PTB Cs 1 in Figure 16. Also plotted in Figure 16 are the time difference residuals between PTB Cs 1 and NBS(AT1). Visually, correlations are apparent even though masked

377

somewhat by the pulsar data noise.

To further study the significance of these annual variations we incorporated a cross–correlation analysis tool[1]. The correlations seemed statistically significant for integration times longer than several months. From this study, the annual variations seem to be primarily in PTB Cs 1; however, this is inconclusive because in the generation of the pulsar data, an annual term had to be removed in conjunction with the determination of the ephemeris for the earth as it orbits the sun. Further study is needed before a definite conclusion can be obtained.

STUDY OF THE COMMERCIAL MERCURY ION STANDARD'S FREQUENCY STABILITIES

Three independent clocks were chosen to study the stability of the two commercial mercury–ion standards located at USNO [6]. Data on the unit called No. 2 covered about a 1 year period and the data on No. 3 covered the last one–half year period. As can be seen in the fractional frequency stability plots shown in Figures 17a, 18a and 19a, there are missing data and some abnormal behavior during the first several weeks of the data. This first part was segmented off for the statistical analysis period, which was from 19 December 1986 to 14 November 1987. The stabilities plotted in Figures 17b, 18b and 19b are for the segmented period.

Assuming independence, the four clocks (unsteered UTC(USNO), NBS(AT1), the APL hydrogen maser and the mercury ion No. 2) were compared in an N–cornered hat analysis. That data are plotted in Figure 20.

For integration times of one, two and four days the GPS common–view noise contaminated the data for APL and NBS. It appears that the NBS and USNO outputs have a flicker frequency modulation (FM) like performance at about a part in 10^{14} over this 11 month data set. The long term frequency drift in the APL hydrogen maser is apparent. The excellent stability performance of the mercury ion standard — as the winner in this 4–cornered hat analysis for integration times of a week to a month — is also apparent. The one, two and four day stability values plotted may be pessimistic, as they are contaminated with measurement noise. However, there appears to be some stability degeneration for integration times of the order of a few months and longer. For completeness the other pair–wise members of the 4–cornered hat are shown in Figures 21a and b through 23a and b.

Over the last one–half year we studied the stability difference between the two commercial mercury–ion standards No. 2 and No. 3. Figures 24a and b show a most outstanding performance of these two standards. Since the stability plotted in Figure 24 is inconsistent with that plotted in Figure 20, we asked whether No. 1 and No. 2 were correlated. To study whether these two clocks have long term correlations and to be able to define a cross–correlation coefficient as a function of τ called $\rho(\tau)$ we proceeded as follows[10]. Given fractional frequency differences:

$$y_1 = \text{clock i} - \text{clock j and}$$

$$y_2 = \text{clock k} - \text{clock l,}$$

we can compute a variance of the difference

$$\sigma^2_{y_1-y_2}(\tau) = \sigma^2_{y_1}(\tau) - 2\sigma_{y_1 y_2}(\tau) + \sigma^2_{y_2}(\tau)$$

We construct:

$$\rho(\tau) = \frac{\sigma_{y_1 y_2}(\tau)}{\sigma_{y_1}(\tau) \cdot \sigma_{y_2}(\tau)}.$$

At a given τ, if $\rho(\tau)$ approached +1 then we could conclude that there are correlations between i and k, or j and l, or -i and l, or -k and j. If $\rho(\tau)$ approached -1, then we could conclude that there are correlations between -i and k, or -j and l, or i and l, or k and j. This cross-correlation analysis was tested with simulated data and gave affirmative results to the above conclusions and to the ability to test in the presence of low frequency divergence processes such as flicker noise FM and random walk FM. Figure 25 would indicate that some of the long-term instabilities are in fact due to mercury-ion No. 2. Figure 26a and b would indicate that No. 2 and No. 3 are positively correlated for integration times of a few months. Using different references, Figures 27a and b lead us to the same conclusion as similarly do Figures 28a and b. All three independent clock pairs lead to the same conclusion that mercury-ion standards No. 2 and No. 3 appear to be long term correlated for integration times of a few months. Figure 29a would indicate no statistical correlation between the four clocks involved. On the other hand Figure 29b shows a definite positive cross-correlation; this is believed to be due to the fact that over the half year analyzed mercury-ion standard No. 2 and the APL maser had positive frequency drifts.

The following independent test of the hypotheses that the low frequency variations could be modelled by long-term correlations between the two mercury ion standards and frequency drifts between the APL maser and the mercury ion standards, was conducted. Frequency drifts were measured using a second difference estimator over the last half year with respect to NBS(AT1) UTC(USNO-unsteered) and the UTC(PTB) time scales. UTC(PTB) has as its reference the PTB primary Cs 1 standard. We observe a very high correlation in the frequency drift numbers measured with respect to the different laboratories (Figure 30). Within this small sample of three clocks, the drifts seem to be statistically significant — indicating, again, that in long term the two mercury ion standards appear to be correlated, and that the frequency drifts of the APL hydrogen maser and the ion standards are in the same direction.

The correlation mechanism is not yet understood and is being studied. Environmental perturbations due to temperature, temperature gradients and pressure are possible candidates. The very outstanding performance of these mercury ion standards gives great hope that if this problem can be identified and fixed, these standards will have a major contribution in the long-term stability analysis of the best frequency standards known.

CONCLUSIONS

The long term frequency stability of time scales has improved dramatically over the last few years. This study has revealed that additional long term frequency stability improvements may be possible if the cause of annual variations in clocks can be identified and fixed. Also, if frequency drift problems can be solved, and if cross-correlation problems through the environment can be identified and fixed, the next few years should show significant improvements in the performance of hydrogen masers and of mercury-ion frequency standards.

It is also apparent from this study that algorithms for combining clock readings can significantly impact the performance of a computed time scale. The NBS algorithm implemented seemed to have merit even where there were significant differences in statistical characteristics of the member clocks contributing to the ensemble.

who helped process a large amount of the data.

REFERENCES

[1] D.W. Allan, Millisecond Pulsar Rivals Best Atomic Clock Stability, Proceedings of the 41st Annual Symposium on Frequency Control, May 27–29 1987, pp. 2–11.

[2] L.A. Rawley, J.H. Taylor, M.M. Davis, and D.W. Allan, Millisecond Pulsar PSR 1937+21: A Highly Stable Clock, Science 238, 761–764 (1987).

[3] D.J. Wineland, Trapped Ions, Laser Cooling, and Better Clocks, Science, 226, 395–400, (1984).

[4] A. DeMarchi, New Insights into Causes and Cures of Frequency Instabilities (Drift and Long Term Noise) in Cesium, Proceedings of the 41st Annual Symposium on Frequency Control, May 27–29, 1987, pp. 53–58.

[5] J.C. Bergquist, W.M. Itano, and D.J. Wineland, Recoilless Optical Absorption and Doppler Sidebands in a Single Trapped Ion, Phys. Rev. A, 36, 428 (1987).

[6] L.S. Cutler, R.P. Giffard, P.J. Wheeler, and G.M.R. Winkler, Initial Operational Experience with a Mercury Ion Storage Frequency Standard, Proceedings of the 41st Annual Symposium on Frequency Control, May 27–29, 1987 pp. 12–19.

[7] F.L. Walls, Characteristics and Performance of Miniature NBS Passive Hydrogen Masers, IEEE Trans. Instr. and Meas., IM–36, 596–603 (1987).

[8] H. Peters, B. Owings, and T. Oakley, Sigma Tau Standards Corporation and L. Beno, Proceedings of the 41st Annual Symposium on Frequency Control, May 27–29, 1987, pp. 75–81.

[9] F.B. Varnum, D.R. Brown, D.W. Allan, and T.K. Peppler, Comparison of Time Scales Generated with the NBS Ensembling Algorithm, 19th Annual Precise Time and Time Interval Applications and Planning Meeting, Dec. 1, 1987

[10] D. W. Allan. Time and Frequency (Time–Domain) Characterization, Estimation, and Prediction of Precision Clocks and Oscillators, IEEE 1987 New Trans. on UFFC.

[11] J.A. Barnes, The Measurement of Linear Frequency Drift in Oscillators, Proceedings of 15th Annual Precise Time and Time Interval Meeting, December 1983, pp. 551–579.

Figure Captions

Figure 1. The open hexagons are a plot of the fractional frequency stability (square root of the modified Allan variance) mod.$\sigma_y(\tau)$ versus τ for the millisecond pulsar as compared against UTC(NBS). The solid hexagons are a plot of an estimate of the stability of the NBS(AT1) time scale as compared against a world's "best clock". Also indicated is where one might measure gravity wave radiation effects between the earth and the millisecond pulsar.

Figures 2a and b through 14a and b. Fractional frequency stability (square root of the Allan variance) $\sigma_y(\tau)$ vs. τ and the time residual plot for the various timing centers as estimated against a world's "best clock" ensemble calculated by using the NBS algorithm.

Figure 15. A plot of the frequency difference between a special terrestrial time scale generated by the International Bureau of Weights and Measures TT(BIPM) and International Atomic Time (TAI). Annual variations are evident. The noticeable frequency change at 1 January 1972 was in TAI, and was purposefully inserted to bring the second of TAI into agreement with the SI second as given by the primary frequency standards.

Figure 16. A plot of the time–difference residuals between PTB Cs 1 and the millisecond pulsar, PSR 1937+21, and the heavy line is a plot of the time– difference residuals between PTB Cs 1 and NBS(AT1). Some correlation is apparent.

Figures 17a and b through 19a and b are fractional frequency stability plots of the commercial mercury–ion standard No. 2 against the three indicated independent reference standards.

Figure 20. A 4–cornered hat analysis estimate of the fractional frequency stability, $\sigma_y(\tau)$, of each of the following four independent time outputs: APL hydrogen maser, NBS(AT1), USNO(MC with steering corrections removed) and the commercial mercury–ion standard No. 2.

Figures 21a and b through 23a and b are fractional frequency stability plots of the other possible combinations of standards individually estimated in Figure 20 and not plotted in Figures 17a and b through 19a and b.

Figures 24a and b. Plots of the fractional frequency stability between two commercial mercury–ion standards, No. 2 and No. 3. The stabilities plotted beyond 10^6 seconds are among the best ever reported, but because of apparent correlations between these two standards the values in this range are probably too optimistic.

Figure 25. A plot of a cross correlation coefficient as a function of averaging time for 11 months data span. That the coefficient is near 1 for averaging times longer than about two months would indicate that the long–term deviations in the two sets of data cross–correlated are primarily due to the mercury–ion standard No. 2.

Figures 26a and b through 28a and b are cross–correlation plots as a function of averaging time to test if there are correlations between the two mercury–ion standards for the last half–year. The two mercury–ion standards were interchanged in their position in the cross–correlation analysis between the "a" figures and the "b" figures. All six of these figures are consistent with the hypothesis that there are significant positive correlations between the two mercury–ion standards for averaging times of the order of two months and some longer.

Figures 29a and b. Figure "a" would indicate that there is no significant correlation between the mercury–ion standard No. 2 and NBS(AT1) or between the APL H–maser and unsteered UTC(USNO). The positive correlation shown in Figure "b" can be explained by the apparent long–term negative frequency drift in both the APL H–maser and the mercury–ion standard No. 2; though logically, we cannot exclude the possibility of correlations between NBS(AT1) and unsteered UTC(USNO), which seems very unlikely.

Figure 30. A tabular listing of frequency drift estimates over the last half–year of data with respect to three principle timing centers with independent standards. This table shows a high degree of correlation between the two mercury–ion standards, and it also shows that the positive correlation shown in Figure 29b is likely due to the negative frequency drift in mercury–ion standard No. 2 and the APL H–maser.
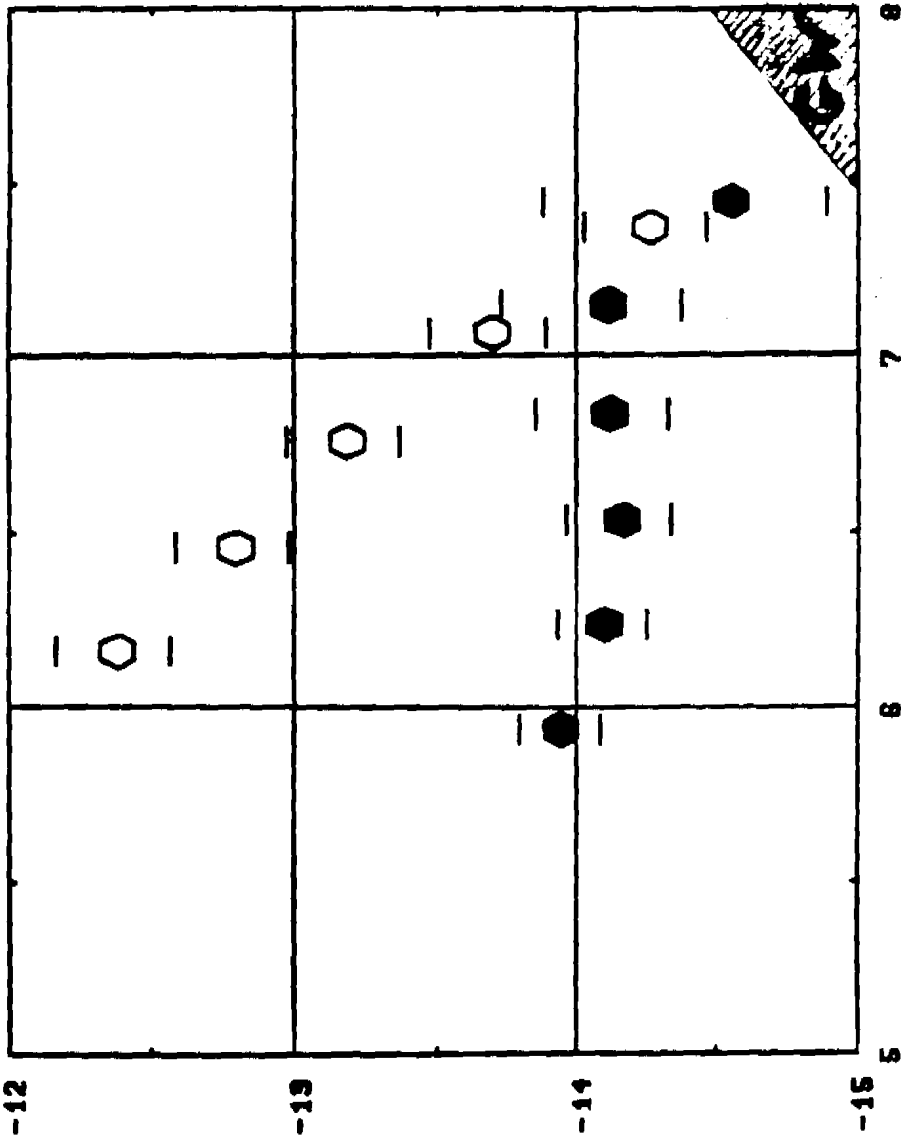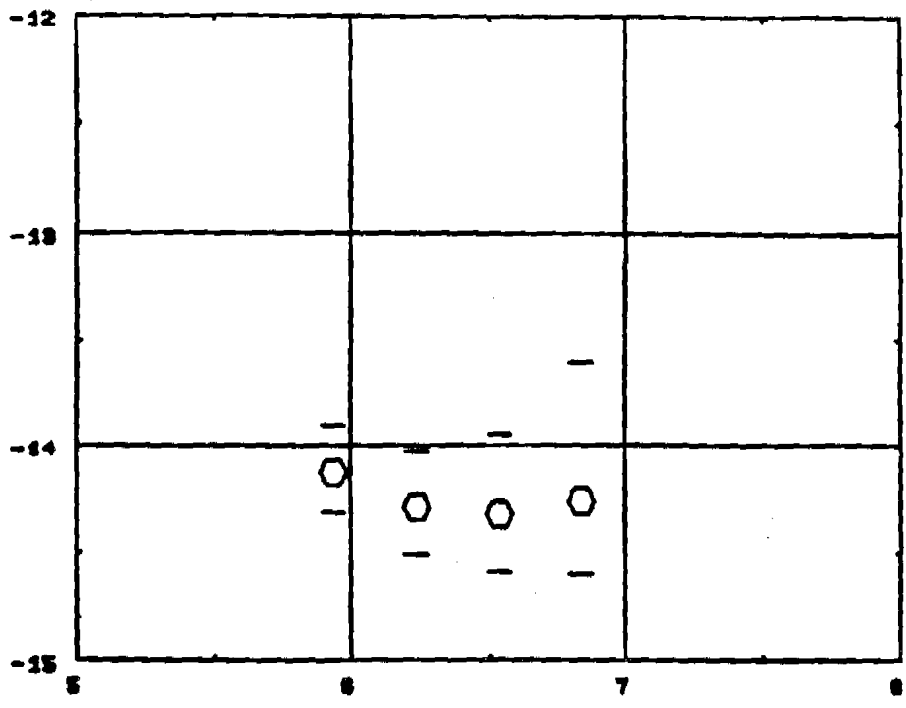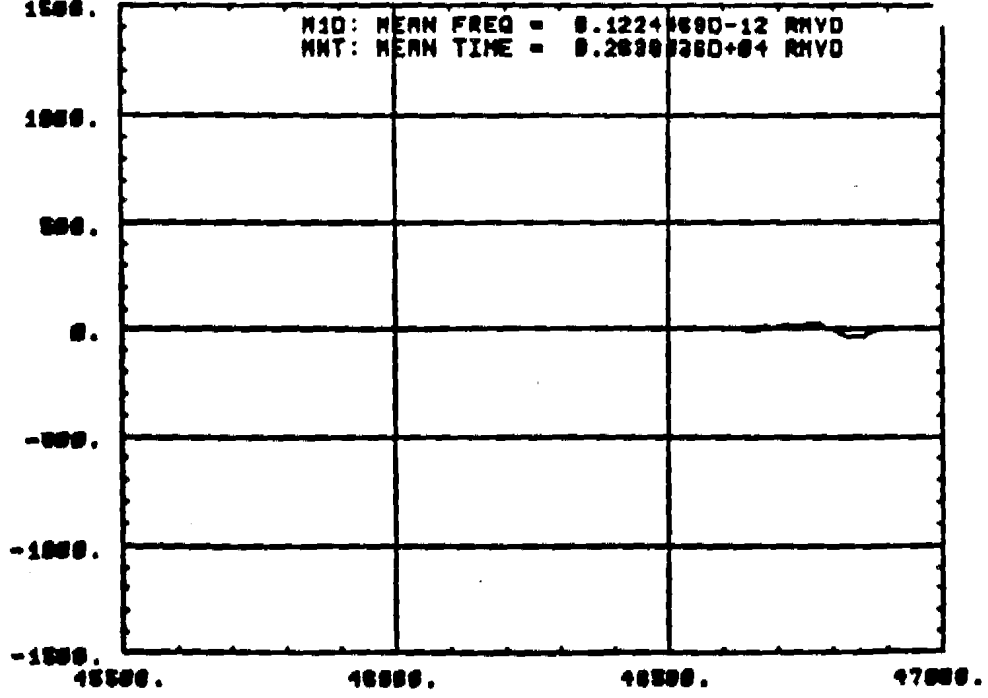
Figure 1

Figure 2a

Figure 2b

LOG MOD SIGy(TAU)
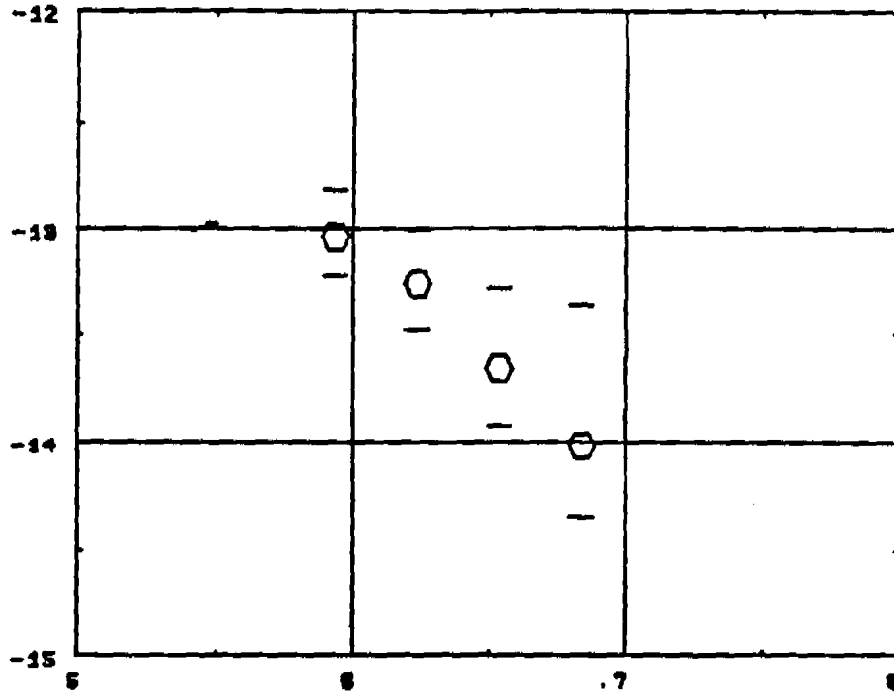
Figure 3a   LOG TAU (Seconds)

TIME (ns)

MJD: MEAN FREQ = 8.3848835D-12 RMVD
MNT: MEAN TIME = 8.5488343D+84 RMVD

Figure 3b   DAY (MJD)

380-5

IEN BEST ESTIMATE VIA MBS ALG.
MJD'S 46579 - 46879

LOG MOD SIGy(TAU)

Figure 4a   LOG TAU (Seconds)

IEN BEST ESTIMATE VIA MBS ALG.
MJD'S 46579 - 46879

TIME (ns)

M1D: MEAN FREQ = -0.1612038D-12 RMVD
MNT: MEAN TIME = 0.2771718D+04 RMVD

Figure 4b   DAY (MJD)

380-6

LOG MOD SIGy(TRU)

−12

−13

−14

−15

5   6   7   8
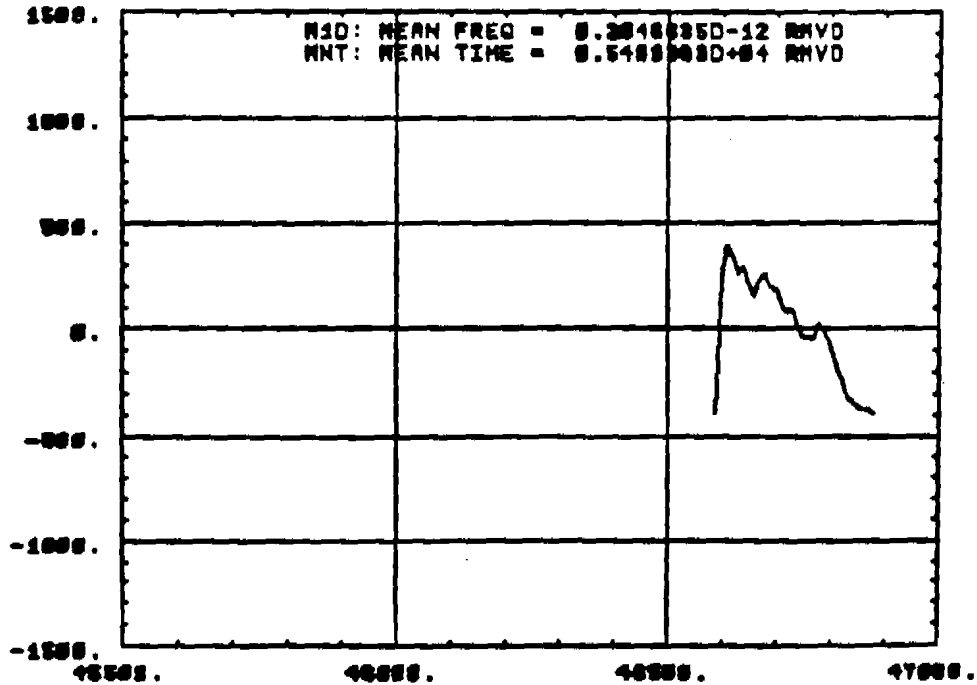
Figure 5a   LOG TAU (Seconds)
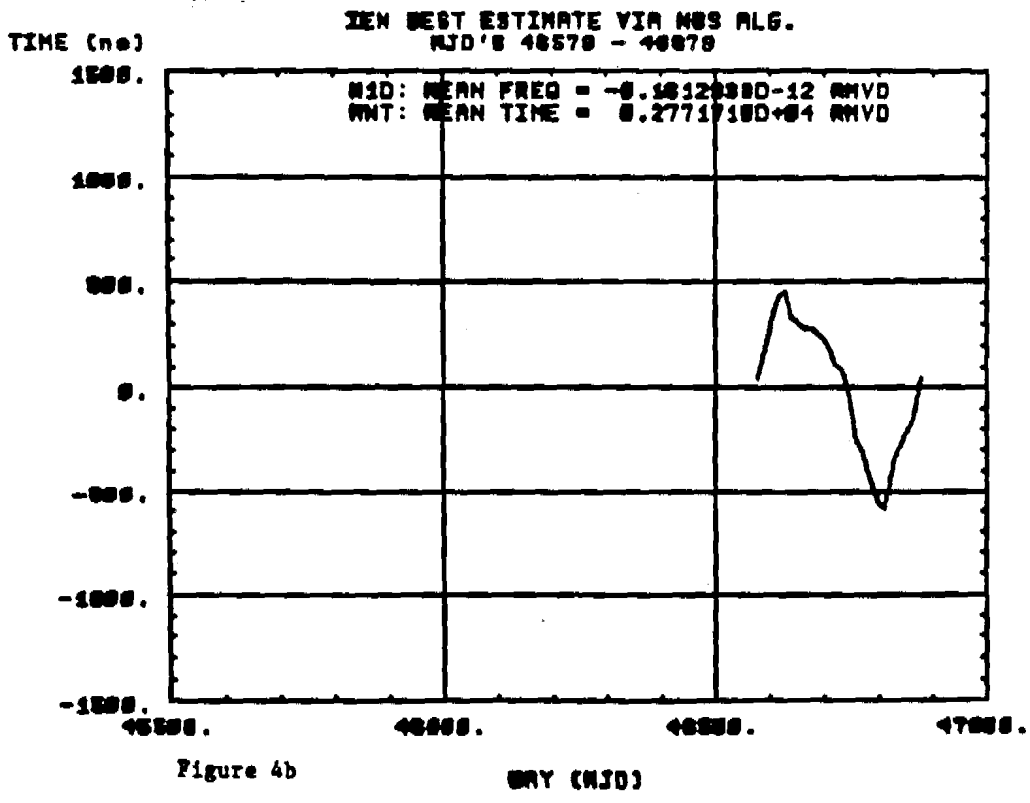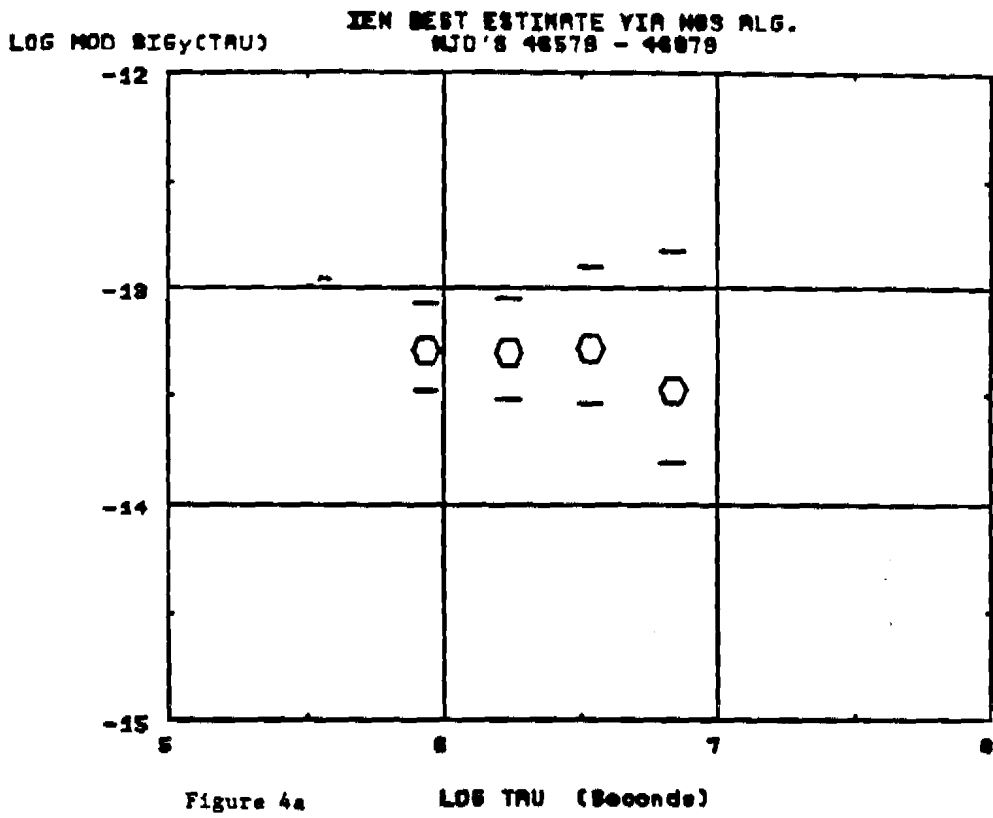
NBS(AT1) BEST ESTIMATE VIA NBS ALG.
MJD's 45769 - 46879

TIME (ns)

1500.

M1D: MEAN FREQ = 8.8853120-13 PHV0
MNT: MEAN TIME = -5.1888780+83 RMV0

1000.

500.

0.

−500.

−1000.

−1500.
45000.   46000.   46500.   47000.
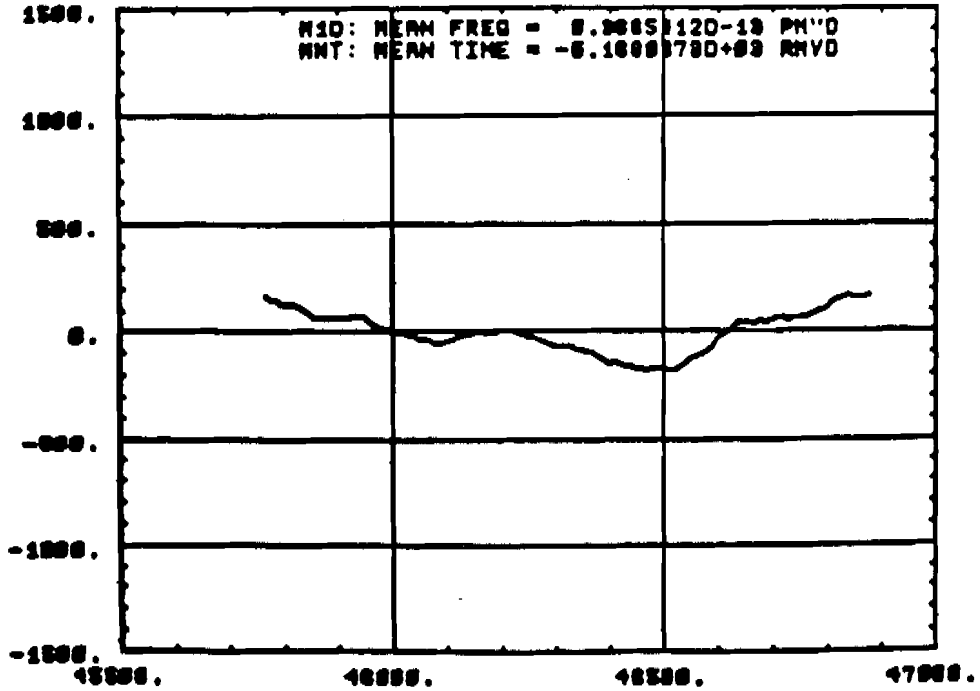
Figure 5b   DAY (MJD)

Figure 6a

LOG TAU (Seconds)

Figure 6b

DAY (MJD)

LOG MOD SIGy(TAU)
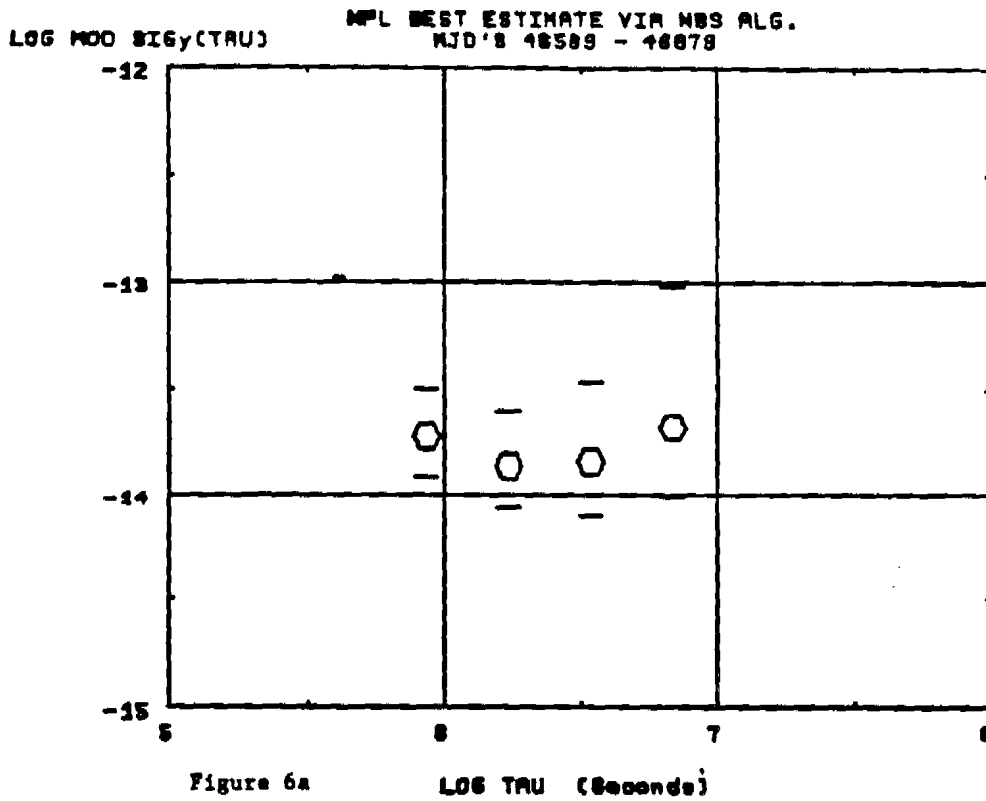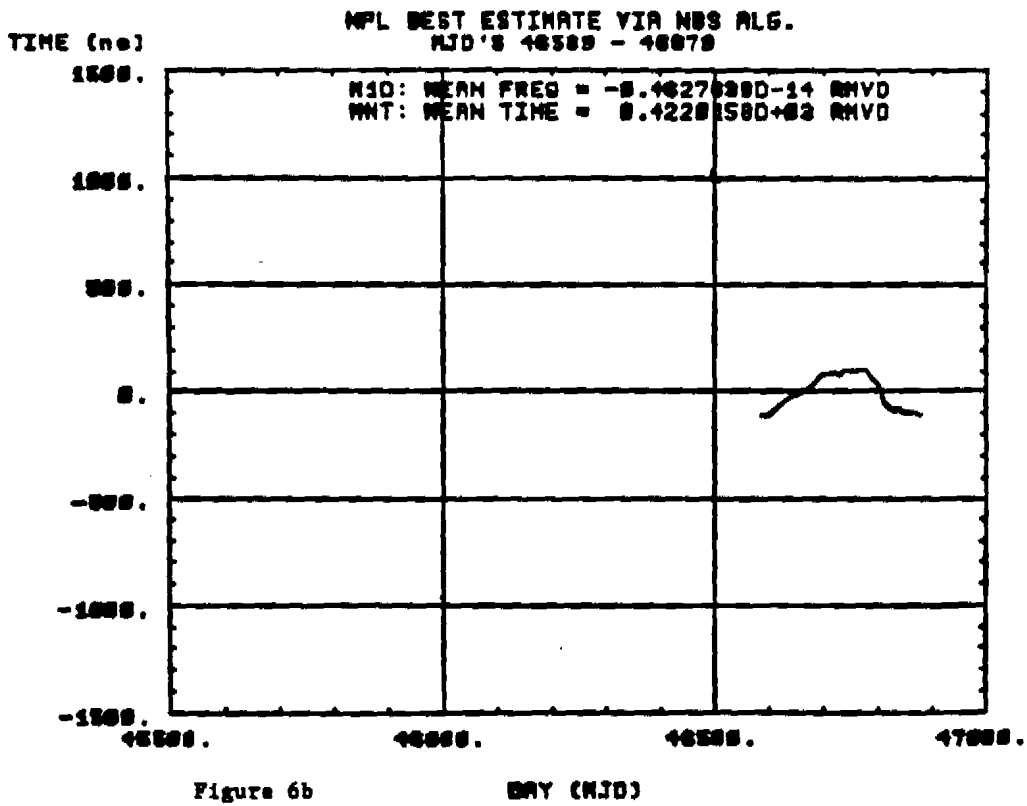
Figure 7a   **LOG TAU (Seconds)**

NRC Cs V BEST ESTIMATE VIA NBS ALG.
MJD 's 45899 – 46879

TIME (ns)
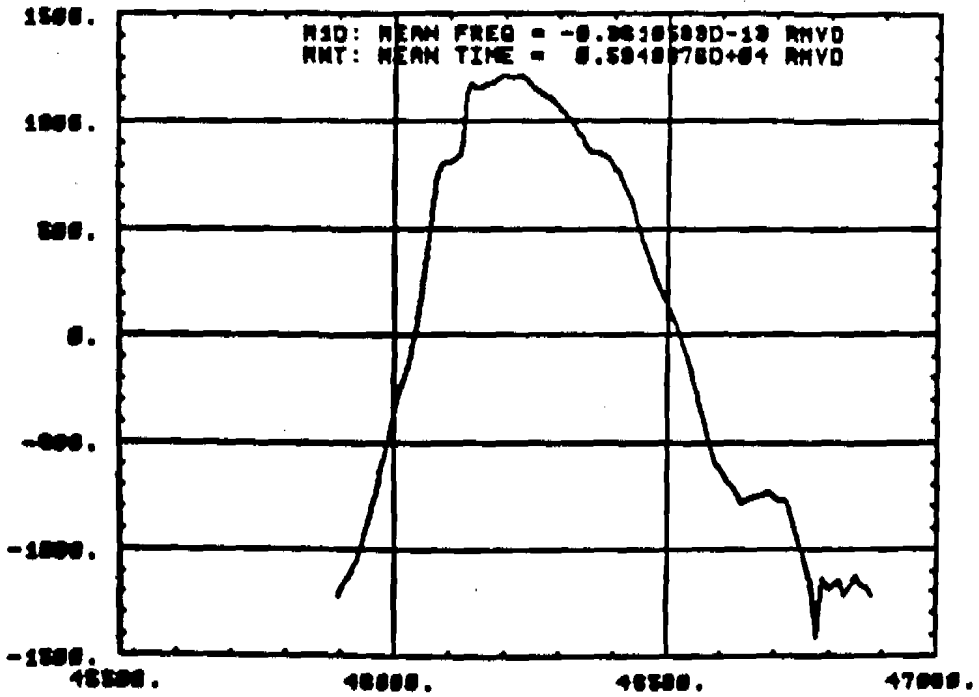
Figure 7b   **DAY (MJD)**

LOG MOD SIGy(TAU)
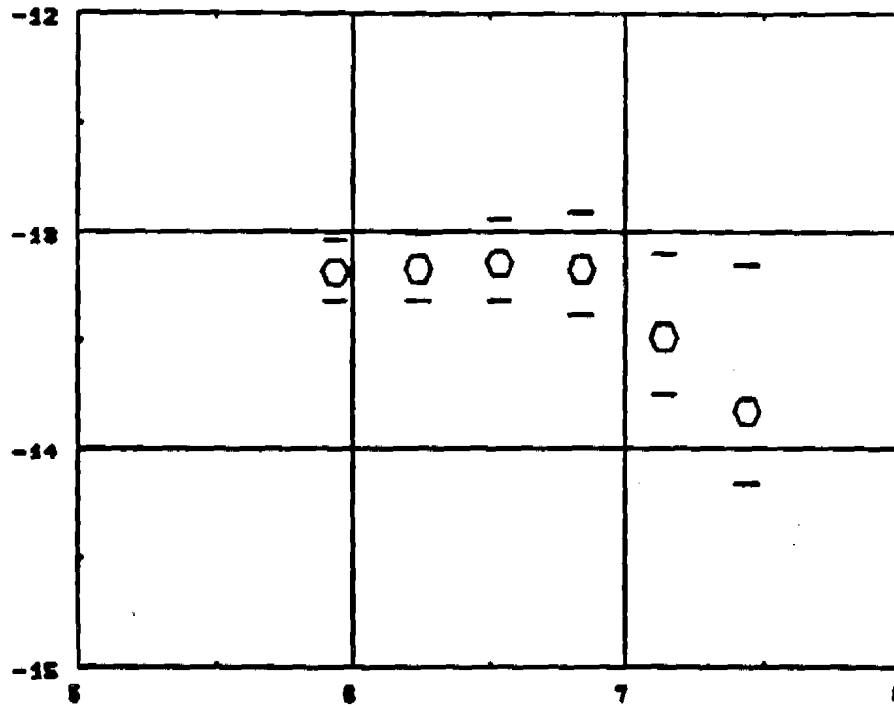
OF BEST ESTIMATE VIA NBS ALG.
MJD'S 45769 - 46879

-12

-13

-14

-15

5　　　6　　　7　　　8

Figure 8a　　　LOG TAU (Seconds)

TIME (ns)

OF BEST ESTIMATE VIA NBS ALG.
MJD'S 45769 - 46879

1500.

MJD: MEAN FREQ = -0.18635680-12 RMVD
MMT: MEAN TIME = -0.24540440+04 RMVD

1000.

500.

0.

-500.

-1000.

-1500.

45500.　　　46000.　　　46500.　　　47000.

Figure 8b　　　DAY (MJD)

380-10
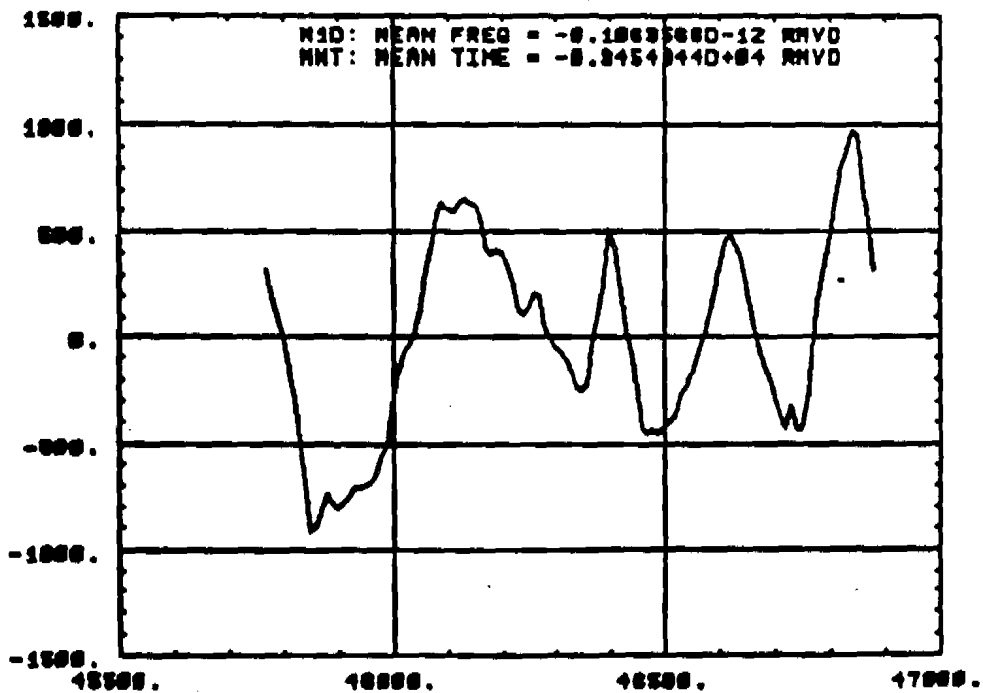
PTB Cs 1 BEST ESTIMATE VIA NBS ALG.
MJD'S 45769 - 46879

LOG MOD SIGy(TAU)
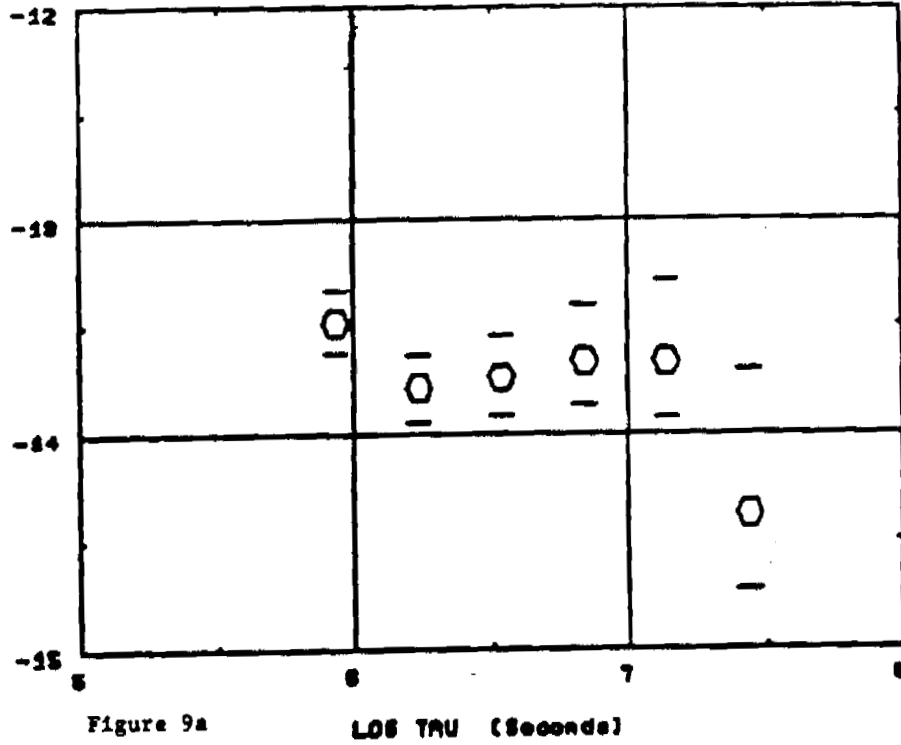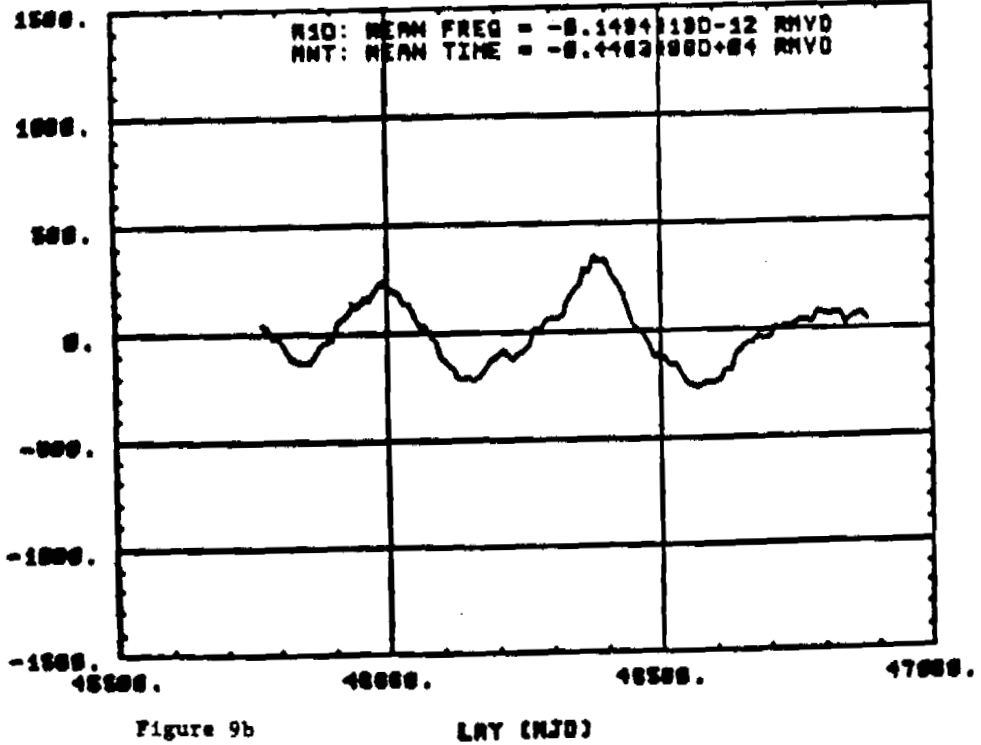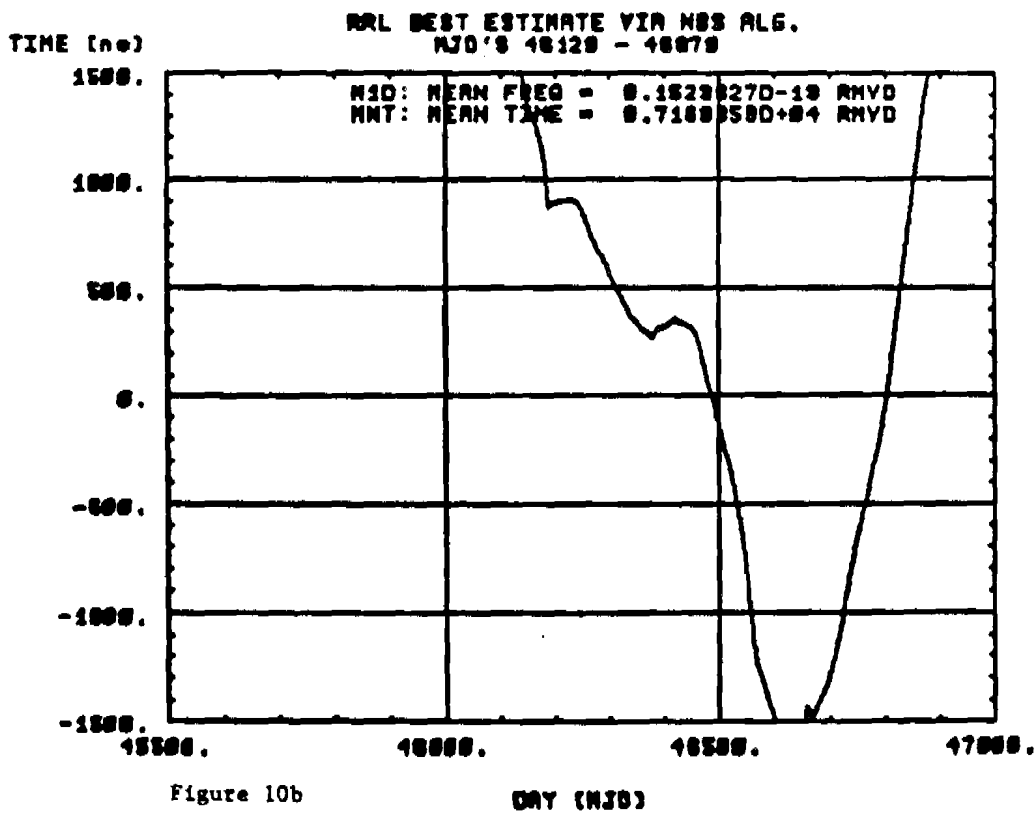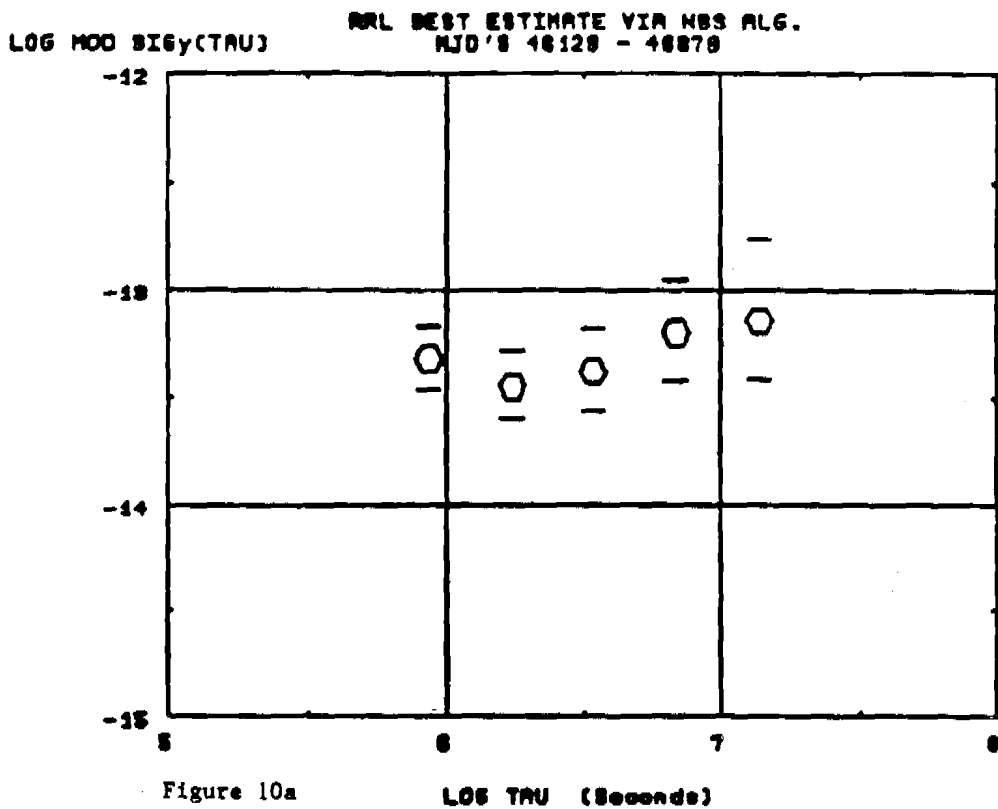
Figure 9a   LOG TAU (Seconds)

PTB Cs 1 BEST ESTIMATE VIA NBS ALG.
MJD'S 45769 - 46879

TIME (ns)

R10: MEAN FREQ = -8.1484119D-12 RMVD
MNT: MEAN TIME = -8.4463488D+84 RMVD

Figure 9b   DAY (MJD)

380-11

Figure 10a

Figure 10b

TRO BEST ESTIMATE VIR NBS ALG.
MJD'S 45859 - 48878

LOG MOD SIGy(TAU)

Figure 11a   LOG TAU (Seconds)

TRO BEST ESTIMATE VIR NBS ALG.
MJD'S 45859 - 48878

TIME (ns)

MFD: MEAN FREQ = -5.1025988D-12 RMVD
MNT: MEAN TIME = -6.2681018D+84 RMVD

Figure 11b   DAY (MJD)

380-13
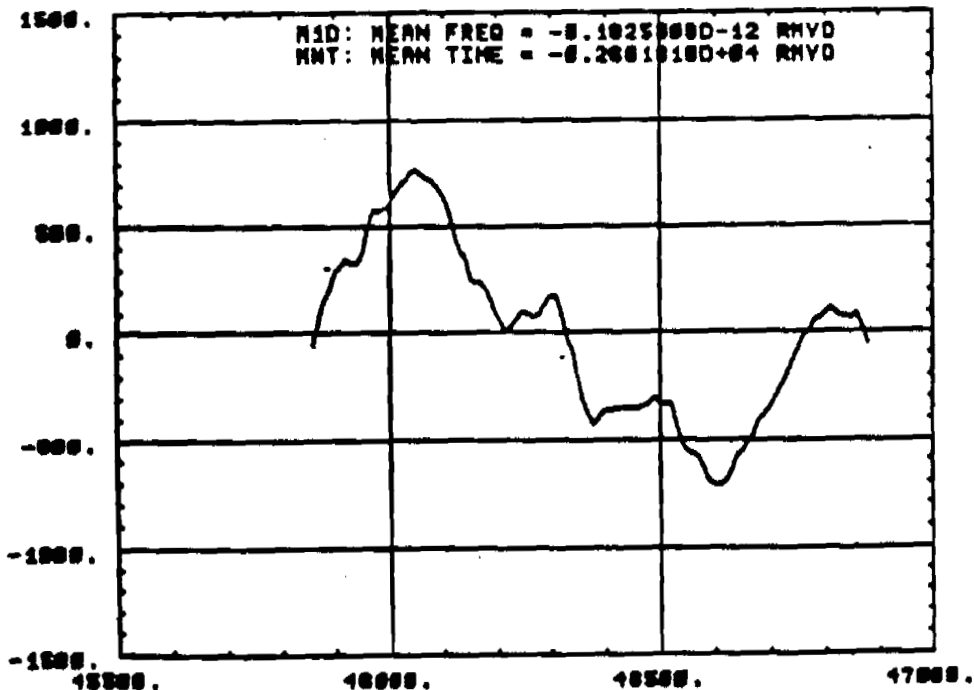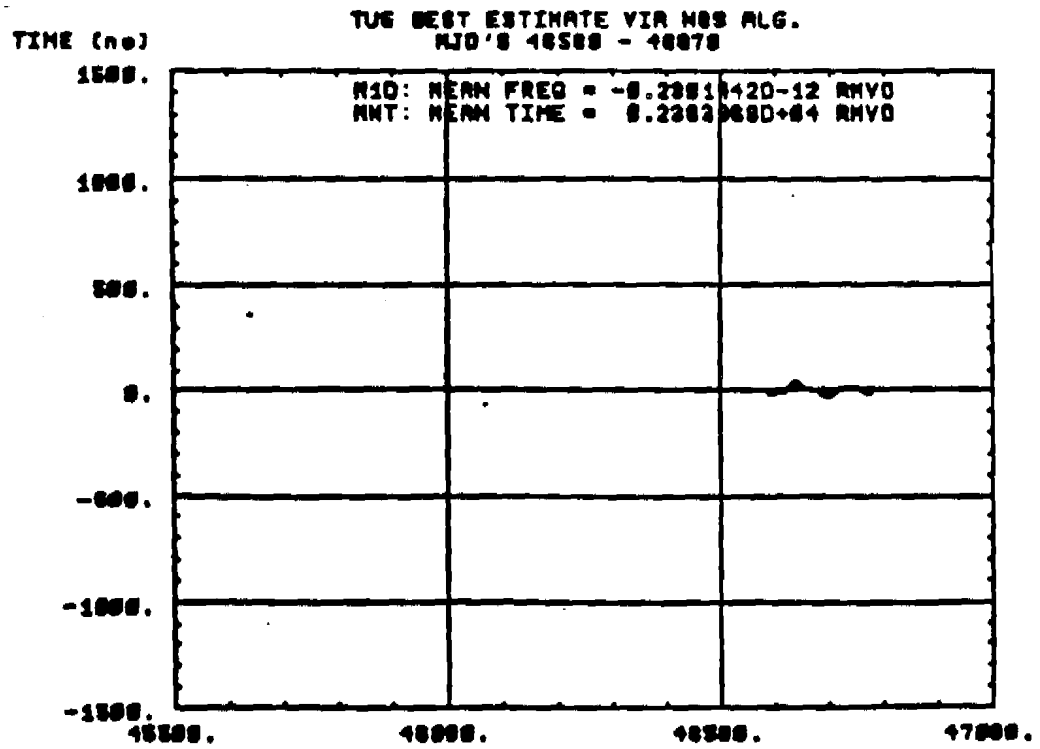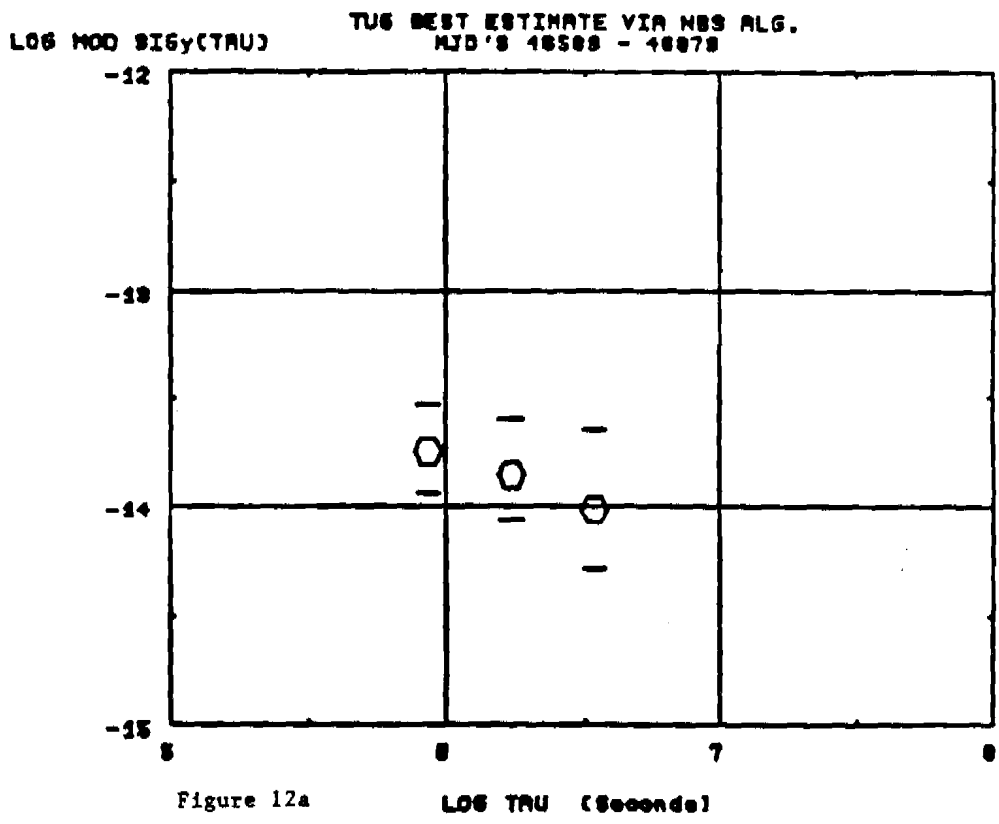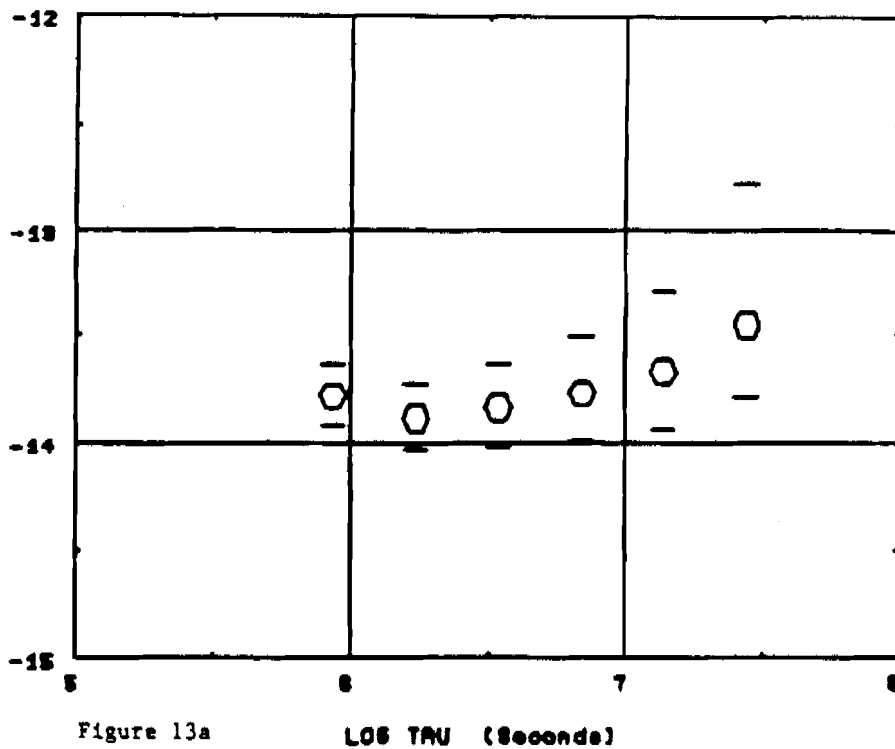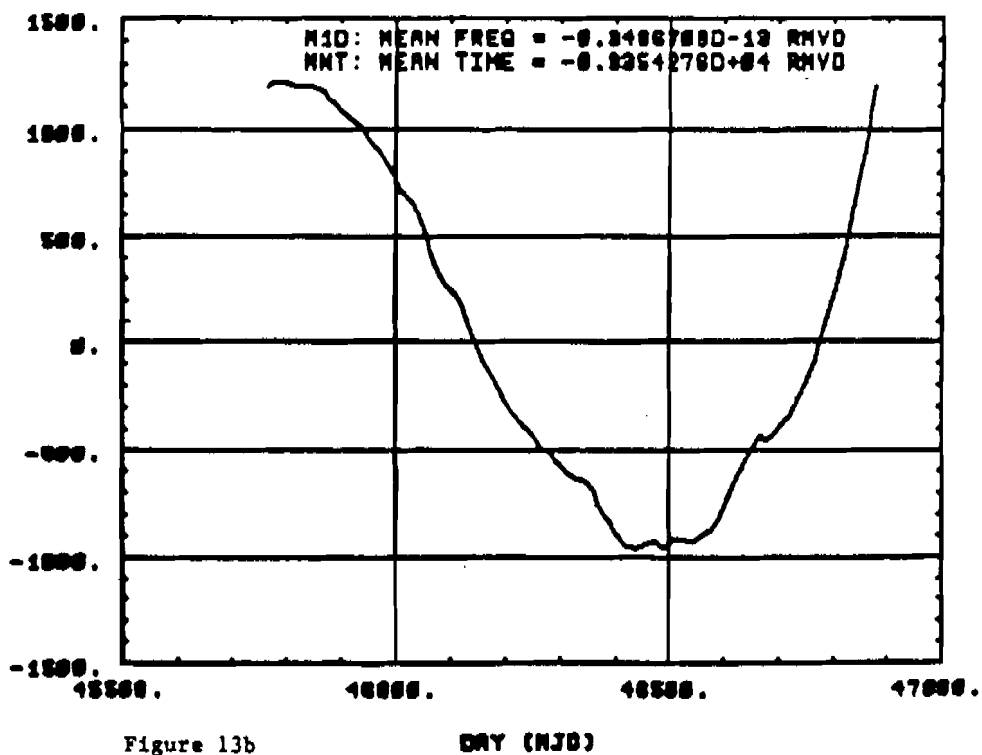
Figure 12a

Figure 13a

Figure 13b
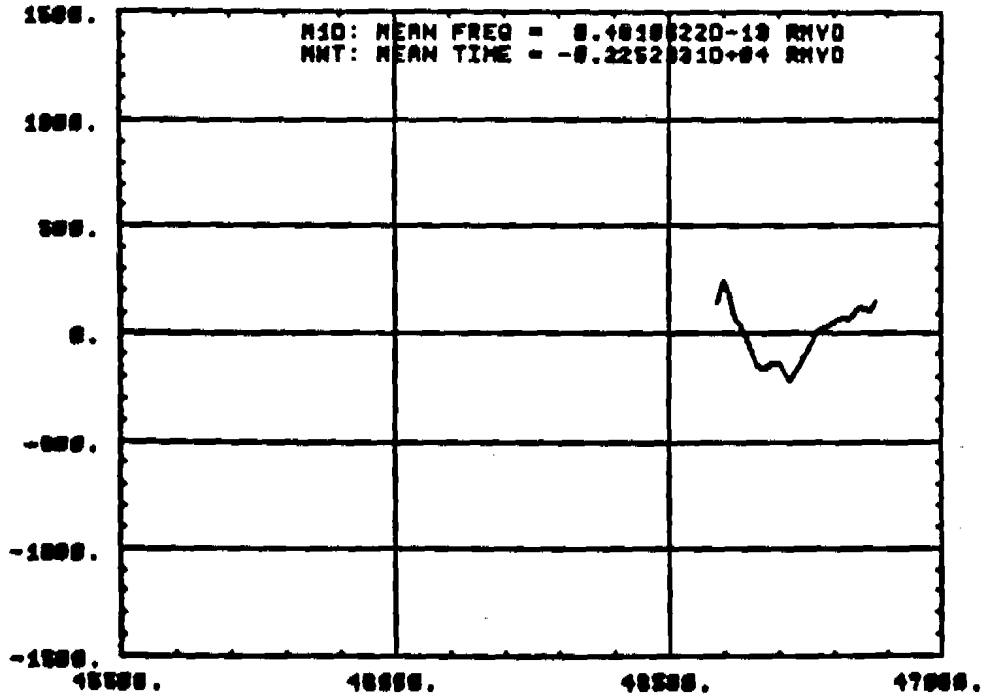
Figure 14a

Figure 14b
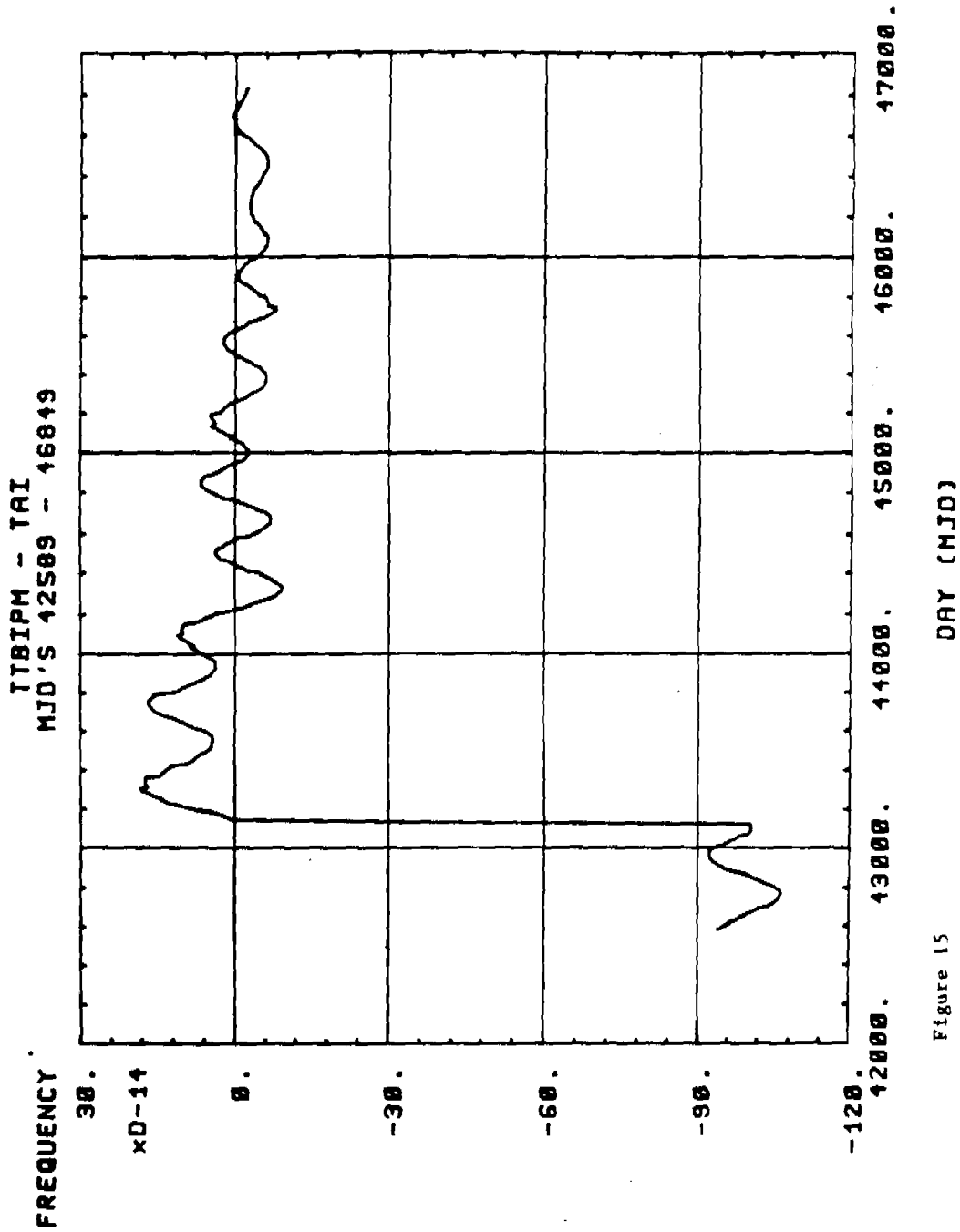
Figure 15

Figure 16

PTB CS1 - NBS(AT1)

PTB CS1 - PSR 1937+21
15 OCT.'84 - 25 DEC.'86
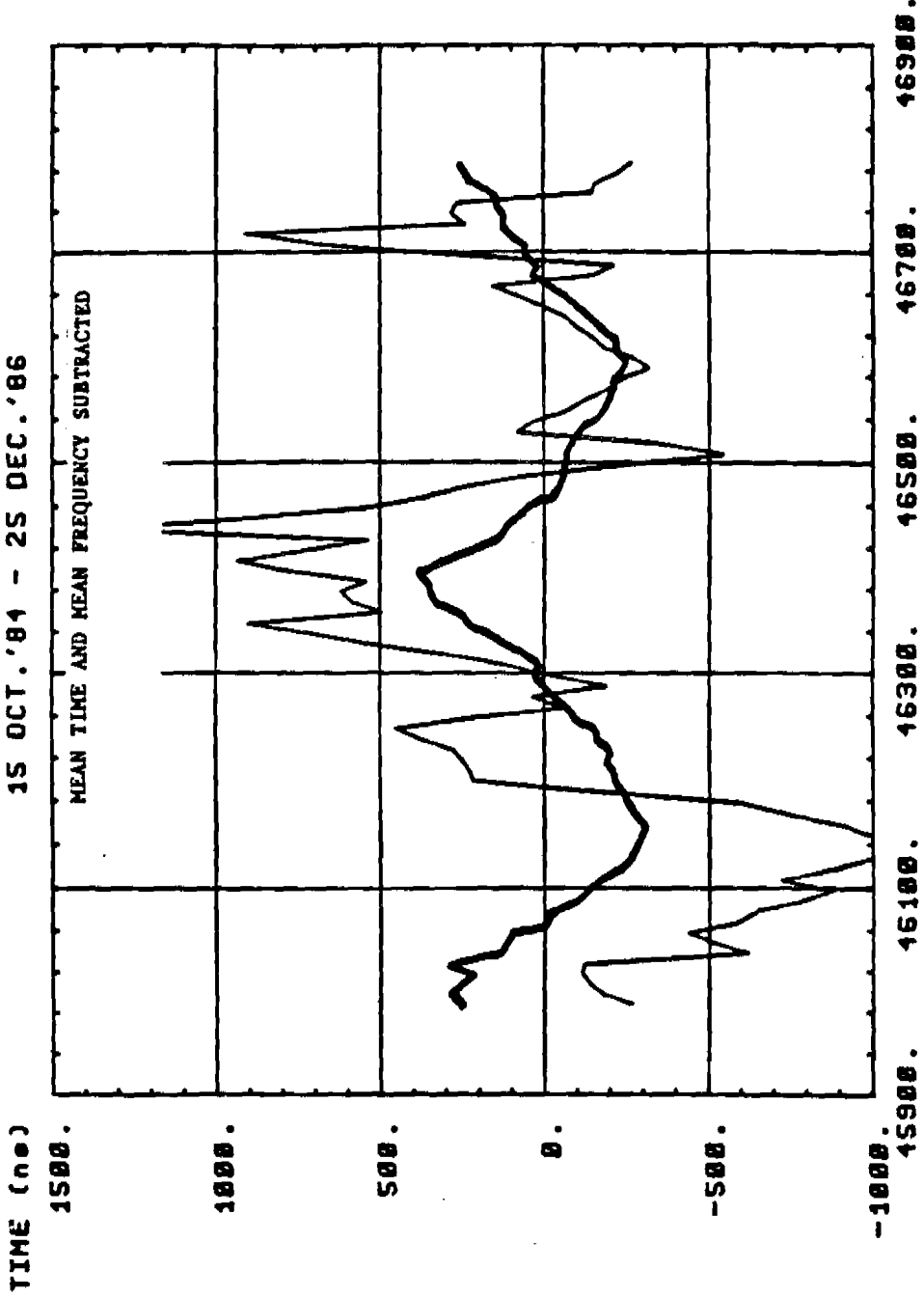
MEAN TIME AND MEAN FREQUENCY SUBTRACTED

TIME (ns)

DAY (MJD)

380-18

Figure 17a   DAY (MJD)

Hg ION #2 - APL H-MASER
18 DEC.'86 - 14 NOV.'87

LOG SIGMAy(TAU)

Figure 17b   LOG TAU (Seconds)

Figure 18a

Figure 18b

Figure 19a

Figure 19b

Figure 20

380-22

Figure 21a

Figure 21b

LOG TAU (Seconds)
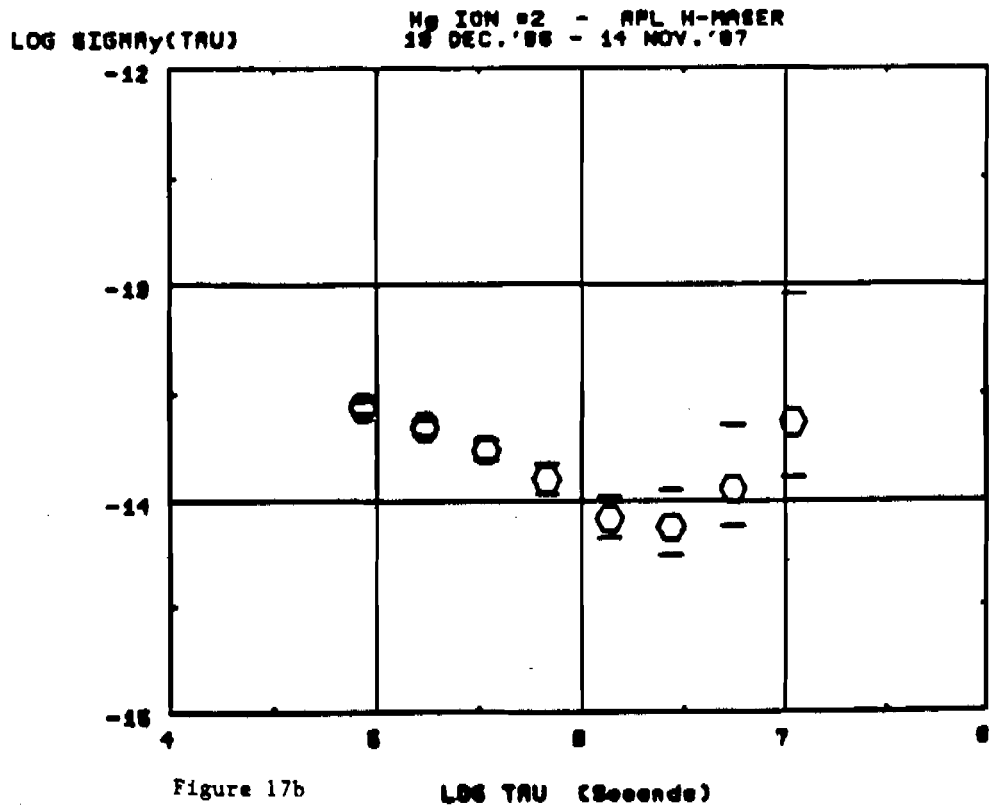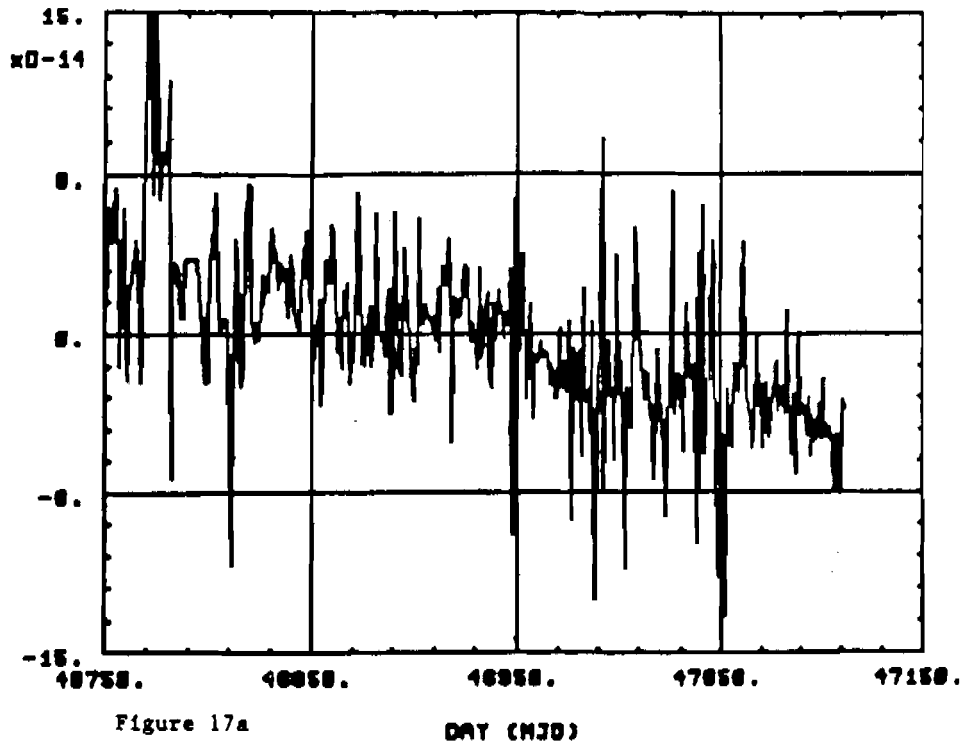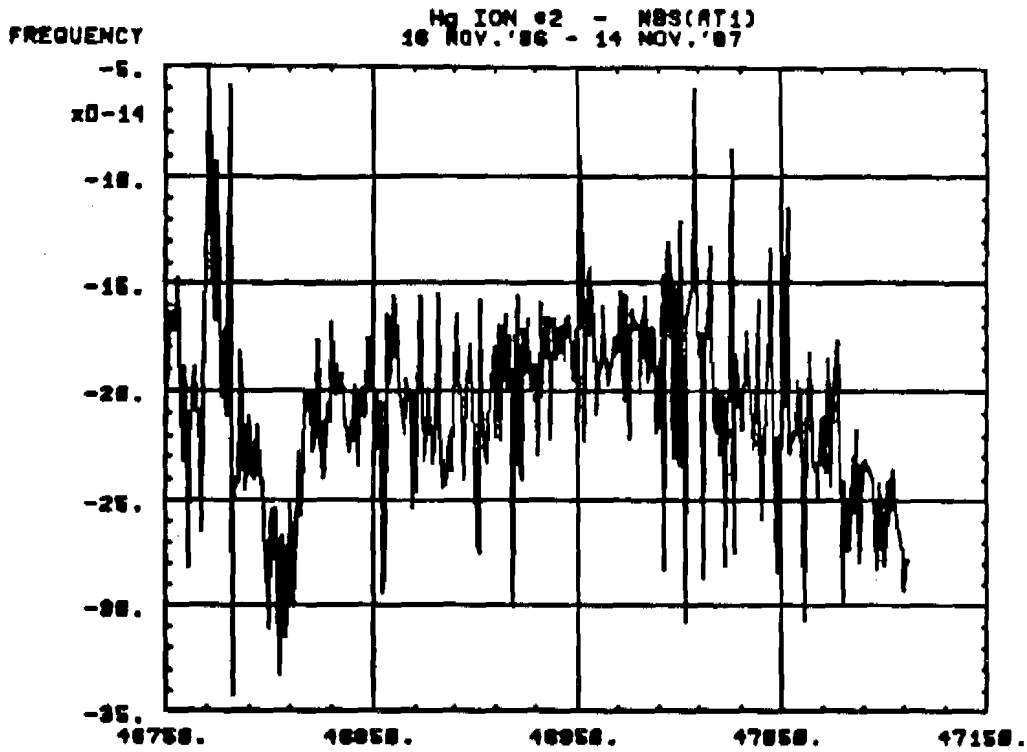
Figure 22a
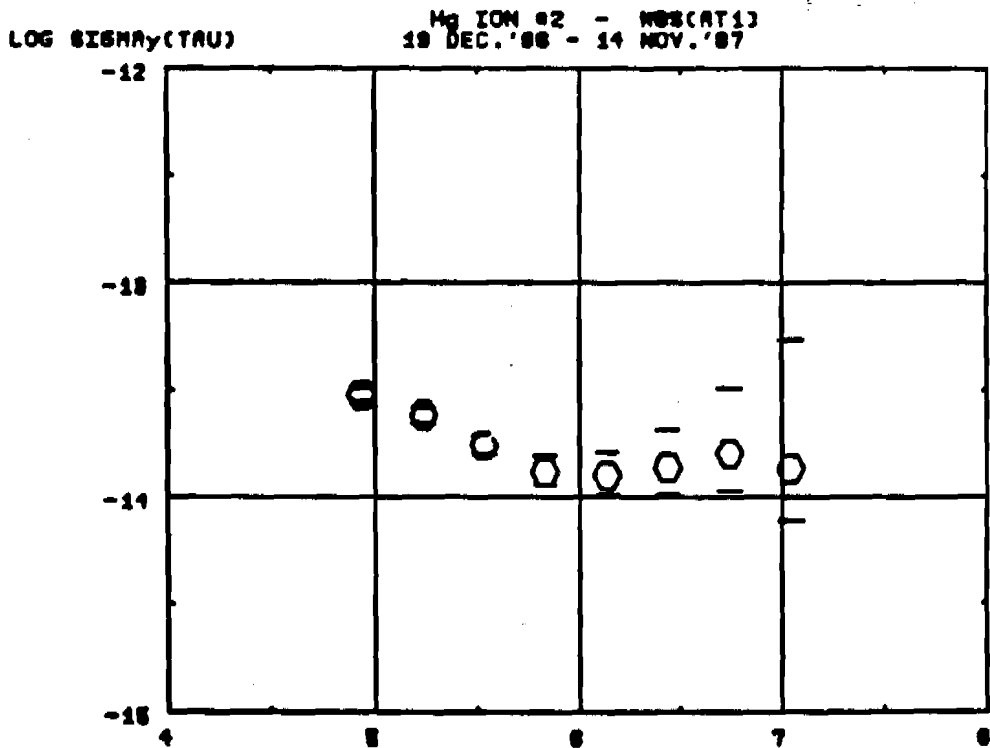
Figure 22b

Figure 23a
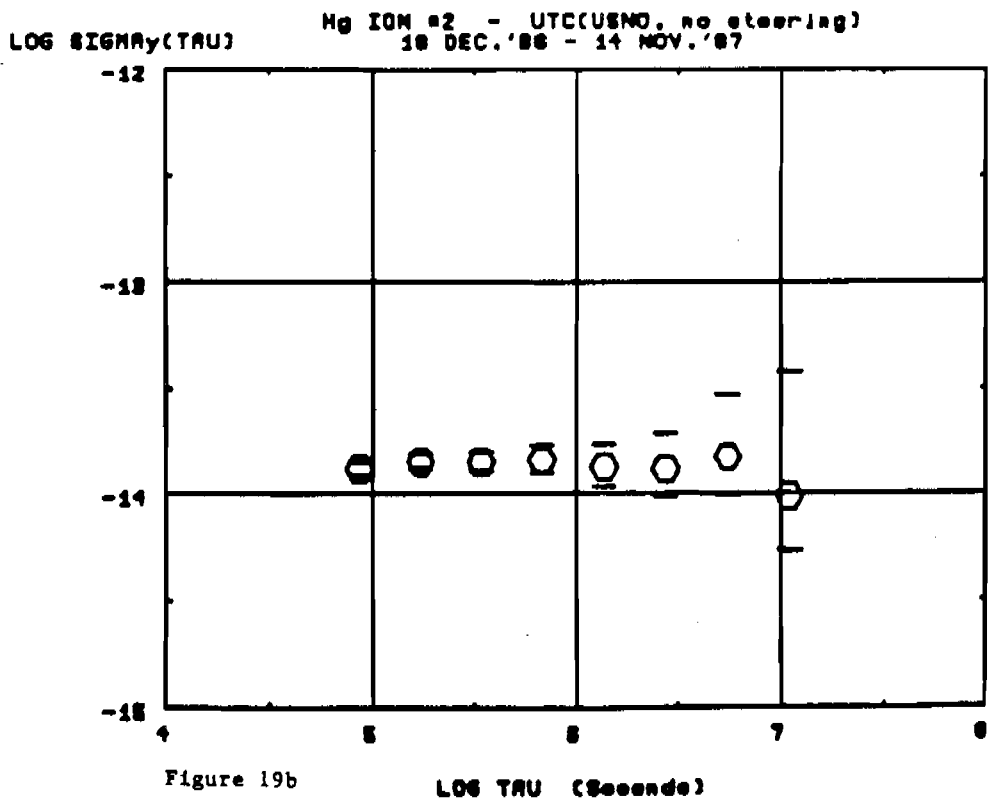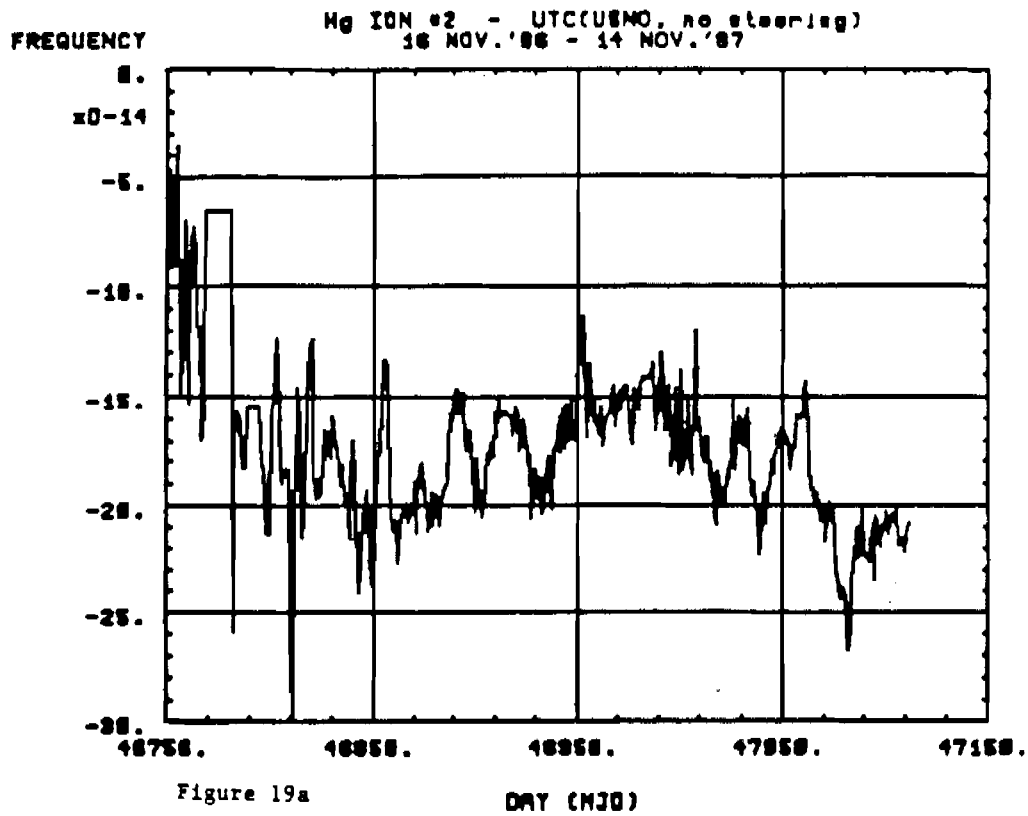
Figure 23b
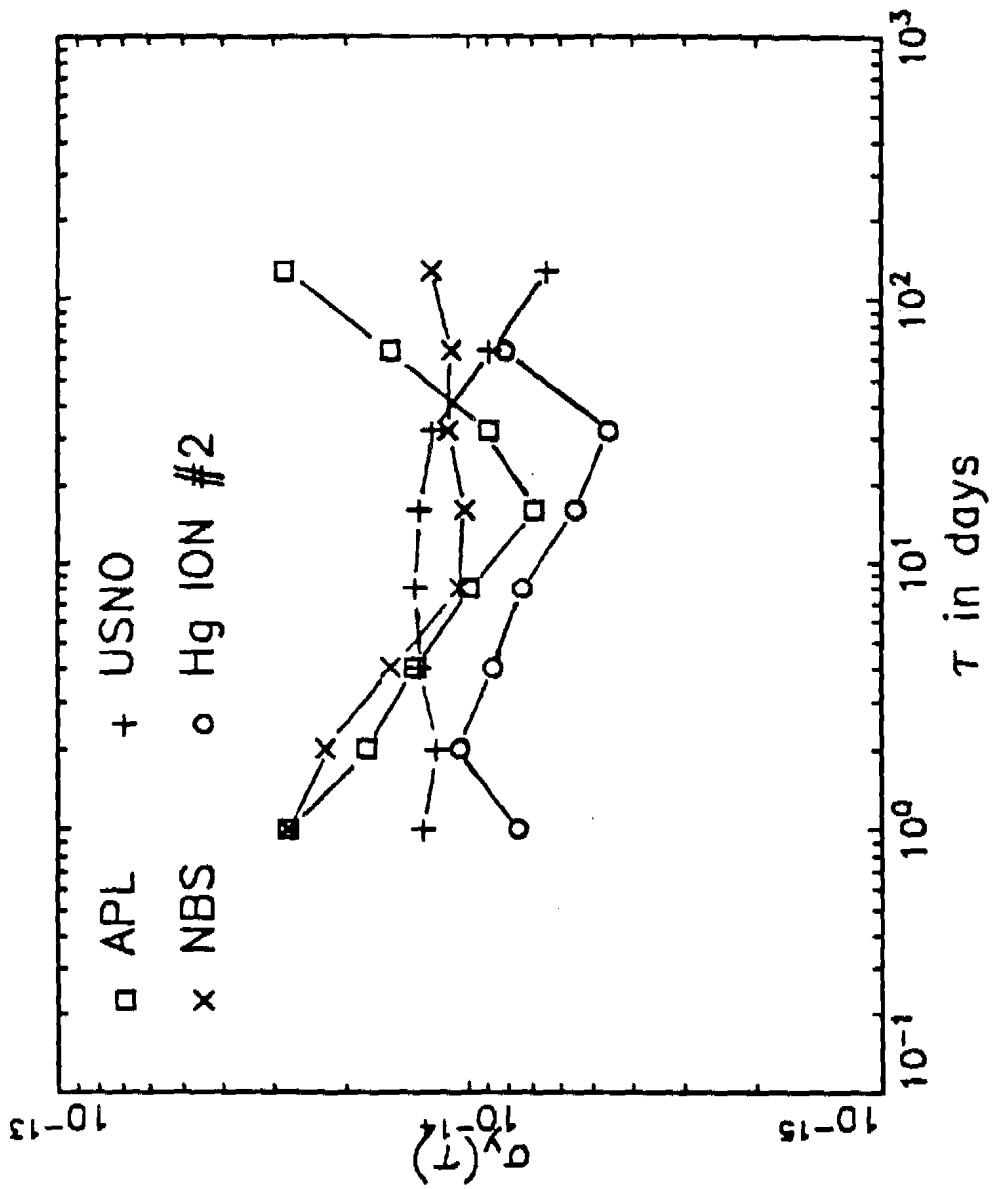
Figure 24a
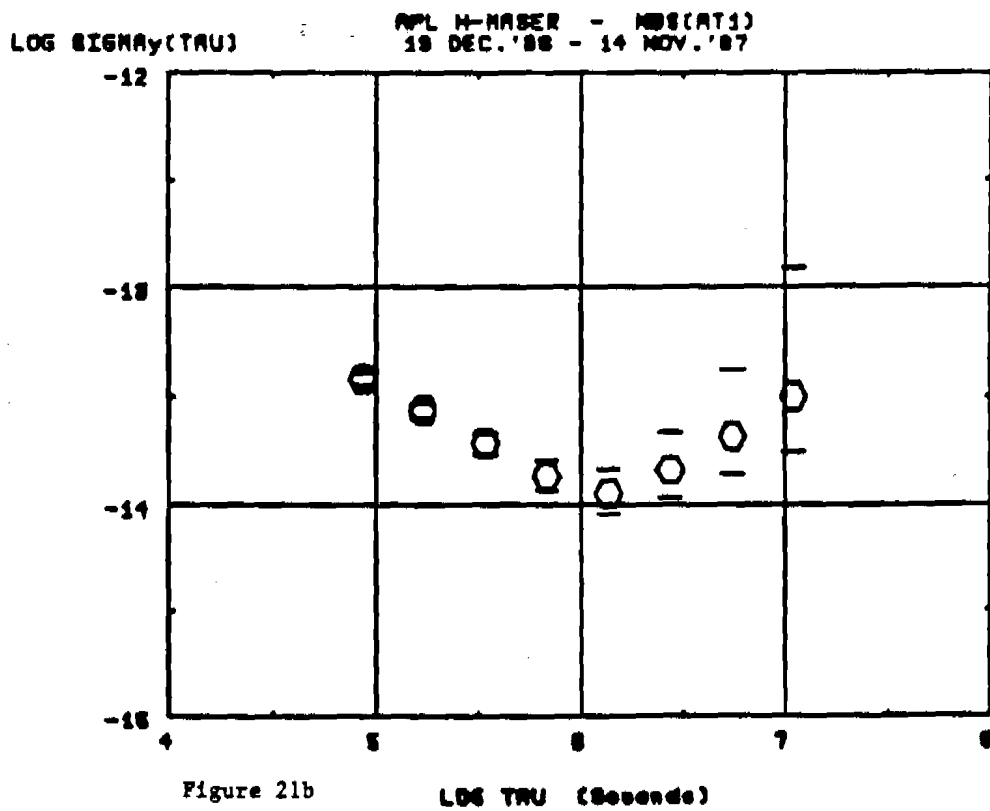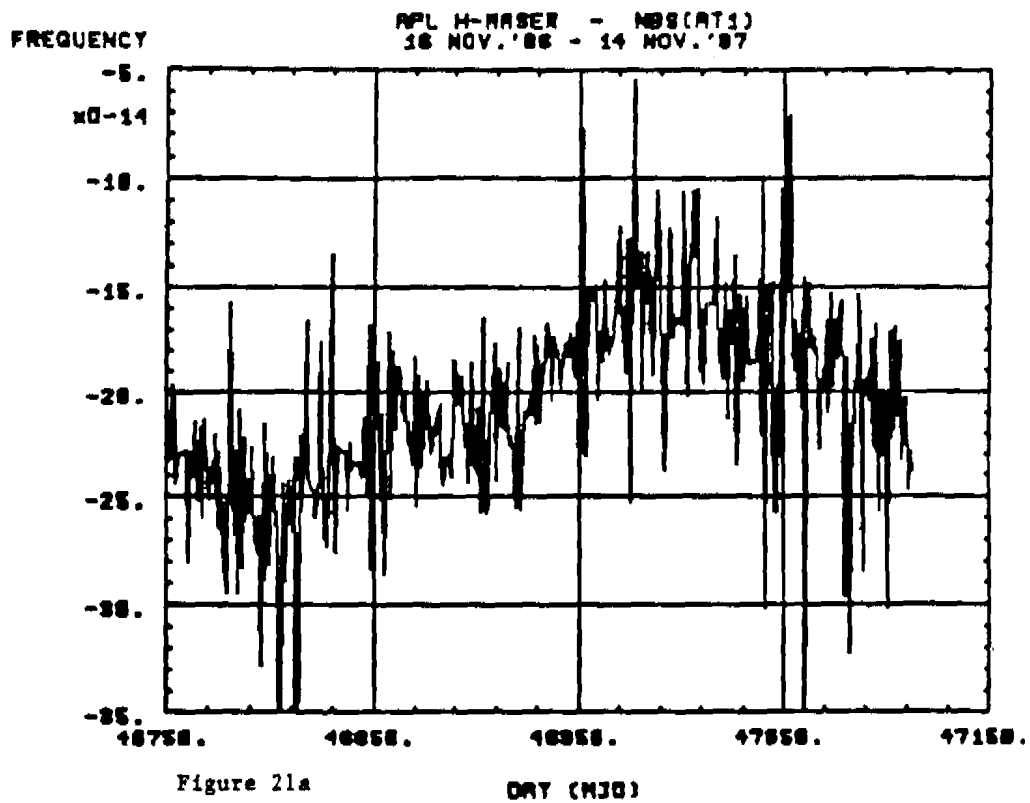
Figure 24b
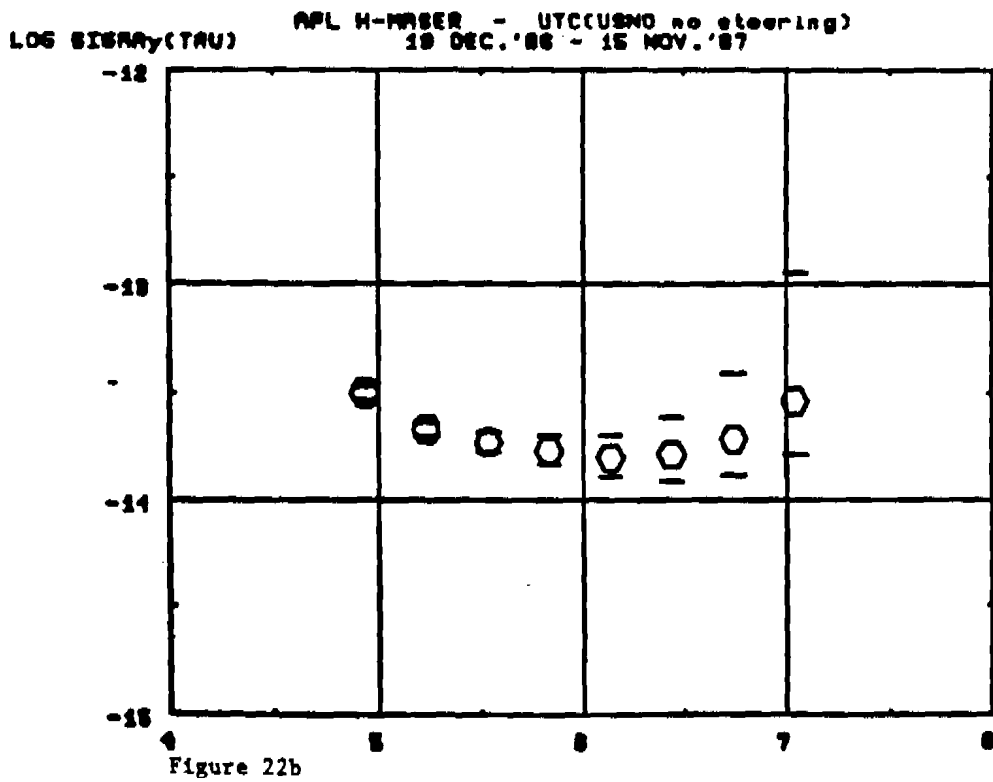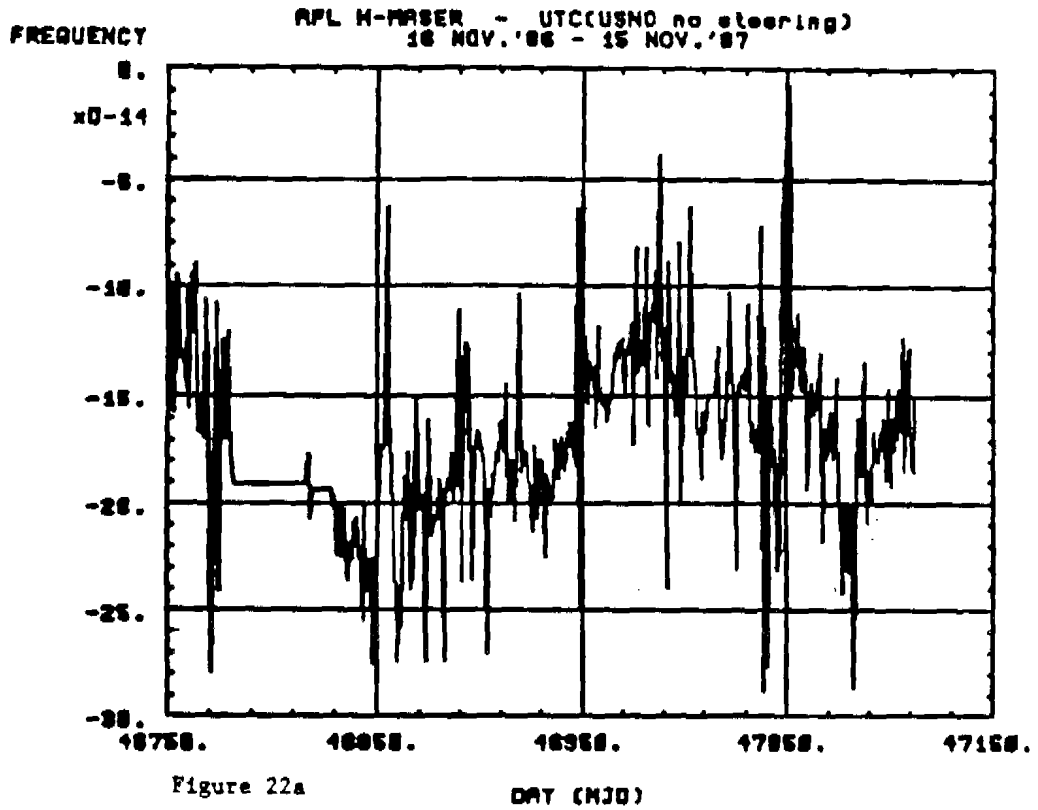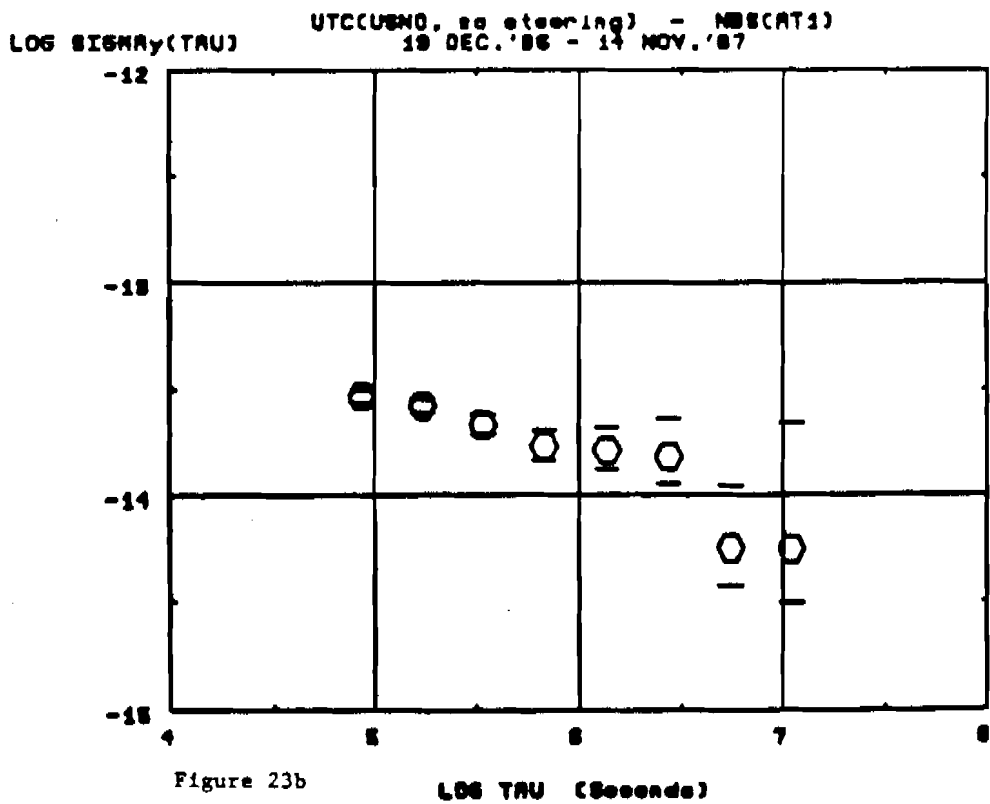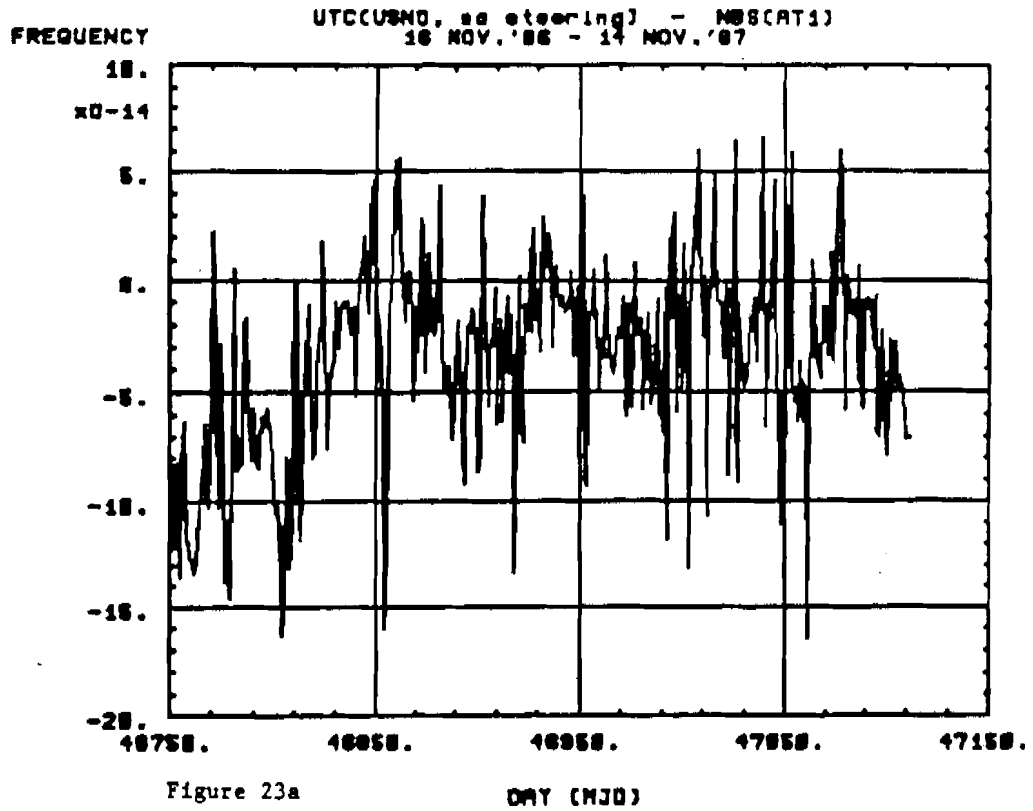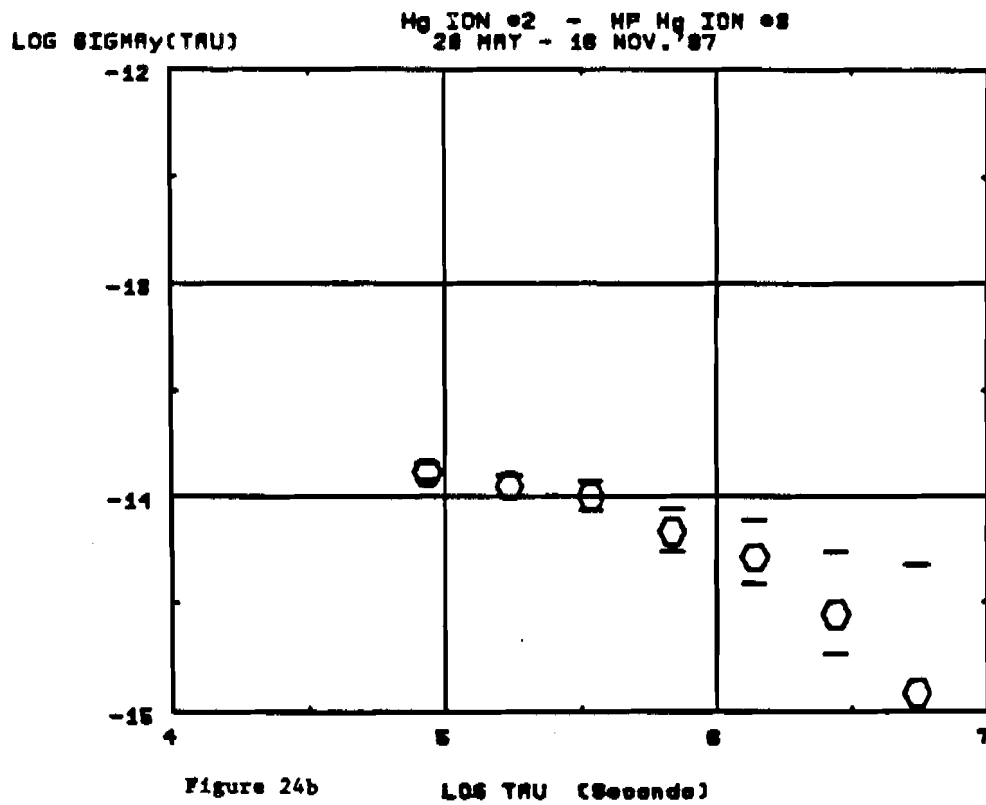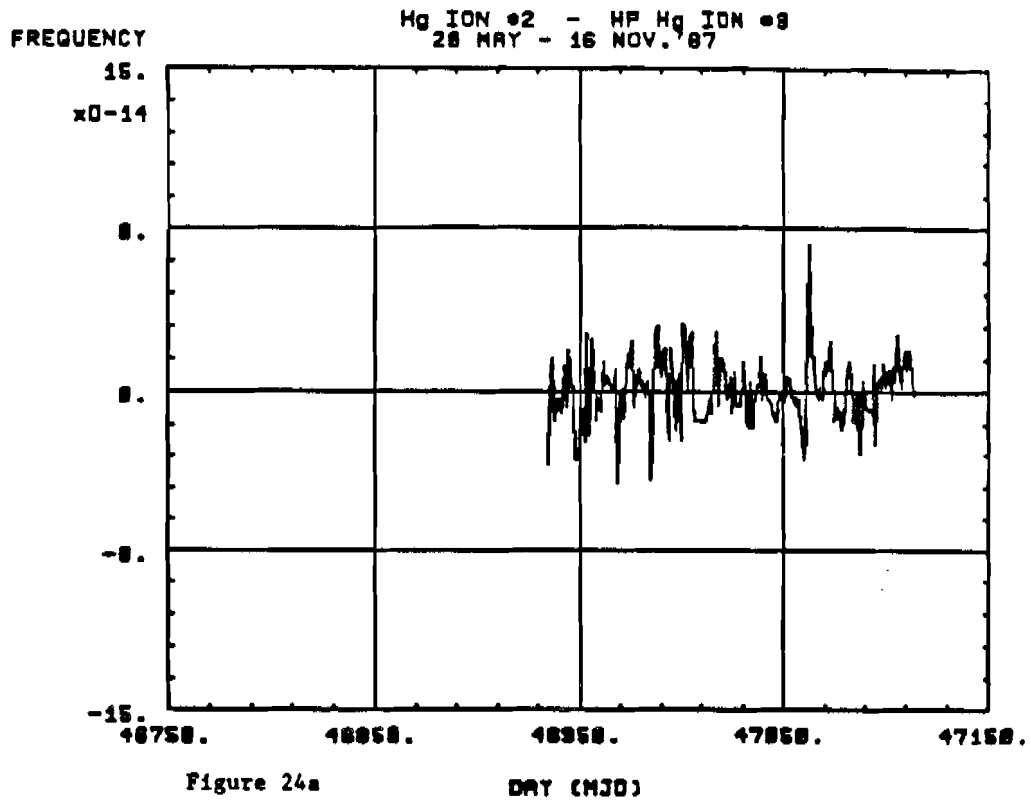
Figure 25

CORR. COEF. (Hg ION #2 – UTC(USNO, NS)) VERSUS (Hg ION #2 – NBS(AT1))
15 NOV.'86 – 14 NOV.'87

SAMPLE TIME, TAU (days)

CORR. COEF. (Hg ION #2 - RPL H-MASER) vs. (Hg ION #3 - NBS(AT1))
20 MAY - 6 NOV. '87

Figure 26a   SAMPLE TIME, TAU   (days)

CORR. COEF. (Hg ION #2 - RPL H-MASER) vs. (Hg ION #2 - NBS(AT1))
20 MAY - 6 NOV. '87
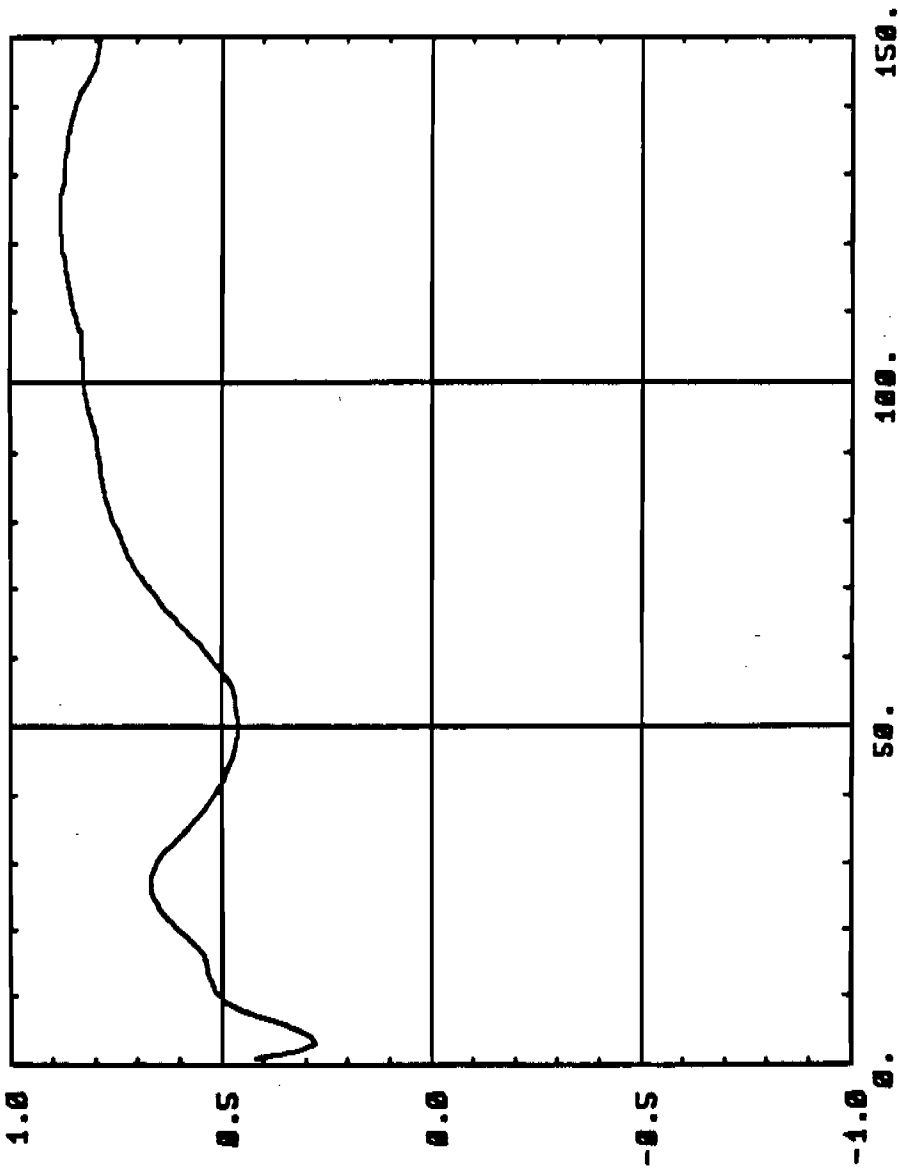
Figure 26b   SAMPLE TIME, TAU   (days)

(Hg ION #2 - NBS(AT1)) vs. (Hg ION #3 - UTC(USNO, MS))
28 MAY - 5 NOV.'87

CORR. COEF.

Figure 27a   SAMPLE TIME, TAU   (days)

(Hg ION #3 - NBS(AT1)) vs. (Hg ION #2 - UTC(USNO, MS))
28 MAY - 5 NOV.'87
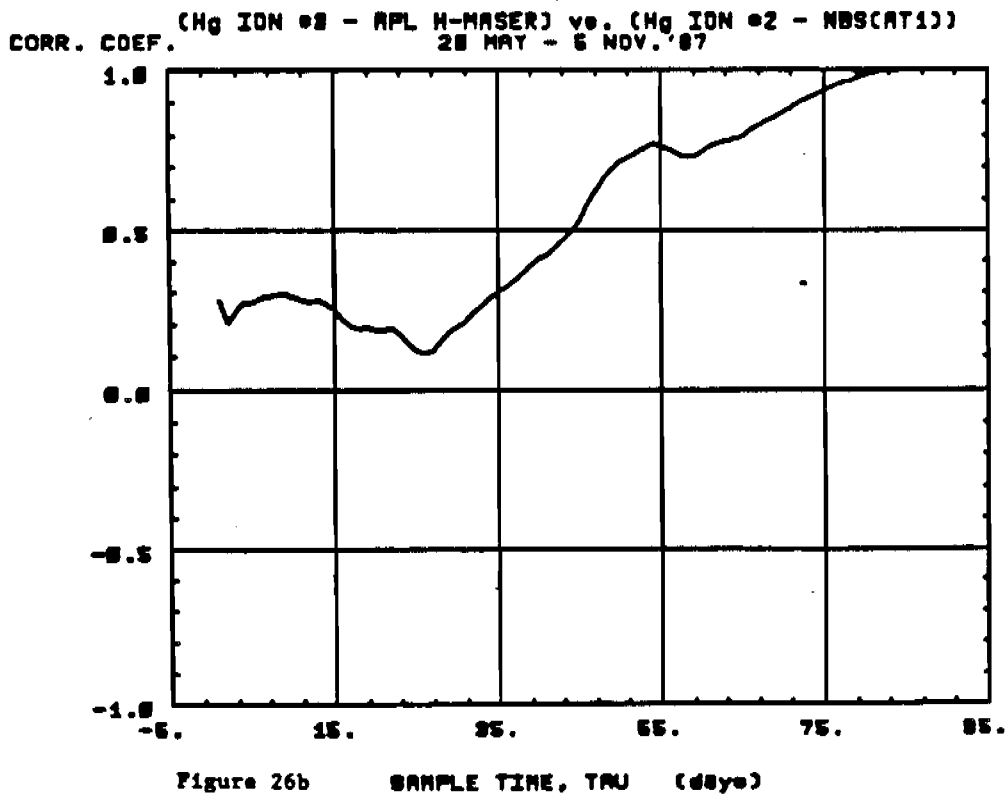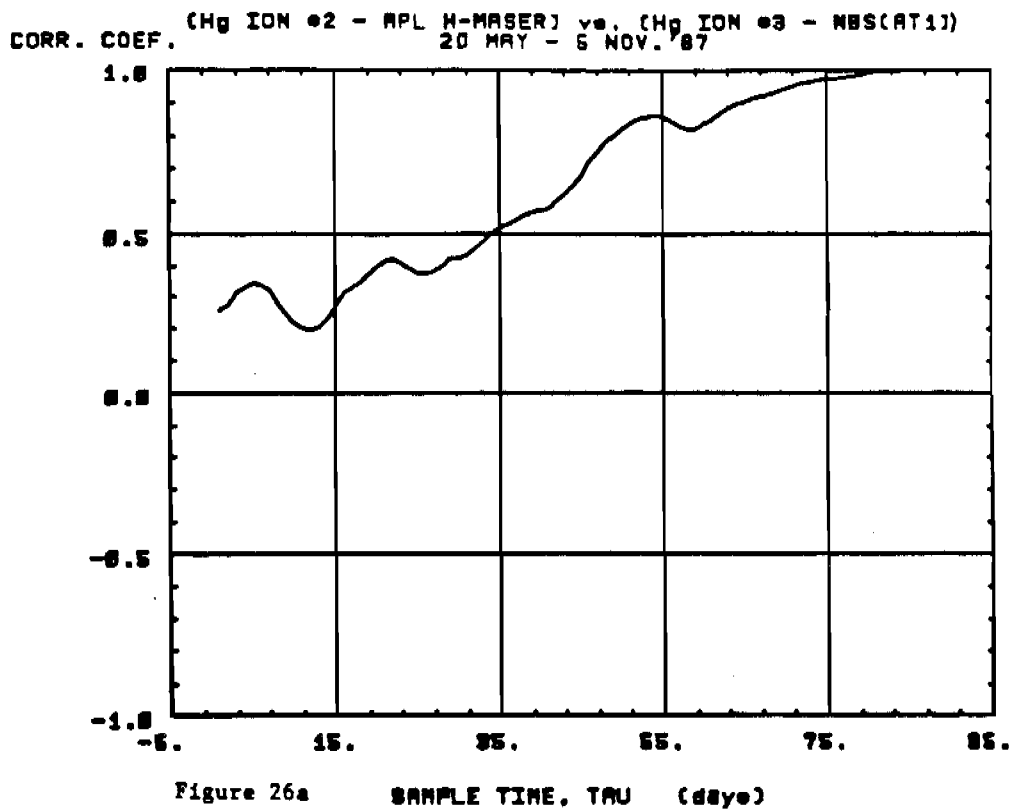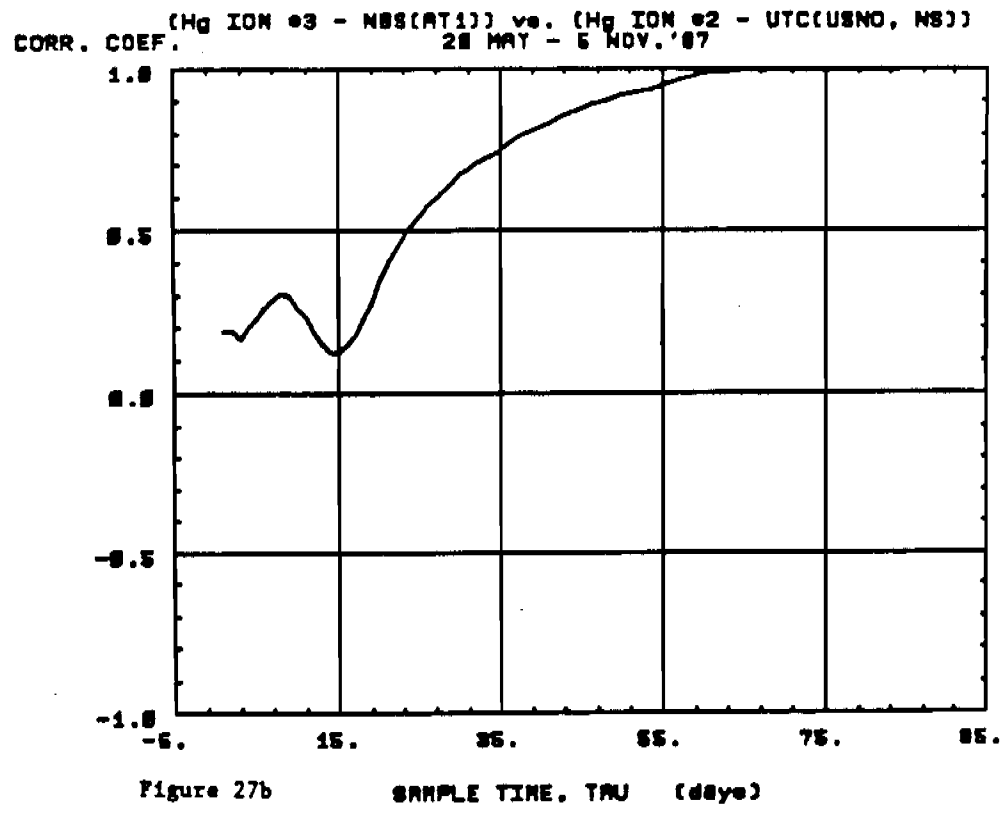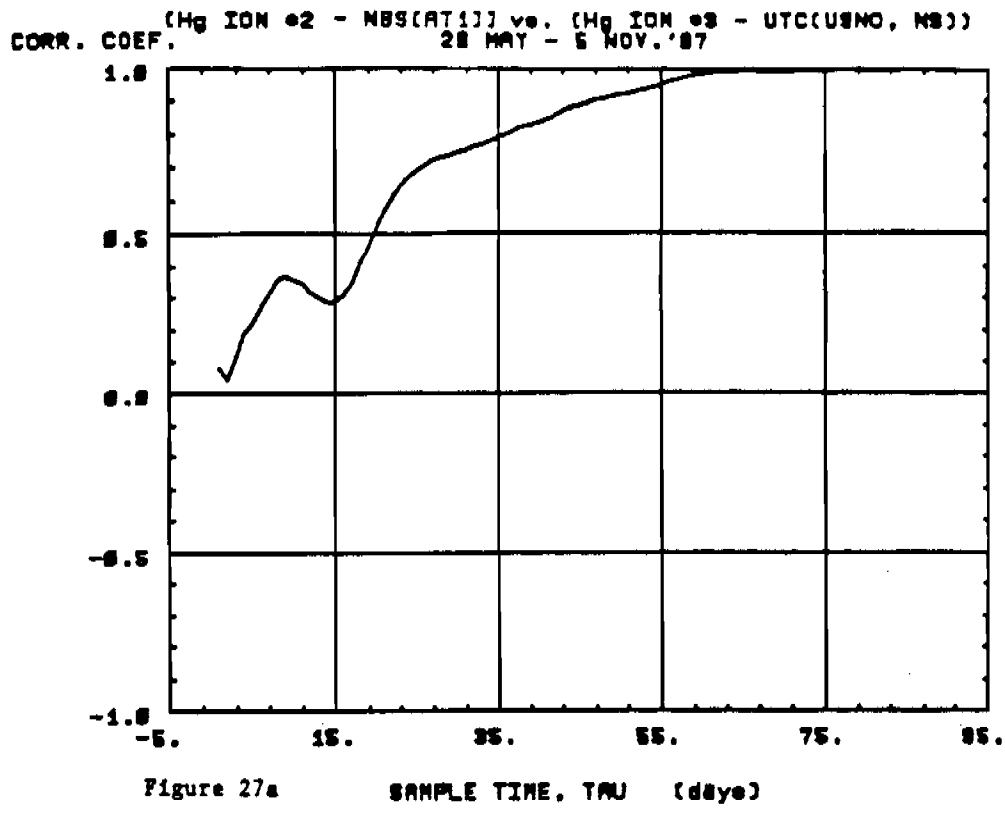
CORR. COEF.

Figure 27b   SAMPLE TIME, TAU   (days)
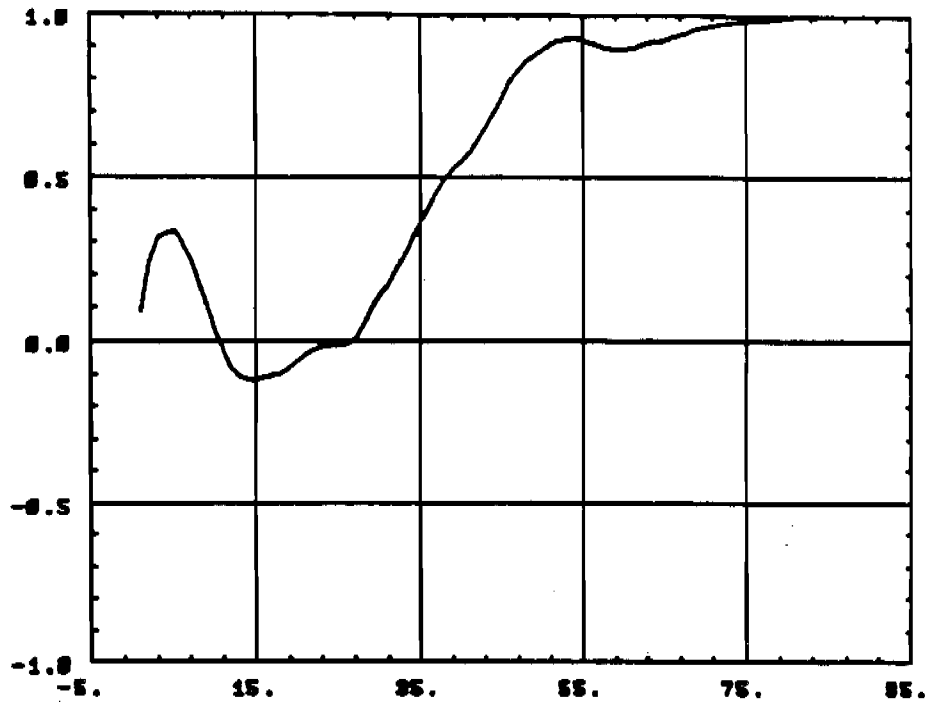
Figure 28a   SAMPLE TIME TAU   (days)
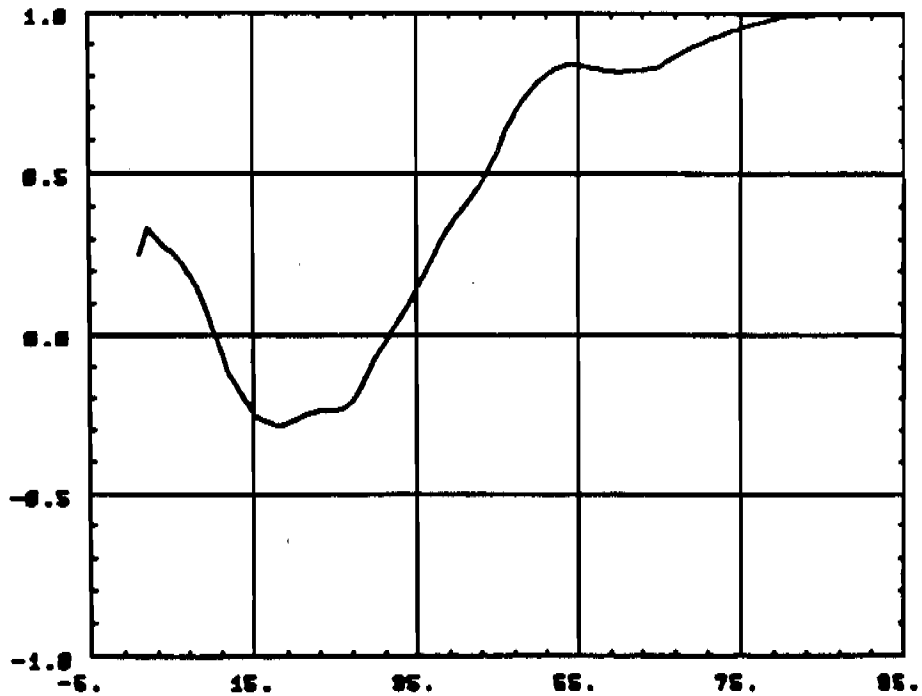
Figure 28b   SAMPLE TIME, TAU   (days)
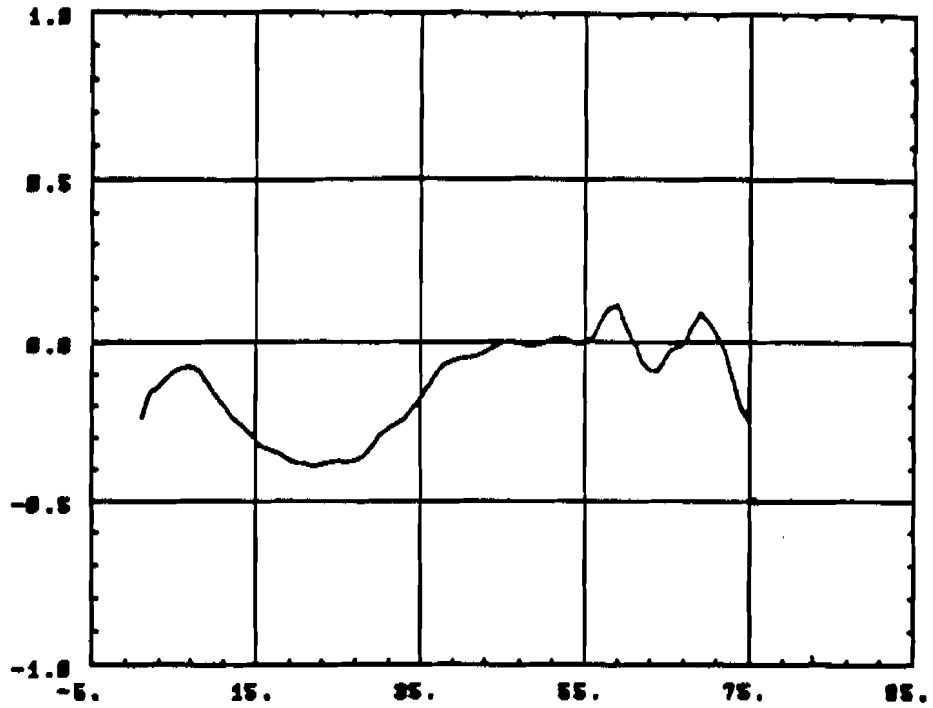
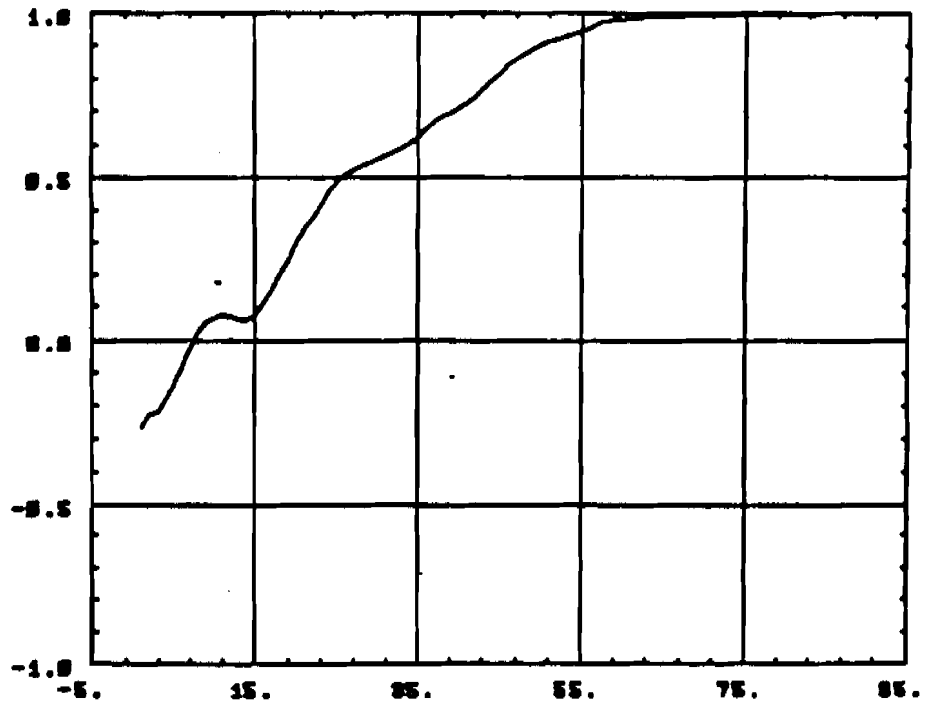Figure 29a   SAMPLE TIME, TAU   (days)

Figure 29b   SAMPLE TIME, TAU   (days)

FREQUENCY DRIFT ESTIMATES (in units of 10^{-15}/DAY)

USING 2nd DIFFERENCE ESTIMATOR FOR MJD 46935 - 47104

HG ION #2	HG ION #3	APL H-MASER	REF. STD.
-0.51	-0.52	-0.31	- NBS(AT1)
-0.44	-0.45	-0.25	- UTC(USNO, NS)
-0.38	-0.38	-0.19	- UTC(PTB)
-0.44 +/-0.06	-0.45 +/-0.07	-0.25 +/- 0.06	AVERAGE

Figure 30